M A G 2 P O L

Navid Qureshi, ILL 2016 - 2022

USER MANUAL

Version 5.1.3

Navid Qureshi

Institut Laue-Langevin

NEUTRONS
FOR SOCIETY

Contents

Bibliography   **103**

1 Preface

1.1 About the program

The MAG2POL source code is entirely written in C++ and can be downloaded in compiled form for the main platforms Windows, MacOS and Linux. The program is based on the Qt5, QCustomPlot, Eigen and OpenGL libraries.

1.2 Purpose of the program

MAG2POL was developed to supply an easy-to-use tool for analyzing spherical neutron polarimetry data obtained from single-crystal neutron scattering experiments using the Cryogenic Polarization Analysis Device (CRYOPAD). In addition it can treat flipping ratios in combination with a multipole expansion of the magnetic form factor. The analysis of nuclear and magnetic structures based on integrated intensites is of course also possible. Since version 2.4 multiple-wavelength integrated intensity data as well as X-ray data can be treated. Version 2.4.1 introduces the calculation of Schwinger scattering flipping ratios. Rietveld refinement of powder data was introduced in version 4.0.

Crystal and magnetic structure models can easily be introduced via the graphical user interface (the latter also with the help of the Irreducible Representation tool) and viewed in 3D in an OPENGL widget. Those models can then be refined to experimental data within a least-squares refinement. Hereby, spherical neutron polarimetry data, integrated intensities from a standard single-crystal diffraction experiment and powder/x-ray diffraction data can be simultaneously analyzed in any combination.

1.3 Disclaimer

MAG2POL is distributed under the GNU Lesser General Public License v. 3 (LGPLv3). The complete Qt5 source code of the used Qt5 libraries can be downloaded from the MAG2POL download page (note that the original code was not modified). The program is distributed with dynamically linked libraries which can be rebuilt by the user, if they

wish to use a different Qt version. A copy of the LGPL license text can be viewed in the *About* window accessible from the main menu.

2 Getting started

2.1 Installation

2.1.1 Windows

In order to run under Windows Qt5 depends on Microsoft Visual Studio. The Visual Studio Redistributable Packages are included in the download of MAG2POL and have to be installed by running `vcredist_x64.exe`. Afterwards, MAG2POL can be started from its executable, which should stay in its folder with all necessary libraries.

2.1.2 MacOS

Open the downloaded `dmg` image and drag the application to your Applications folder or directly download MAG2POL from the Mac App Store. Once the prompt appears saying that the application cannot be opened (after the first attempt of starting the application downloaded from the MAG2POL website), cancel it and launch *System Preferences*. Navigate to the *Security & Privacy* section, and under the *General* tab you'll see the blocked program. Simply click *Open Anyway* to launch it.

2.1.3 Linux

- AppImage (only 64 bit Linux versions)

  Download and launch the AppImage.

- Debian package (only up to MAG2POL version 3.0)

  Download gdebi from a terminal by typing `sudo apt-get install gdebi`. Then install the debian package with `sudo gdebi mag2pol_3.0.0-1_amd64.deb`, which will download the necessary libraries from the internet. Start the program by typing `Mag2Pol`.

2.2 Setting up a structure model

The main window contains a toolbar for the most frequently used menu entries and dockable widgets, which can be reorganized to one's individual taste. Moving a widget on top

of another will automatically create a tab widget and single tabs can be extracted to form new widgets. All the settings related to the toolbar and the dock widgets can be found in the *View* menu. Six different presets of different window dispositions can be accessed with the shortcuts CTRL/CMD + 1-6. Note that the exact position and size of the individual widgets are saved, when the program is closed and restored at the next start.

The first step for a meaningful use of MAG2POL is the parametrization of a nuclear and eventually magnetic structure model in the main window. This is done in the tab widget on the upper left part of the main window, when MAG2POL starts up (shown in red in Fig. 2.1) or by loading a `*.cif` or `*.mcif` file.

   The crystallographic space group (CSG) of the underlying nuclear structure has to be entered in Hermann-Mauguin notation in the corresponding field under the *Symmetry* tab. It is also possible to enter a magnetic space group (MSG) or a magnetic superspace group (MSSG), see also Sec. 6.2 for more information about space groups. Note that all information related to MSGs and MSSGs is based on the tables available at the ISOTROPY SOFTWARE SUITE [1], and in particular ISO-MAG [2] and ISO(3+D)D [3–6]. The entry of a CSG, MSG or MSSG is case dependent, i.e. the first letter should be upper case and any following letters lower case. Eventual additional spaces will be removed. Note that for MSGs and MSSGs lower-case symbols need to be preceded by an underscore (e.g. `P2_1'` in order to distinguish $P2'_1$ from $P21'$) in order to avoid ambiguity, while this is not necessary for CSG. For MSGs having the same label as a CSG an underscore should be added (e.g. `Pmna_` for the MSG and `Pmna` for the CSG). The symbol will be shown in green, if the space group has been recognized, and in red in the contrary case. In the case of CSGs, all alternative monoclinic settings are included as well as space groups with different origin choices or trigonal space groups with different axes settings (hexagonal or rhombohedral). For MSGs and MSSGs the following conventions are chosen by default: monoclinic unique axis b, monoclinic cell choice 1, hexagonal axes for trigonal groups and origin choice 2 for groups with more than one origin choice. Alternatively, the space group can be entered by its number or its numerical label in case of a MSG or MSSG. If the entry is followed by `#` the numerical entry will be replaced by the space group label (e.g. `139#` for space group $I4/mmm$). If an entered CSG has origin or axes setting choices a combo box will appear next to the space group field, in which the corresponding choice can be entered. For cell transformations the *Space group tables* tool has to be used (see Sec. 6.2).

The lattice parameters should be given in Ångströms and degrees. If a CSG was entered the magnetic symmetry should be given by a number of symmetry operators (generators) which can be constructed from the drop-down menues. The first part featuring xyz refers to the symmetry operator which is applied to the atomic position, whereas the second part featuring uvw is the corresponding symmetry operation acting on the magnetic moment.
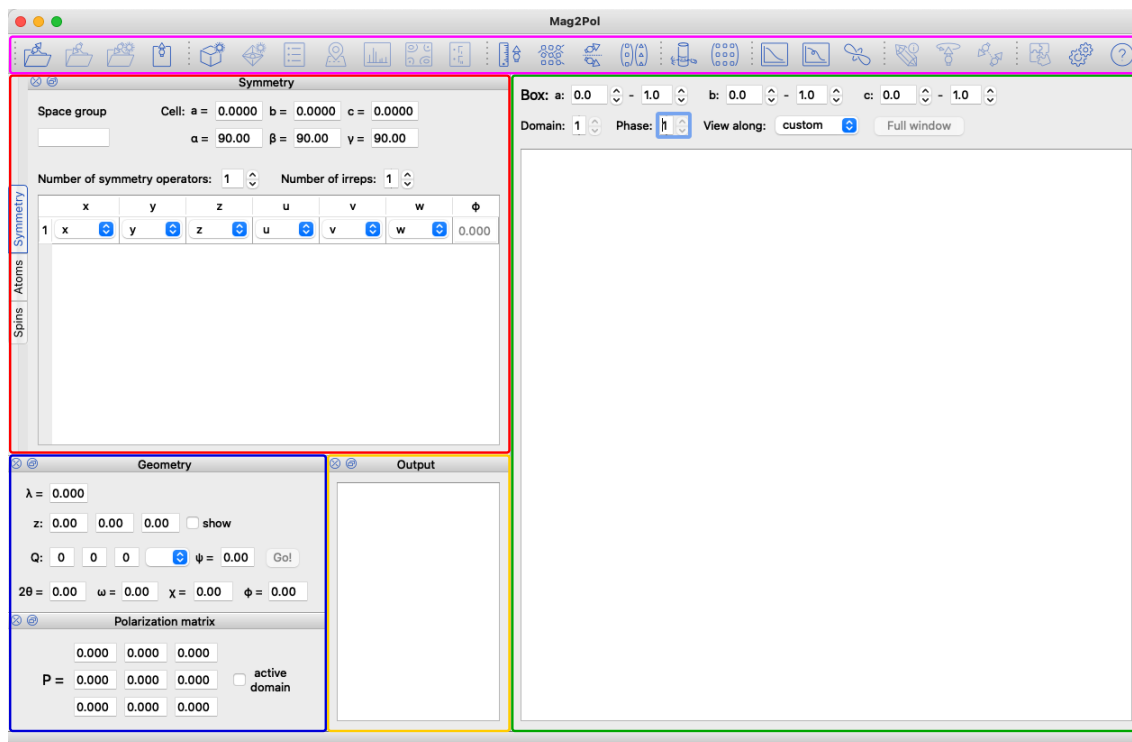
Figure 2.1: MAG2POL main window at the program start (in the *Compact 1* preset). The cyan box shows the toolbar from which most of the menu entries can be triggered. The crystal and magnetic structure information are entered in the tab widget marked by the red box. The green box contains the OPENGL widget for the 3D visualization of the nuclear and magnetic structure and the drawing box given in relative lattice coordinates. The blue box is devoted to the experimental geometry including wavelength and sample orientation. Individual calculations for a given (hkl) reflection can be triggered from here. The calculated angles corresponding to the instrument geometry are shown in the respective boxes. The results of the calculations (nuclear/magnetic structure factors, flipping ratios, etc.) are shown in the orange output box.

Each symmetry operator can be combined with a magnetic phase. Note that the magnetic symmetry can be obtained from calculating the irreducible representations through the menu item *Generate→Irreducible representations* (see Sec. 6.4). In that case it is not necessary to enter the magnetic symmetry operators by hand. The use of a MSG or MSSG will automatically set the magnetic symmetry. MAG2POL supports the loading of `*.mcif` files for MSGs and MSSGs together with the appropriate transformations.

Under the tab *Atomic positions* the different sites can be entered by adjusting the corresponding number. Each site needs an atom label which corresponds to the element symbol in case of a purely nuclear scatterer. For a magnetic atom, the label starts with an `M` or `J` followed by the element symbol and the oxidation state, e.g. `MCo3` or `JHo3`. The `M` refers to the magnetic form factor containing only spherical Bessel functions $\langle j_0 \rangle$, while `J` denotes a magnetic form factor of rare-earth elements approximating $\langle j_0 \rangle + c_2 \langle j_2 \rangle$. For the calculation of Schwinger flipping ratios the exact x-ray form factor is needed for which the oxidation state should be given as e.g. `Co2` for a non-magnetic atom. Contrarily to the space group symbol, the entry is case independent, however, no spaces can be used.

An isotropic temperature factor B and an occupation factor (1 for a fully occupied site) can be entered for each site. Anisotropic temperature factors can be chosen by right-clicking the isotropic value, which opens a pop-up menu for activating and setting the values. Depending on the site symmetry certain entries of the anisotropic temperature tensor may be 0 or constrained. In MAG2POL this is handled automatically by determining the site-symmetry group. As stated in [7] one should choose the first atomic position of an equivalent set given in the International Tables Vol. A [8] in order to obtain the correct restrictions. When the tensor is the zero matrix it will be initialized as isotropic according to the isotropic temperature factor following [9]. The inverse operation is also possible: the isotropic temperature factor can be set as an *equivalent* one from the anisotropic tensor by evoking the previously mentioned pop-up menu. Anisotropic displacement ellipsoids can be visualized in the unit cell by checking the corresponding checkbox in the settings menu (see this demo video).

If a magnetic ion has been recognized, it will be displayed in the *Magnetic structure* tab, where its complex Fourier components and a phase factor can be entered (in the case of user-defined basis vectors or basis vectors of irreducible representations, the coefficients of those basis vectors should be entered here, see Sec. 3.5 and Sec. 6.4). In addition, the propagation vector can be entered here, which relates the translational symmetry of the magnetic cell to the nuclear one. The checkbox $+q \neq -q$ is automatically set when the propagation vector or the space group is changed. It should be activated, when $\mathbf{q} - (-\mathbf{q})$

does not correspond to a vector of the reciprocal lattice. The automatic setting can always be overridden, e.g. if the reflections were measured with a component 0.501 which in fact should be commensurate.

A generated structure can be converted to space group $P1$ by right-clicking the label *Space group* and selecting *convert to P1*. This will add all atoms (formerly generated by the space group symmetry) to the list in the *Atoms* tab, which can be useful if one wants to treat the nuclear/magnetic structure without symmetry constraints. If a structure is already expressed in $P1$ symmetry, an additional menu entry *create supercell* is visible in the context menu. When clicked, the supercell can be given in the form of n_a x n_b x n_c (note that the x are optional, spaces work as well), which will then be applied to the lattice parameters and to all atomic positions.

It is possible to set up multiple phases. When treating single-crystal data, this feature can be useful in the presence of co-existing magnetic structures which have the same propagation vector and therefore contribute to the same magnetic reflections. Multiple phases may also be used to generate or analyze a powder pattern.

In order to create an additional phase simply right-click the *Phase* label above the OPENGL widget and under the *Add phase* menu choose either *New phase* or Duplicate current phase. In the latter case a copy of the present phase will be generated which can then be modified. The different crystal and magnetic structures can be visualized by modifying the phase number through the arrow buttons. A volume fraction is associated to each phase which can be set in *Structure→Phases, domains and twins.*

Different example videos are available for setting up a structure model, setting up a simple magnetic structure or setting up a complex magnetic structure.

2.3 Visualizing crystal and magnetic structures

Once all necessary parameters have been entered, the crystal and magnetic structures can be visualized by triggering the menu entry *Generate→Unit cell* or using its shortcut (CTRL/CMD + U). In case of a missing or erroneous input, the corresponding error message should pop up. MAG2POL can optionally check, if the atomic positions entered by the user are not too close to a special position of the space group. This would lead to generated atoms which are too close to each other and trigger a warning. This option and also the shortest allowed distance between generated atoms can be set in *Settings→Symmetry.*

The perspective can be modified by dragging within the OPENGL widget. A rotation around the axis vertical to the viewing plane can be achieved by dragging within the upper or lower left corner of the widget. Zooming in and out is done via the mouse wheel, wheras the original zoom can be restored with a right click. The view can be

shifted by keeping the CTRL/CMD key pressed while dragging. The bounding box of the volume to plot can be modified in the spin boxes corresponding to relative units of the lattice constants. If more than one phase or magnetic domain is present, each individual structure can be viewed by selecting the respective phase/domain number in the spin box. The position of the light source can be modified by dragging the scene while pressing the ALT key. The default position is restored by ALT+rightclick.

The appearance of every atom/spin site can be modified with the plot options shown at the right of the atomic position. A site can be turned invisible by removing the tick below *plot*. A right-click on either of the *plot* check boxes opens a context menu from which it can be chosen wheter all, only nuclear or only magnetic atoms will be plotted. The color can be chosen by clicking on the colored square and then by setting the *RGB* values in the pop-up window. The color boxes also provide convenient shortcuts through a context menu: a selected color can be applied to all atoms, all nuclear atoms, all magnetic atoms or all atoms with the same label. The sizes of the atoms and spins can be defined in the boxes *size a* and *size s*, respectively. If the Fourier components are imaginary and the imaginary part is perpendicular to the real part (within 1°) then an envelope will be drawn automatically emphasizing the rotation plane of the spin.

The objects to be plotted can be chosen from the *Settings* menu together with the quality and resolution of the objects. The coordinate axes can be plotted in the lower-left corner instead of the colored unit cell axes. Also, a smart legend can be added in the upper-left corner, which will automatically adjust the legend entries depending on repeated elements with the same appearance (such sites will automatically be numbered, e.g O1, O2, O3...). Furthermore, multiple unit cell edges can optionally be plotted as well as multicolored atoms representing the respective occupation of shared sites. Furthermore, MAG2POL features antialiasing by using multisampling per pixel and the objects' distance to the viewer is calculated for each view which allows for a correct back-to-front rendering of transparent objects. Those features massively increase the quality of the rendered picture. The OPENGL objects have been designed in order to minimize the calls to the frame buffer, for which the improved graphics don't come alongside with slower performance.

2.4 Distances and angles

Once a (magnetic) structure is drawn in the OPENGL widget the user can visualize atomic positions, magnetic moment values, bond distances, angles between 3 atoms and angles between two spins. In order to get information concerning the position of an atom or the Fourier components of a magnetic moment, just click on the atom (sphere) or on the cone of the spin, respectively. The information will be shown in the status bar of the main window and the object will be drawn with a different texture. In order to get distances

between 2 atoms click the first atom and then SHIFT-click a second one, which will show the distance in the status bar and will draw the bond between those 2 atoms. The same procedure has to be done to get the angle between 2 spins. For the angle made up by 3 atoms simply SHIFT-click the 3 atoms. Note that you can rotate the perspective in between SHIFT-clicks if necessary.
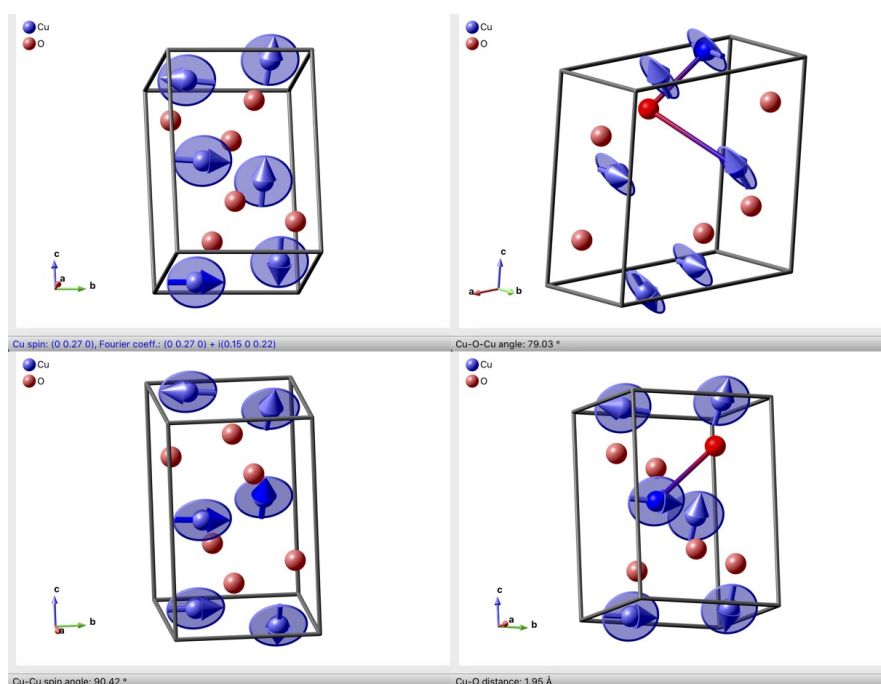
Figure 2.2: Geometry options in MAG2POL.

2.5 Bonds and polyhedra

MAG2POL features the plotting of bonds and polyhedra. After a structure has been generated this can be done via the *Generate→Bonds* menu or the toolbar icon. A control window will open up, which is shown in the upper part of Fig. 3.1. Here the number of bond types to search and generate can be entered which creates the according number of rows in the *Bonds* and *Polyhedra* tables. The center (atom1) and ligand (atom2) atoms can be chosen from the combo boxes. Note that the content of these boxes is a list of elements followed by the list of sites. In the example shown in Fig. 3.1, the structure contains two Co sites, so in order to plot all possible Co-O bonds, irrespective of the specific site, the elements have been chosen from the first (element) list. A number of parameters can be adjusted in order to control the bond distances and the appearance of the rendered objects. The meaning of these parameters are explained when hovering

the mouse over the horizontal header items. Note that the minimal distance between the center atom and the polyhedron faces should be increased, if the resulting polyhedra look unexpected. This can be the case for heavily distorted polyhedra. The information about bonds created in the OpenGL widget can be retrieved by clicking on the center of the bond. This will show the two connected atoms, their positions and the bond length in the status bar of the window.

The parameters for the bond search as well as for the appearances of bonds and polyhedra are saved in the *.xml file.
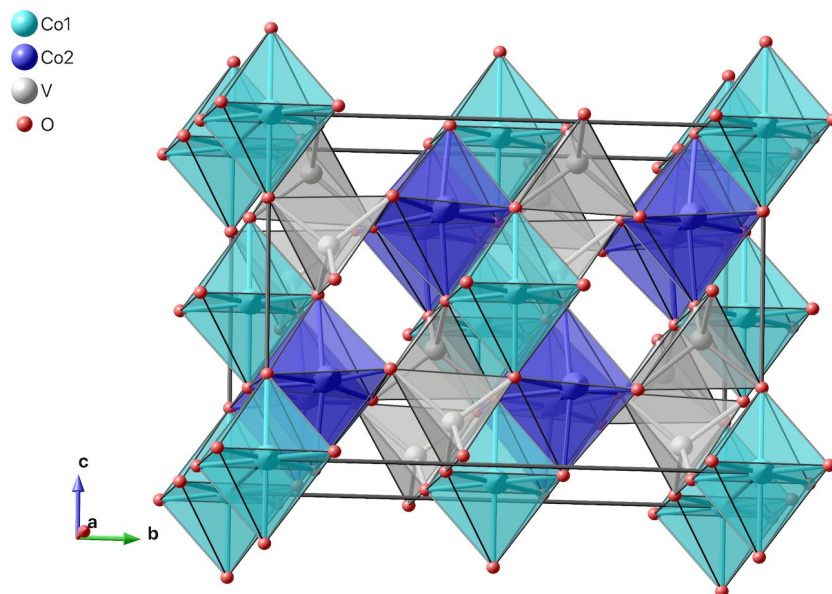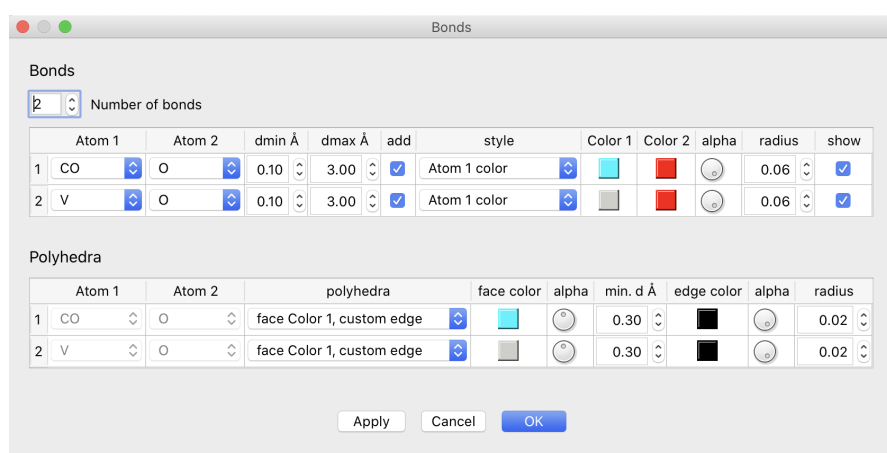

Figure 2.3: Bonds and polyhedra plotting in Mag2Pol.

2.6 Saving and loading input files

All parameters which have been entered or modified can be saved into an input control file in XML format from the menu entry *File→Save/Save as*. Additional information concerning scale and extinction factors, magnetic domains, fit parameters and constraints, user-defined magnetic form factors, powder patterns, plot parameters like the cell range, the perspective and the zoom are saved as well. Note that if a magnetic (super) space group is used after having calculated irreducible representations, the latter will not be saved in the XML file. The respective parameters will be explained in Sec. 3. Saved input files can be loaded via *File→Load*. The MAG2POL main window can also be reset by *File→Reset*.

Crystal and magnetic structures can also be exported in `*.cif` or `*.mcif` format. When the propagation vector is 0, the magnetic symmetry will be exported either using the user-defined magnetic symmetry operators or that given by an irreducible representation. Note that only 1-dimensional irreps can be exported and that for mixed representations only the first will be considered. For non-zero propagation vectors the magnetic moments (real vectors) will be calculated for all atomic sites and the structure will be exported in $P1$ symmetry.

2.7 Calculation of structure factors and polarization matrices

Besides the correct description of a magnetic structure, MAG2POL needs information concerning the experimental geometry in order to calculate the nuclear/magnetic structure factors and the polarization matrices. Herefore, the wavelength should be given in Ångströms, which already allows the calculation of structure factors. The calculation of the polarization matrix depends on the orientation of the sample, which can be given either by defining the vertical sample axis (reciprocal lattice vector) or by supplying the orientation matrix of the experiment in the menu *Geometry→Orientation matrix*. In the latter case the instrument angles are automatically calculated and shown in the respective boxes. For the 4-circle geometry a ψ value can be given, which is the rotation angle around the scattering vector, where $\psi = 0$ refers to bisecting geometry. From any given angles the corresponding (hkl) indices can be calculated by right-clicking any angle value and selecting *calculate hkl*.

Note that that the flipping ratio geometry requires the use of the vertical axis (not Cryocradle). The vertical axis will automatically be calculated and set after setting the normal-beam orientation matrix. Since in a flipping ratio experiment one usually assumes the magnetic moments to be aligned parallel to the vertical direction (magnetic field di-

rection) one can align the moments automatically by right-clicking the label *z axis* and choosing *set moments parallel*. If the UB matrix is not given the program will calculate the moment direction from the values given for the vertical axis. Note that the *uvw* components of the magnetic moments will have to be constrained in a refinement. Another option is to use user-defined basis vectors before aligning the moments vertically, which requires the refinement of only one parameter.

With MAG2POL it is possible to calculate flipping ratios due to Schwinger scattering [10–13], which is automatically done in the absence of magnetic ions in the unit cell (e.g. use `Fe2` instead of `MFe2`). Note that the polarization axis of the neutrons is taken to be parallel to $\mathbf{k}_i \times \mathbf{k}_f$.

The calculations are done for the Bragg reflection $(hkl) \pm \mathbf{q}$ entered by the user by pressing *Go!* (see also this demo video). If the propagation vector is 0, there is no difference concerning the combo box. When more than one propagation vector was entered in the *Domain* window (see Sec. 3.3), they will all be shown in this combo box and by selecting e.g. (hkl)-$\mathbf{q}_2$ the program will automatically check if a contribution from another configuration domain is present at the $\mathbf{Q}$ position.

If the checkbox *show* is activated, the local coordination system (see Sec. 7) and the magnetic interaction vector $\mathbf{M}_\perp$ are drawn.

The results of the calculation are shown in the output text window (orange box in Fig. 2.1) and the individual polarization matrix entries are shown in their respective boxes in the Geometry section of the window (blue box in Fig. 2.1).

Whole lists of reflections can be generated under *Generate→Reflection list* for given criteria like *hkl* range, intensity, polarization and diffractometer angles. This can be useful as a preparation for an experiment e.g. by selecting those magnetic reflections which show a large chiral component in the P_{yx} term. The reflections which fullfil the given criteria are shown in a table after clicking *Create hkl list*. By right-clicking on a respective horizontal header the list can be ordered according to that parameter, either ascending or descending. The reflection list can be saved in `ASCII` format which is directly readable by MAD or NOMAD due to the comments marked by '!'.

3 Further parameters

In addition to simple calculations as shown in the previous section, scale/extinction parameters and magnetic domains can be defined, which obviously affect the observed intensities and polarization values. In case of a crystallographic site being shared by multiple magnetic ions, user-defined magnetic form factors can be created, plotted and saved.

3.1 Global settings

The global settings of the application can be evoked from the *Settings* or *Preferences* menu (depending on the platform). General parameters concerning the application, the instrument, symmetry and the view can be found in the *General* tab. Most of the settings are self-explaining. Note that the theme colors and the dark mode can also be set via the shortcuts ALT + 1 to ALT + 8 from within the main window.

Under the *Symmetry* tab, the option *Check special atomic positions* assures that the user does not define an atomic position (by mistake) which is too close to a special Wyckoff position. If after generation of the unit cell, atoms of the same site reveal a distance shorter than the one defined under *Shortest allowed distance*, the program will show a warning. The option *Constrain lattice parameters in powder fit* will automatically add constraints concerning the lattice parameters during Rietveld refinement depending on the space group. The setting *Constrain propagation vector in powder fit* constrains e.g. $q_y = q_x$ for a tetragonal, trigonal (hexagonal setting) or hexagonal space group or e.g. $q_z = q_y = q_x$ for a cubic or trigonal (rhombohedral setting) space group.

Under the *Refinement* tab different least-squares fit parameters can be set. The convergence criterium is defined as the maximum parameter shift divided by its standard deviation. The range in multiples of the peak FWHM can be defined for which the peak profile will be calculated in a powder pattern. When the *Calculate pattern in excluded regions* option is disabled, only the peak positions will be calculated and shown, but no intensities will be calculated. This can be a convenient choice for low-symmetry structures with hundreds (thousands) of reflections in the high-Q region of the powder pattern. The setting *Ignore secondary phases for single crystal* should be unchecked when those secondary phases are only present in a powder diffraction pattern. It should be checked when two nuclear and/or magnetic phases are actually present in the single-crystal sample

and contribute to the same reflections.

All settings concerning the unit cell plot in the OpenGL widget can be found under the *Plot* tab. Here the objects to be rendered can be chosen as well as the mouse sensitivity for zooming and rotating the plot. Several options exist to adjust the rendering quality which affect the fluidity with which you can manipulate the drawing. The level of multisampling can be set by the number of samples per pixel, which affects the rendering of edges (smoother edges for increasing multisamples). The object resolution is a measure of the number of vertices which are calculated for the creation of an object. The minimum number is 3 and corresponds to a triangle in comparison to a circle with higher resolution. In order to correctly render transparent objects, when they are aligned one behind the other, the order is crucial. Since the perspective is constantly changed by the user, the order of the transparent objects is automatically recalculated on-the-fly. For a large number of transparent object this means a lot of calculation cost, of course. Therefore, the threshold for continuous reordering can be adjusted, the default value being 1000 objects, e.g. 100 octahedra (each containing 8 transparent planes) and 200 spin envelopes. Above this threshold, the order will only be recalculated when the mouse button is released after dragging the perspective. In order to avoid too long calculation times when a very large supercell with a lot of transparent objects is plotted, the automatic reordering can be turned off with the second threshold value (default is 5000).

Under the *Labels* tab the position, scale and font size of the coordinate axes and legend can be customized. It is also possible to enter individual translation values for the axes labels. These settings are also saved in the `*.xml` file.
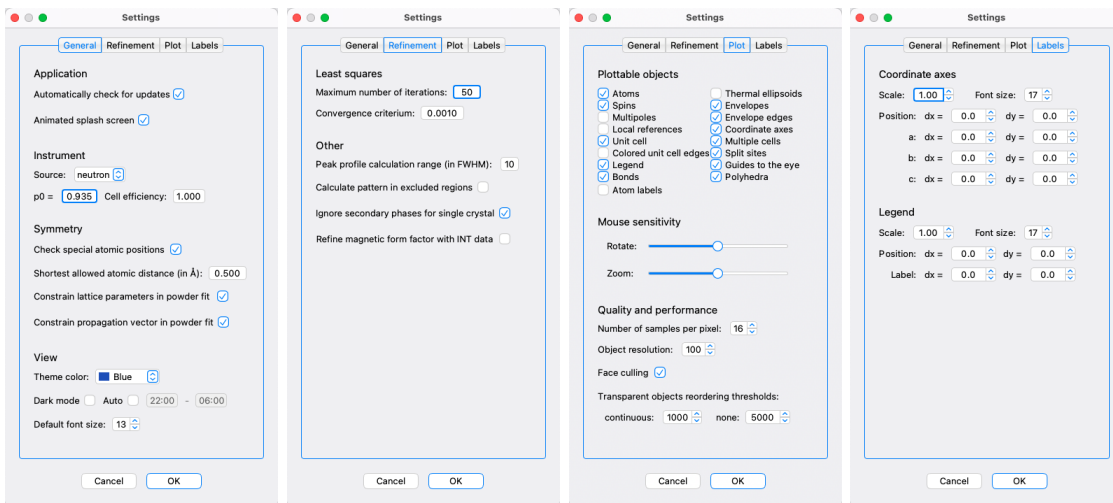

Figure 3.1: Global settings in Mag2Pol.

3.2 Scale and extinction parameters

The scale factor and extinction parameters can be set via the menu entries *Structure→Scale factor* and *Structure→Extinction*, respectively. The scale factor is multiplied to the calculated intensities of Bragg reflections in order to be compared with the observed ones. The extinction parameters x_{ij} build up the tensor **x** which allows the treatment according to an empirical model which represents a compromise to treat both primary and secondary extinction. It is also implemented in FULLPROF [14] and in SHELX [15] and has shown to work well in practice. The extinction correction is given by

$$y = \left(1 + \frac{p\mathbf{x_{aniso}}F_c^2\lambda^3}{4\sin(2\theta)(\sin\theta/\lambda)^2}\right)^{-\frac{1}{2}} \tag{3.1}$$

where x is the anisotropic extinction parameter and F_c is the calculated structure factor. p is $1e^{-3}$ for neutrons and $1e^{-6}$ for x-rays. x_{aniso} is obtained by operating the tensor **x** subsequently on the scattering vector (hkl):

$$x_{aniso} = \left[\begin{pmatrix} x_{11} & x_{12} & x_{13} \\ 0 & x_{22} & x_{23} \\ 0 & 0 & x_{33} \end{pmatrix} \begin{pmatrix} h \\ k \\ l \end{pmatrix}\right] \begin{pmatrix} h \\ k \\ l \end{pmatrix} = x_{11}h^2 + x_{22}k^2 + x_{33}l^2 + x_{12}hk + x_{13}hl + x_{23}kl \tag{3.2}$$

3.3 Domains and twins

An unlimited number of magnetic domains and structural twins can simply be added via the menu *Structure→Domains and twins* (see demo video). The program differentiates between S-domains and k-domains, see [16] for a review. For k-domains at least two propagation vectors have to be set to which the magnetic domains (see below) can be attributed.

For magnetic domains, first the number of different domains has to be set, which automatically applies an even population between the domains. Then, the symmetry operators (usually the ones from the paramagnetic space group which have been lost in the magnetic phase transition) have to be entered using the combo boxes. In addition, check boxes can be activated to define inversion or chiral domains. The first simply reverses every magnetic moment, whereas the latter takes the complex conjugate but keeps the phase shift of the user-given Fourier components describing the magnetic structure. If a symmetry operation is not included in the little group, i.e. it transforms $+\mathbf{q}$ into $-\mathbf{q}$, the program calculates the complex-conjugate and inverts the phase. That means that if a magnetic structure breaks inversion symmetry and therefore two magnetic domains are related by the inversion center, the *chiral* checkbox should not be checked. When only

one propagation vector is present, then all magnetic domains are considered as S-domains. When more than one propagation vector is entered, then each of the magnetic domains can be attributed to a specific k-domain by choosing the arm of the propagation vector star through the combo box with q_1, q_2, etc.

Structural twins are set up in the same way, however, in this case the rotation matrix relating the (hkl) reflections of the different twins has to be given. For the calculation of structure factors those rotations matrices will be multiplied to the observed (hkl) values and if the result corresponds to integer indices ($\pm$ the propagation vector) it will be considered as a contribution from another twin.

3.4 X-ray and magnetic form factors

3.4.1 Built-in form factors

In the present version of MAG2POL the scattering length, absorption cross section, incoherent cross section and X-ray form factor of all elements and the magnetic form factors of the $3d$, $4d$ and actinide ions are implemented. The latter are described by the analytical expression

$$f_M(\mathbf{Q}) = A \exp(-as^2) + B \exp(-bs^2) + C \exp(-cs^2) + D \tag{3.3}$$

with $s = \sin(\theta)/\lambda$. The magnetic form factors marked with the letter M (e.g. MCo2 for Co^{2+}) consist of only spherical Bessel functions $\langle j_0 \rangle$. For the rare-earth elements additional magnetic form factors are implemented which are marked with the letter J (e.g. JHo3 for Ho^{3+}) which approximate $\langle j_0 \rangle + c_2 \langle j_2 \rangle$.

The atomic or X-ray form factor is given by

$$f(\mathbf{Q}) = \sum_{i=1}^{4} a_i \exp(-b_i s^2) + c \tag{3.4}$$

The form factor is then corrected for anomalous dispersion which modifies it to

$$f(\mathbf{Q}) = f_0 + f' + if'' \tag{3.5}$$

where the real and imaginary part of the anomalous dispersion f' and f'' are stored wavelength-dependent in MAG2POL. The complete list of built-in scattering lengths and (magnetic) form factors can be accessed under *Form factors→View list* (see this demo video). The list can be ordered either by element name, by atomic number or alphabetically by right-clicking on the combo box and selecting the appropriate menu entry. By selecting an element from the combo box the scattering lengths, cross sections and the (magnetic) form factor coefficients will be displayed as well as a plot of the x-ray and

magnetic form factor as a function of $\sin(\theta)/\lambda$. Multiple form factors can be plotted by clicking *Keep* before selecting another element (see Fig. 3.2). Parts of the plot can be
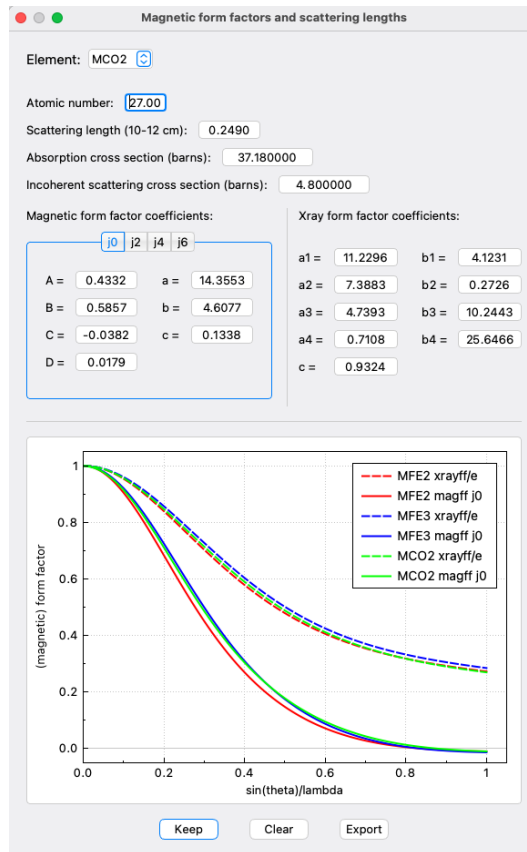
Figure 3.2: Example of the comparison of multiple form factors.

zoomed in by the usual controls of clicking and dragging, while the original view is reset by a right click. The plot can be cleared by clicking *Clear*.

3.4.2 User-defined form factors

In some cases it is desirable to use a custom magnetic form factor, e.g. if the magnetic form factor under question is not tabulated or if one crystallographic site is shared by different magnetic ions. In this case MAG2POL offers a simple method to add user-defined magnetic form factors which can then be saved in the input control file. In order to add (or delete) custom magnetic form factors, open the respective window under *Form factors→Manage user-defined* (or the corresponding toolbar icon), where you will find two tabs for the respective actions. Under *Add* either enter the form factor coefficients and the scattering length manually or type in a linear combination of built-in magnetic form factors. The number of elements is unlimited, however, the weights have to sum

to 1. Interstitial sites can be handled through the occupation factor in the main window. Fig. 3.3 shows an example of a compound in which Co and Fe ions in bi- and trivalent oxidation state share the same crystallographic site. The corresponding input is

Figure 3.3: Example of a user-defined magnetic form factor.

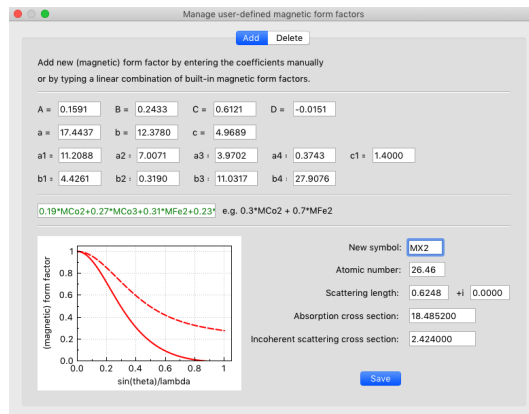`0.19*MCo2+0.27*MCo3+0.31*MFe2+0.23*MFe3`, which is case-independent. A correct entry, i.e. the sum of weights is 1 and the (magnetic) ions have been recognized, is signalled by green text (red otherwise). Note that you can only mix either only magnetic or only non-magnetic ions. Instantly, the weighted magnetic and atomic form factor coefficients and scattering length will be displayed as well as the plot of the form factors as a function of $\sin(\theta)/\lambda$. In order to save the new element a symbol has to be given. Any name (different from any built-in element) can be used for the new element. Upon clicking *Save* a pop-up window will inform the user, if the new element has been saved as magnetic or non-magnetic ion.

Built-in form factors can be viewed in the complete list as well as under the *Delete* tab. In the latter you can remove the selected one by clicking the button *Delete*.

3.5 User-defined basis vectors

For magnetic structures with higher symmetries it may be of advantage to use symmetry-adapted basis vectors instead of manually putting constraints between the individual components before refining the structure. Therefore, under *Structure→Basis vectors* up to 6 basis vectors can be defined (see Fig. 3.4). Once the *use basis vectors* check box is activated MAG2POL will interpret the values under the *Magnetic structure* tab as well as in the *Fitting* window as coefficients to be multiplied to the basis vectors. This is signalled by the label *<- BVs ->* between the first and last 3 basis vector coefficients. Note that

symmetry-adapted basis vectors can be deduced with the Irreducible Representation tool which is described in Sec. 6.4.
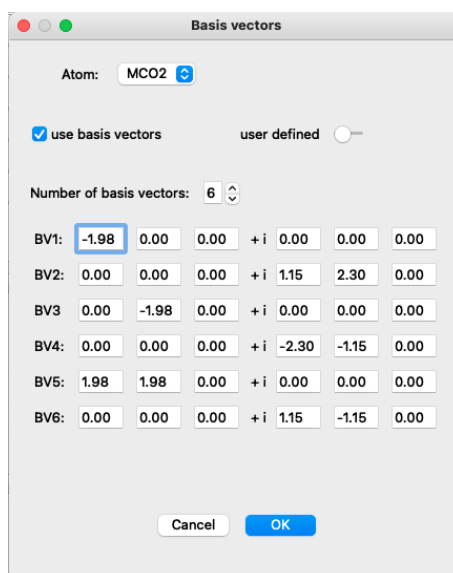
Figure 3.4: Example of a user-defined basis vectors.

3.6 Mixed irreducible representations

Two one-dimensional representations can be combined to a two-dimensional one. This can be achieved by setting the number of representations to 2 under the *Symmetry* tab of the main window. This will duplicate the symmetry operations where the first half corresponds to representation 1 and the second half to representation 2. The nuclear symmetry can obviously not be changed, however, the magnetic symmetry should be set by adjusting the (uvw) combo boxes according to the individual representations. Under the tab *Magnetic structure* you can now attribute the indivudal real and imaginary parts of the Fourier components to a respective representation by right-clicking on its value, which will open a context menu. Here you can select either *irrep1* or *irrep2* as shown in Fig. 3.5. Note that symmetry-adapted basis vectors of the irreducible representations can also be mixed using the Irreducible Representation tool (see Sec. 6.4).

3.7 Magnetic form factor models

When defining a magnetic ion the default magnetic form factor corresponds to a spherical magnetization density which is expressed by the radial integral $\langle j_0 \rangle$. Further magnetic
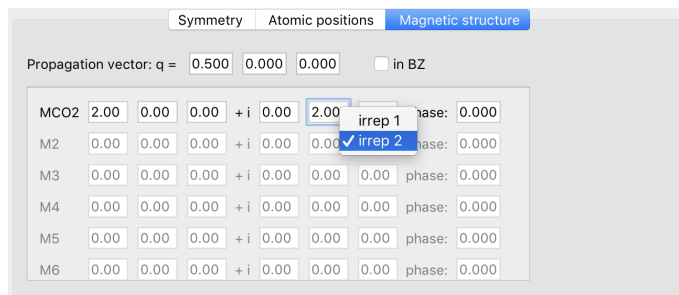
Figure 3.5: By right-clicking on the value of the Fourier component it can be defined according to which irreducible representation it transforms.

form factor models can be chosen for each magnetic ion individually by entering the *Multipoles* window via *Form factors→Multipoles* (or its toolbar icon). Note that those parameters (not belonging to the default model) can be refined in the fitting procedure by activating the *use multipoles* checkbox when the refinement is done on flipping ratios. When integrated intensities are analyzed the checkbox *Refine magnetic form factor with INT data* should be activated in the settings.

3.7.1 Sum of radial integrals

This model still yields a spherical magnetization density and the magnetic form factor is given by

$$f_M(\mathbf{Q}) = \langle j_0 \rangle + w_2 \cdot \langle j_2 \rangle + w_4 \cdot \langle j_4 \rangle + w_6 \cdot \langle j_6 \rangle \tag{3.6}$$

with the $\langle j_n \rangle$ being spherical Bessel functions and the w_n refinable parameters. The coefficients of the analytic approximation of the $\langle j_n \rangle$ integrals are stored inside the program and can be looked up in the form factors window (*Form factors→View list*). The analytical approximation of the different spherical Bessel functions is given by

$$\langle j_0 \rangle = A \exp(-as^2) + B \exp(-bs^2) + C \exp(-cs^2) + D \tag{3.7}$$

with $s = \sin(\theta)/\lambda$ and

$$\langle j_n \rangle = \left(A \exp(-as^2) + B \exp(-bs^2) + C \exp(-cs^2) + D \right) \cdot s^2 \tag{3.8}$$

for $n \neq 0$.

The resulting magnetic form factor is plotted together with the spherical $\langle j_0 \rangle$ in order to point out the differences and can be exported as a `PDF` or `ASCII` file.

3.7.2 Multipole expansion

If the data allows for a more sophisticated description of the magnetic form factor, the deviation of the magnetization density from the spherical symmetry can be achieved by a linear combination of basis functions. In Mag2Pol those basis functions are the real spherical harmonics which describe the angular dependence of the magnetization density. The radial dependence is calculated according to a Slater-type function (see Sec. 7.4 for a complete description). The description of each combination of multipoles is always in relation to a orthogonal local reference system, where for $\theta = \varphi = \chi = 0$ the local x axis is parallel to the unit cell's a axis, y is within the a-b plane and z is perpendicular to a and b. By selecting the multipole expansion for a particular magnetic ion the coefficients of the different basis functions (multipoles) can be set together with the Slater-type function coefficients and the local reference angles for each magnetic ion. Non-magnetic ions, e.g. O^{2-} can in principle be treated by first creating a new magnetic ion as described in Sec. 3.4.2 and then using that ion in the multipole expansion.

The respective ion to which the local reference and the multipole/Slater coefficients apply can be chosen in the combobox. The tab widget then offers a clearly arranged representation of the coefficients C_l^m, the Slater exponent n and the parameter Z, diveded into monopole, dipoles, quadrupoles, octupoles and hexadecapoles. Note that the monopole coefficient C_0^0 represents the global magnetic moment of that ion and that the values in the magnetic structure tab are ignored. As soon as a coefficient C_l^m is different from zero the respective multipole can be plotted in the OpenGL widget (see Fig. 3.6, left panel). When using many multipoles it can be difficult to see the individual ones clearly, so in this case the tickboxes above the OpenGL widget can be used in order to only plot the ones of interest. Clicking on *color scale according to coefficients* changes the color code in dependence on the values of C_l^m. It is also possible to visualize the weighted sum of the individual multipoles, which plots the angular dependence of the magnetization density distribution (see Fig. 3.6, right panel). Since the magnetization density is non-spherical the magnetic form factor in the right panel can now be plotted along a user-defined reciprocal lattice vector. It can also be chosen to show the amplitude, the real or the imaginary part.

On clicking *OK* all parameters are saved for each atom. In the main window the (angular dependence of the) magnetization density distribution around the ion can be visualized in the unit cell, if the *Multipoles* and eventually the *Local references* check boxes are checked in the *Plot* tab of the settings window. Note that the scale can be modified by the spin and atom plot scales, respectively.

A demo video can be seen here.

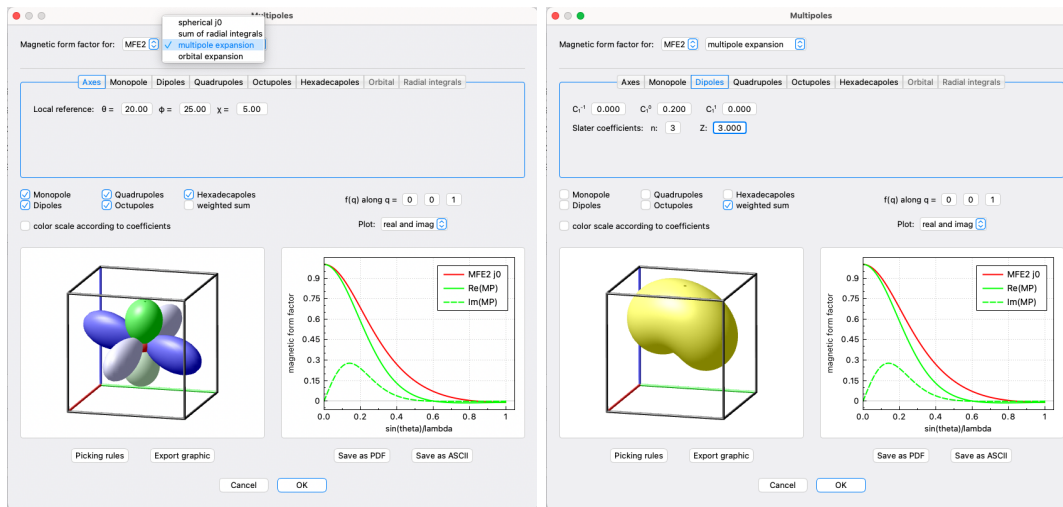Figure 3.6: Multipole window allowing to the set the coefficients of the multipole expansion of the magnetization density. Left: Visualization of the individual orbitals with positive and negative lobes. Right: Weighted sum of the individual orbitals.
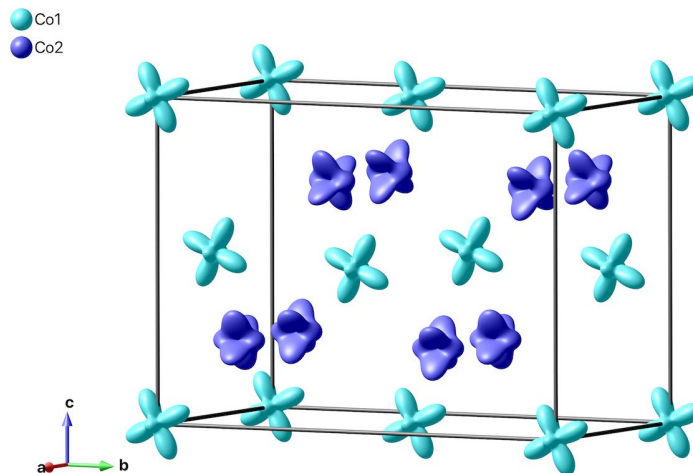

Figure 3.7: Multipole expansion of the magnetization density for each magnetic ion in the crystallographic unit cell (arbitrary population coefficients).

3.7.3 Orbital expansion

The relation between multipole population parameters and orbital occupancies can be generalized as shown in [17] for which the magnetization density distribution can be expressed in a similar way as in the previous section, but by using well-defined orbitals centered at the atomic position. The angular dependence can be chosen between $2p$, $3d$, $4f$ and a hybridized sp orbital, while the options for the radial dependence are the tabulated $\langle j_n \rangle$ values, a hydrogen-like orbital or a Slater-like orbital as in FULLPROF. Note that the coefficients C_l^m are normalized before being converted to the multipole population parameters (see Sec. 7.5) for which a single non-zero coefficient does not have any effect in a least-squares refinement.

3.8 Orientation matrix

As mentioned briefly in Sec. 2.7 the orientation matrix of a Cryocradle experiment is necessary to calculate the sample orientation for each (hkl) reflection. In other geometries the orientation matrix is necessary e.g. for calculating the absorption correction or the diffractometer angles. This UB matrix can either be entered manually in the window which opens by clicking *Geometry→Orientation matrix* or by selecting *Get UB* in that window. Here the individual observations with their respective angle values after centering can be entered manually or a list of reflections can be loaded by clicking *Browse*. The program reads `*.dat` files which are generated and filled by the MAD centering commands on the instrument D3. The refinement of the UB matrix is done according to the formalism presented by Busing and Levy and is based on the conventions of the instrument given in the *Geometry→Instrument* menu, see next section. The positioning of the sample with the Cryocradle setup does not correspond to the bisecting geometry as for standard four-circle geometries due to the fact that the angle ω is fixed. The positioning by using the angles χ and ϕ basically correspond to a non-zero ψ value (ψ being the angle around the scattering vector, which is 0 in the bisecting geometry). Fig. 3.8 shows the corresponding window for calculating and refining an experimental UB matrix after the centered reflections have been read from a file.

The refinement is presently reserved for the lattice parameters only (by activating the respective check boxes), i.e. the wavelength cannot be varied. The symmetrical constrains, e.g. $a = b$ and $\gamma = 120°$ are automatically set and fixed from the space group. By clicking the *Refine* button a least-square refinement will be started, where the initial orientation matrix is calculated form the first two reflections in the list and then refined on all observations.
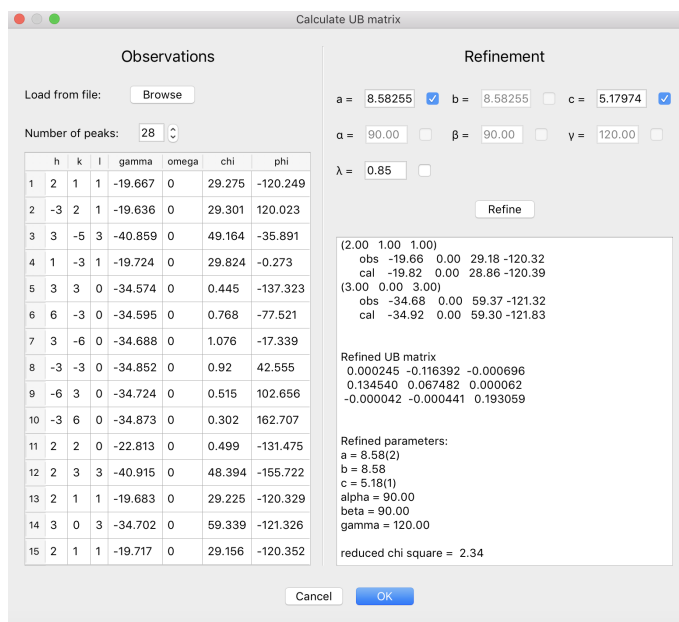
Figure 3.8: The experimental orientation matrix can be calculated and refined from a number of observed reflections.

The results of the calculation/refinement are shown in the text field and consist of the initially calculated UB matrix, a list of all observations and their observed and calculated angles, the refined UB matrix, the refined lattice constants including their respective standard deviations and the reduced χ^2. By clicking *OK* the refined UB matrix will be passed on to the previous window, which can than be saved by clicking *OK* on the latter.

Another possibility is to set the orientation matrix by choosing two vectors - either direct or reciprocal - pointing along the positive z axis and the positive x axis of the instrument (i.e. according to the definition of the instrument geometry), respectively. The corresponding UB matrix will be calculated by clicking on *Calc UB*. If the given vectors are not perpendicular (2-digit precision in reciprocal Å), the program will show a warning. It is possible to add an offset on ω (rotation around the vertical axis), χ (rotation around the beam axis for ω=0) and φ (rotation around the vertical axis for χ=0) which will automatically update the calculated UB matrix. Note that the rotation senses of the ω, χ and φ angles also follow the definition of the actual instrument geometry.

If a crystal model has been setup in the *Sample info* window (under *Absorption*) (or in the *Data reductioni* window), it will be shown in a 3D plot on the right-hand side of the window (see Fig. 3.9). The usual OPENGL controls like rotating, zooming, panning and changing the light direction (ALT + rotating) are available. The plottable objects can be switched on/off using the checkboxes on top of the 3D plot, which can be exported to a

`*.png` file by clicking on the export button. Recalculating the UB matrix from the given sample orientation (through the 2 definable vectors) or by moving the angle sliders will update the sample orientation in real time.

Furthermore, it is possible to visualize the successive rotations of the sample when posi-
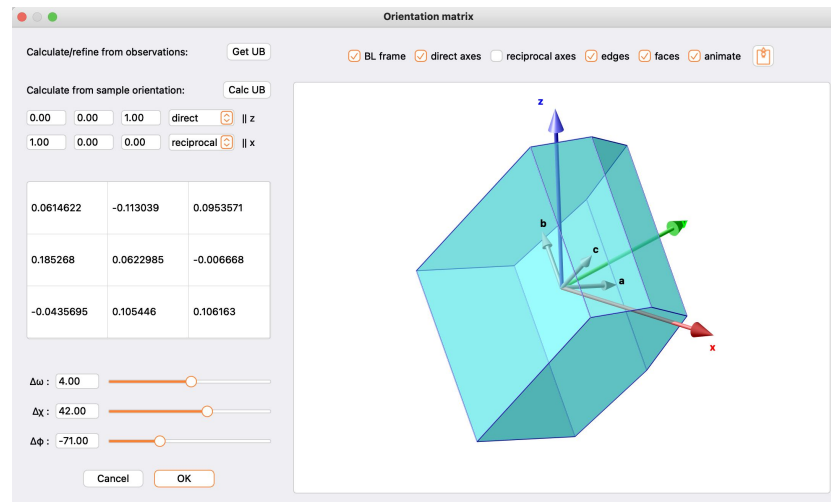
Figure 3.9: Orientation of the 3D sample model with respect to the Busing-Levy frame (colord axes). The instrument geometry definition is taken into account for the visualization.

tioning it for a particular Bragg reflection. In addition, the scattering vector, the incoming beam and the diffracted beam will be shown. This can only be achieved, when the UB matrices between the main window and the UB window are synchronized, i.e. the UB window was just opened without modifying the orientation matrix. Then, when calculating the angles and structure factors of a Bragg reflection $\mathbf{Q}$ in the main window, the sample will be positioned in the 3D plot of the UB window. If one wishes to see the final orientation only, the *animate* checkbox can be unchecked before clicking *Go!* in the main window.

3.9 Instrument

All instrument angle calculations are based on the definitions given in the *Geometry→Instrument* menu (Fig. 3.10). On the one hand it is necessary for calculating the vertical sample axes for a given (hkl) reflection for polarization matrix calculations, on the other hand it is needed by the absorption correction module in order to calculate the beam path lengths in the sample (see Sec. 4.2).

Five ILL single-crystal diffractometers (D3, D9, D10, D19, D23) can be selected from the

combo box and their axes definitions, angle rotation senses and standard angle limits will be automatically set. It is also possible to either change the definitions for another instrument or to choose a *Custom* instrument. The angle definitions are taken with respect to the conventions of Busing & Levy [18], i.e. the incident beam is directed along the positive y axis, z is the vertical axes and x completes the right-handed coordinate system. E.g. the definition *x: -x, y: +y, z: -z* means that the x axis according to Busing & Levy is actually the $-x$ axis according to the instrument's definition. In this example the reference frame is rotated by 180 degrees around the y axis. In case the instrument axes definition does not coincide with the Busing & Levy convention the instrument orientation matrix is internally transformed before the calculation of the diffractometer angles. The scattering geometry can be chosen between *normal beam* and *4 circle* as well as *Cryocradle* for D3. In 4-circle geometry the chi quadrant in which the instrument performs should be given, but is automatically set to the standard value for the ILL diffractometers. The calculated angles are converted back to the instrument's convention with respect to the rotation senses and whether the neutrons are diffracted to the left or to the right. The diffraction direction is taken in the reference frame of the neutron, i.e. standing at the source and looking towards the sample. The rotation sense of the angles θ, ω and ϕ (ϕ for $\chi=0$) are called clockwise or anticlockwise when viewed from the top. The sense of χ is defined for $\phi=0$ and looking towards the source. These definitions are shown as tooltips when hovering the mouse above the respective combo boxes. The angle limits are used in order to calculate the exact position of the sample in case the bisecting scattering geometry cannot be achieved and/or another chi quadrant has to be tried. Note that the offsets are not yet used.

Figure 3.10: Instrument axes and angles definitions used for the calculation for the sample orientation at a particular (hkl) reflection.

4 Fitting

The main purpose of MAG2POL is the refinement of a nuclear and/or magnetic structure model to different kinds of data sets: spherical neutron polarimetry data, flipping ratios, integrated intensities from a monochromatic single-crystal diffraction experiment and powder diffraction patterns. Correlated refinements can be done in any combination of the previously mentioned data types. After the structural data, the magnetic structure model, magnetic domains, scale factor and extinction parameters have been entered and the unit cell has been successfully generated and visualized, one can proceed to the refinement module by clicking *Fit→Fit* or the icon in the toolbar.

4.1 Loading raw data

The raw data are loaded in the *Data* tab using the respective buttons. In the present version of MAG2POL the accepted data types are

- D3 `*.fli` files containing the polarization values of the individual polarization matrix entries and/or the flipping ratios

- D3 raw data Numors

- FULLPROF `*.int` files containing (a) integrated intensities of integer reflections plus eventually two propagation vectors corresponding to $+\mathbf{q}$ and $-\mathbf{q}$ or (b) flipping ratios together with the beam polarization and the orientation matrix.

- `*.col` files as an output of a RACER integration [19] of two-dimensional detector data

- `*.fsq` files as an output of a COLL5 integration of single-detector data

- `*.sf` files as an output of a CCSL program

- `*.bra` files as an output of a D19 large-detector integration

- powder data in different formats (see below)

When data files have been successfully loaded a message will be displayed in case of polarized neutron data and a list will appear in the case of integrated intensities and powder patterns. By right-clicking on a list entry the wavelength, source and weight can be adjusted or the loaded data set can be deleted (note that the wavelength and source of powder patterns can be entered in the respective tab, which will be explained in Sec. 4.5). When loading `*.fli` files the program will detect if the data has been collected in polarimetry or flipping ratio geometry of D3 and will set the corresponding checkbox (*Refine on flipping ratios*) and disable the spin-filter related information eventually. In case of flipping ratio data the checkbox *Use multipole expansion* appears, which if set will add a multipole tab to the fit window. If flipping ratio data were loaded from a `*.fli` file the data reduction window will open, which will be explained in more detail below for integrated intensity data. The loaded data can be viewed by clicking on *View data*. Right-clicking on a vertical header opens a context menu, which permits to delete a single reflection (*Delete*) or all reflections of the same (*hkl*) values (*Delete all*). This is useful to remove nuclear reflections, which have been measured to calibrate the efficiency of the ^{3}He spin-filter cell, from a list of polarization matrices. Activating the checkbox *Refine nuclear structure* for any data type will add an *Atoms* tab containing the atomic positions, isotropic temperature factors and occupation factors as well as the scale and extinction factors. In the case of integrated intensities the checkbox *Purely magnetic scattering* should be checked, if the loaded data was obtained from a subtraction of a nuclear background.

When opening a `*.col`, `*.fsq`, `*.sf`, `*.bra` or a flipping ratio `*.fli` file a data reduction window will open (see Fig. 4.1), in which the user can merge the loaded data with respect to a given space group (at the beginning the space group from the main window is automatically set). The reflections will be shown regrouped and the R_{int} value will be printed together with reflection statistics (unique, symmetry inequivalent, forbidden reflections). The internal R value is calculated according to

$$R_{int} = \frac{\sum\limits_n I_n - \bar{I}}{\sum\limits_n I_n} \tag{4.1}$$

and the sum is taken over all n reflections without previously averaging repeated observations. Forbidden reflections can be excluded from the calculation. The reflection list is ordered by scattering angle by default, but it can be ordered with respect to h, k, l, I/R, dI/dR or 2θ by right-clicking on the corresponding horizontal header and by choosing either *ascending* or *descending* from the sort menu. A particular reflection can be searched by opening a find dialog using the *Ctrl/Cmd+Shift+F* shortcut. The (*hkl*) indices can by transformed by entering a transformation matrix in the upper-right part of the window

and then clicking *Apply*. Any further application of different transformation matrices will be applied to the original indices and the applied changes can be reverted by clicking the corresponding button.

The data can then be transfered to the fit window or be exported in a format corresponding to a FULLPROF `*.int` file (this is also possible for flipping ratio data). Furthermore, for integrated intensity data a second data set can be subtracted from the first one by clicking on *Subtract dataset*, which is useful for removing the nuclear contribution from $\mathbf{q} = 0$ reflections. If the second data set lacks reflections which are present in the first data set, there are two options: either ignore (delete) the corresponding reflection or treating the missing reflection as $I = 0$. The latter can be convenient, if a low-temperature magnetic data set contains (hkl) reflections which are forbidden and have not been measured in the high-temperature nuclear data set.
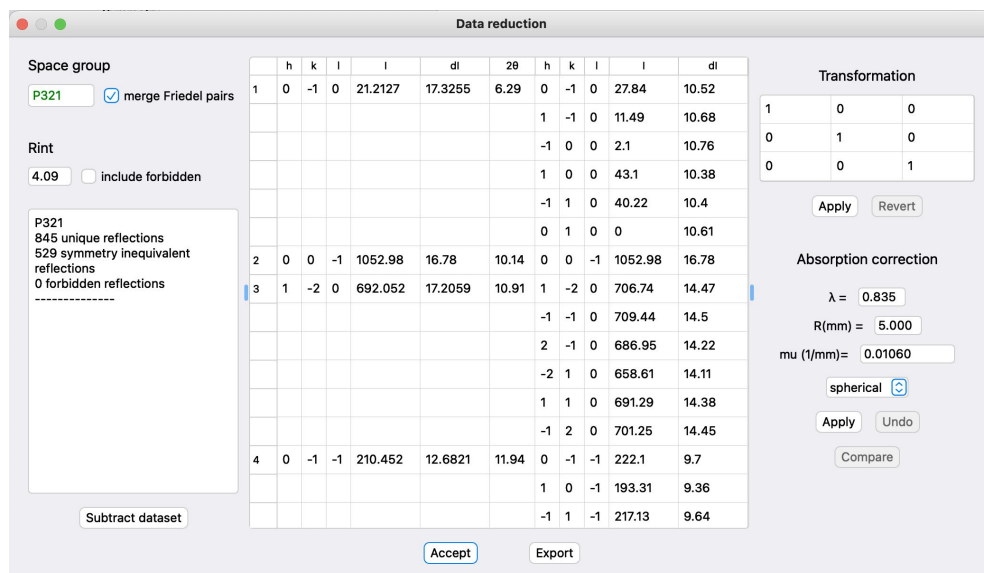
Figure 4.1: Data reduction window permitting to merge integrated intensities with respect to a given space group.

From within the data reduction window an absorption correction of integrated intensities can be applied for different sample shapes, see next chapter.

The integrated intensity data transferred from the data reduction window to the fit window as well as the data directly loaded from an `*.int` file will be shown as a list in the *Integrated intensities* section. A right-click on a data set offers different options in a context menu, e.g. deleting or replacing the data set. The *replace* option is useful if one wants to use the same structure including the scale factor for the refinement of another data set. Note that deleting a data set also deletes its corresponding scale factor. Other parameters which can be addressed from the context menu are the source, the wavelength and the weight of the

data set in the least-squares algorithm.

Before loading powder patterns the corresponding format of the file has to specified in the drop-down menu. The different options are

- MAG2POL format. It consists of a header with title, wavelengths, ratio and temperatures followed by the data in values of 2θ, counts and sigmas. Powder patterns in other formats can be exported in this format by clicking on *Save data* after successful opening.

- XYSIGMA corresponding to FULLPROF INS = 10

- D1A, D2B corresponding to FULLPROF INS = 6

- D1B, D20 corresponding to FULLPROF INS = 3

- FREE FORMAT corresponding to FULLPROF INS = 0

- DMC, HRPT corresponding to FULLPROF INS = 8

- GSAS TOF corresponding to FULLPROF INS = 12

- ISIS TOF corresponding to FULLPROF INS = 14

When a wrong format was specified an error message will be shown, otherwise, after successful opening a *Patterns* tab will appear in the tab widget in which the loaded data can be viewed and analyzed (see Sec. 4.5). A successfully opened diffraction pattern of any format can be exported into MAG2POL format with `*.m2p` extension. The data is stored in three columns - 2θ, counts and σ - and is preceded by a header containing the lines `TITLE`, `WAVE`, `TEMP`, `COMP` (composition parameter x, e.g. in A_xB_{1-x}) and the corresponding metadata. Further lines might be added in future versions while obviously maintaining compatibility. A pattern is exported by selecting it in the table of loaded patterns and clicking *Save data*. Input dialogs will pop up in which the metadata can be entered. As for integrated intensity data, a right click on the data set evokes a context menu with the possibility to delete or replace the data set as well as to change the weight in the least-squares algorithm.

4.2 Absorption correction

4.2.1 Simple sample shapes

An absorption correction can be applied for spherical sample shapes and cylindrical sample shapes with normal-beam geometry, which is based on [20]. The linear absorption

coefficient is automatically calculated based on the structure model and displayed in the according box, but of course, one is free to enter whatever value. The calculation is done according to:

$$\mu = \frac{\sum\limits_{i} o_i(\sigma_{i,a} \cdot \lambda / 1.798197 \text{ Å} + \sigma_{i,inc})}{V} \tag{4.2}$$

where the sum is done over the atoms i of the unit cell with volume V. o_i is the occupation, $\sigma_{i,a}$ is the absorption cross section (at $\lambda = 1.798197$ Å) and $\sigma_{i,inc}$ is the incoherent scattering cross section of atom i. The incoherent scattering cross section is wavelength independent for most elements, with a notable exception being hydrogen for which it is given by

$$\sigma_{H,inc} = 19.2 \cdot \lambda + 20.6 \tag{4.3}$$

with λ given in Å resulting in $\sigma_{H,inc}$ in barns [21].

After setting the radius of the sample in mm one only needs to click *Apply* to perform the absorption correction. The internal R value will directly be recalculated. The corrected, uncorrected and normalized uncorrected data can be verified under *Compare*. The button *Undo* permits to remove the applied correction.

4.2.2 Special sample shape

Mag2Pol offers the possibility to index the bounding faces of a convex crystal shape based on a sequence of picture frames which can be loaded into the program (note that a crystal model can be set up *blindly* even without such frames, see hints below). This is done within an interactive OpenGL widget, which can be opened by selecting the *special* sample shape and clicking *Set faces*. When first opened the crystal model utility should show a red crosshair on a white or black background (for dark mode off/on, respectively). Depending on the platform (as seen for Linux and Windows) borders in a different color can be present, which should be removed by right-clicking witin the widget and selecting Adjust size (furthermore Linux and Windows machines display a wrong aspect ratio of the frames which is not a problem for the following treatment). The program assumes that the picture frames are taken during a successive rotation of the sample around the φ axis for 4-circle geometries or around the ω axis for normal-beam geometries. For the first, it is necesssary to indicate the χ value at which the frames have been taken. Before opening the picture files the lower and upper angles spanned by the rotation should be entered in the corresponding boxes. When selecting the files in the file browser, they should be ordered according to angles with the first file selected corresponding to the lower angle. Since the camera position and rotation can be general, it should be stated to which diffractometer axes the right and up directions of the OpenGL widget refer to. The file names and camera parameters will automatically be saved in a `crystalFrames.info` file which

can conveniently be chosen for the next time. The diffractometer axes should be given according to the convention of Busing & Levy, i.e. the incoming beam is along the positive y axis and the z axis is vertical, x completes the righthanded set. The orientation matrix will internally be transformed according to the instrument's definition (see Sec. 3.9). On the ILL instruments the camera is mounted on the omega table and is pointing upwards. With the neutrons entering from the top part of the taken picture the correct settings for this geometry are those which are loaded by default, i.e. right $= +x$, up $= -y$. The frames are then taken by rotating around the φ axis with $\chi = 90°$ and the sense of rotation is calculated based on the instrument's definition.

Camera and sample offsets can be set in the *Offsets* tab on the right. x sample offsets should be set, when a picture close to $\varphi = 0$ is viewed, while y sample offsets can be seen for $\varphi \approx 90$. The buttons for ± 90 or ± 180 rotations can be used for finding the offsets conveniently. A z sample offset concerns the height along the sample pin. The camera offsets refer to the lateral misalignment of the camera and its rotation around the z axis. The goal is to have the crystal's center of mass in the center of the crosshair. In the *View* tab it is important to set the zoom factor so that the radius of the crosshair (in mm) corresponds roughly to the real crystal dimensions.

The frames can be viewed by dragging the horizontal slider below the OPENGL widget or by using the buttons below it. The play speed can be adjusted and the loop checkbox can be set, if you want to see a continuous rotation.

In order to add a plane to the crystal model, one has to rotate the crystal to a position in which the face is parallel to the view direction. In this position simply click and drag a line along the edge, which will add a plane (converted to *hkl*) to the table. The length of the line is not very important and only serves for drawing unbound planes as a square having the edge length according to the drawn line. By adding more planes in different sample positions the program will redraw the bound volume and show the model on top of the picture. Note that it is of course possible to draw a sample model without having loaded any frames. In that case, it is recommended to change the plane color under the *View* tab to a different color than the background. First, one should draw e.g. four lines in the shape of a square around the crosshair, then move the φ slider by $+90°$ or $-90°$ and draw two horizontal lines above and below the center position, which should create a closed volume.

In order to highlight a plane simply click on it in the table or in the model. When a parameter in the table is highlighted, it can be adjusted using the horizontal slider or a

new value can be entered directly. The crystal model will be updated instantaneously. If a plane is actually needed to draw the smallest possible volume will be shown with a *yes* or *no* in the last column of the table. Planes can be removed by right-clicking the vertical header and selecting *Delete*. Multiple planes can be deleted simultaneously. For very irregularly shaped crystals it may be more intuitive to uncheck the *Hide planes behind picture* option in the *View* tab. An example of a complex crystal shape is shown in Fig. 4.2 and a tutorial video can be seen here. By clicking *OK* the created planes will
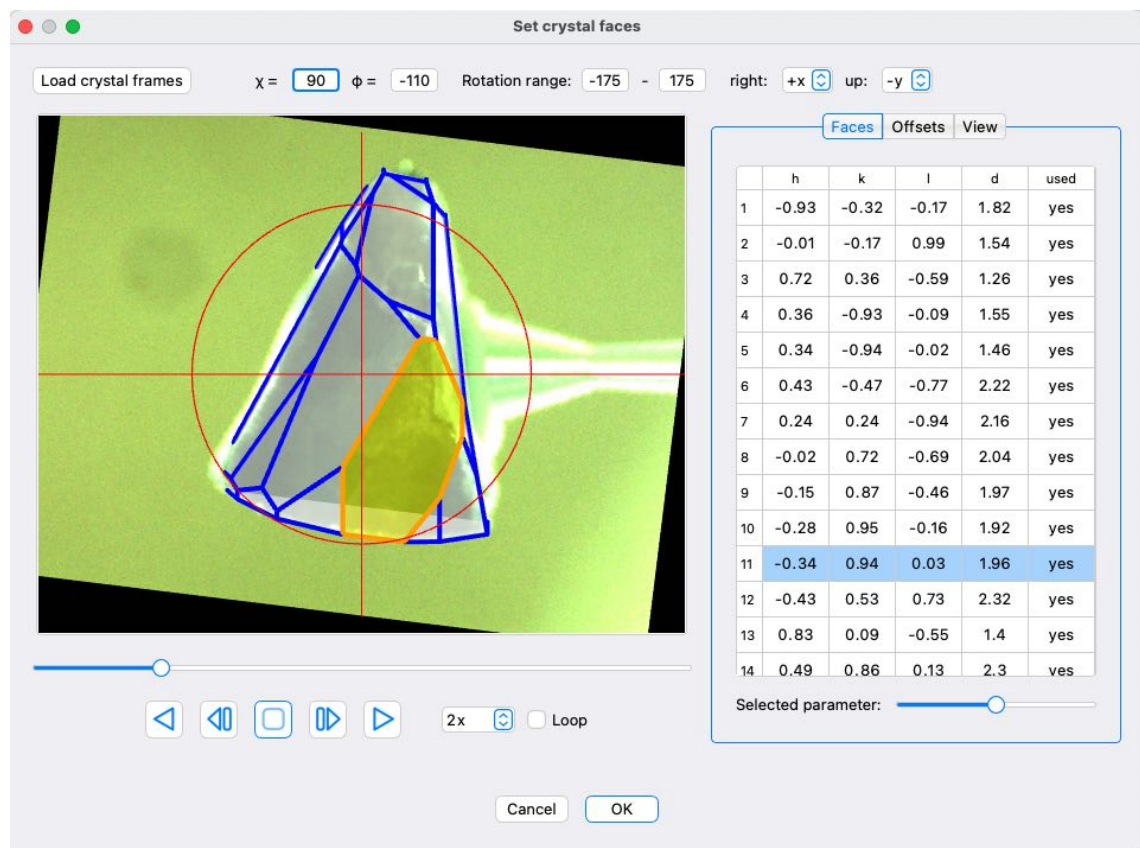
Figure 4.2: Complex crystal shape containing 19 limiting faces.

be transfered to the Data reduction window. Note that the planes are only saved when at least 4 used planes are present. Unused planes are not saved. Mag2Pol will automatically calculate the corresponding diffractometer angles for every measured reflection based on the instrument definition and will determine if a non-zero ψ angle or a different χ quadrant was necessary to measure a particular reflection. Furthermore, the number of integration samples should be given along the a, b and c axes of the sample by clicking on *Set grid*. The grid points will be distributed according to the Gaussian integration procedure described in [22].

Once all the necessary information are entered, the absorption correction is done like for simple sample shapes by clicking the *Apply* button. By clicking on any *hkl* index in the table the orientation of the crystal model and the integration points are shown together with the diffractometer axes and the incoming/outgoing neutron beams (see Fig. 4.3). The planes of the model which are intersected when diffracting from the origin are marked by orange edges. The diffractometer angles are shown below the OPENGL widget together with the average path lengths along the incoming (r_1) and outgoing beam (r_2). The average transmission T is approximated by a Gaussian integration [22] according to

$$
\begin{aligned}
T &= \int\limits_V \frac{1}{V} \exp[-\mu(r_1 + r_2)]dV \\
&\approx \sum_{i=1}^{n_x} \sum_{j=1}^{n_y} \sum_{k=1}^{n_z} (b-a)[d(x_i) - c(x_i)][f(x_i, y_j) - e(x_i, y_j)]R_i R_j R_k 1/V \exp[-\mu(r_1 + r_2)],
\end{aligned}
$$

(4.4)

where the a, b, c, d, e, f are the corresponding limits of integrations and the R_i, R_j, R_k are the respective weights which are taken from [23]. The visualization of the scattering geometry is animated by default, i.e. the successive rotation of angles will be shown. By unchecking *animate* the final diffraction position will be shown immediately. For a more fluid rendering the grid points can be omitted in the rendering process. The absorption
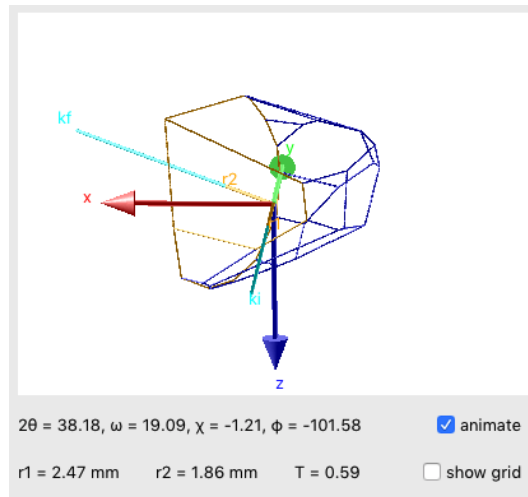

Figure 4.3: Orientation of the sample for a given (*hkl*) reflection within the Busing-Levy frame (colored axes). The diffractometer angles are give together with the average beam paths inside the sample and the transmission factor.

correction in MAG2POL has been compared to the subroutine AVEXAR of the CCSL

subroutine library for normal beam and 4-circle geometries. The results are identical within rounding errors starting from $n_x = n_y = n_z = 3$ as can be seen in Fig. 4.4.
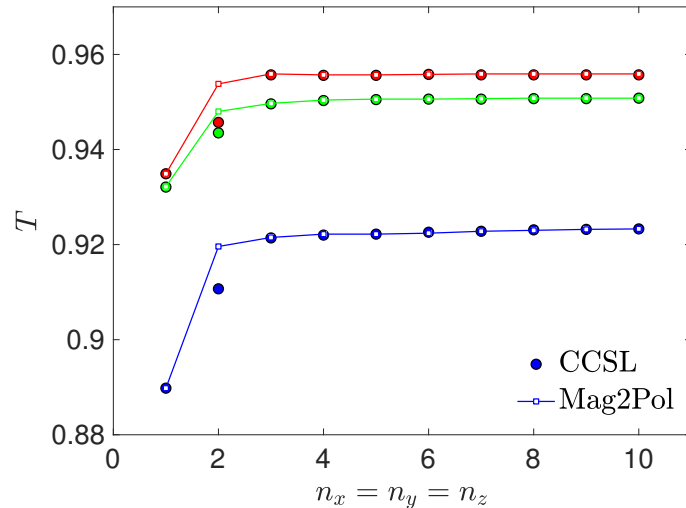

Figure 4.4: Transmission as a function of integration points $n_x = n_y = n_z$ for three different Bragg reflections calculated by MAG2POL and CCSL.

4.2.3 On-the-fly absorption correction

The absorption correction mentioned in the section above can be applied to correct the dataset of integrated intensities which was opened in the data reduction window. In that case the correction factors are applied to each measured (hkl) reflection before an eventual merging with respect to the given space group. The corrected data can directly be used in the analysis or they can be exported into an `*.int` file.

It is also possible to use the convex-hull crystal model to do an *on-the-fly* absorption correction, which is useful if one wants to refine the occupation of a heavy absorber as it influences both the absorption through the linear absorption coefficient and the scattering potential through the scattering length (e.g. incomplete ^{11}B or ^{160}Gd substitution). This possibility allows for a self-consistent analysis of the data. In order to activate this feature a crystal model needs to be present before entering the fit window, which can be done by opening the *Sample info* window (see Sec. 6.1) and clicking *Edit* under the *Absorption* tab. In that case, when the fit window is entered the option *On-the-fly absorption correction* becomes visible below the loaded integrated intensity data. When it is activiated the program will calculate the neutron beam path lengths for all the reflections only once before starting the refinement iterations. In each iteration the linear absorption coefficient may be different, if the atomic occupations are refined parameters. Note that the use of this feature is even possible for multiple integrated intensity files as long as the data were

recorded in the same instrument geometry (e.g. different wavelengths).

If the occupation of a heavy absorber is uncertain and needs to be refined, the recommended procedure is the following:

In a first step, the integrated intensities should be reduced in $P1$ or P-1 symmetry (the beam path lengths are identical for Friedel pairs, however, small deviations may be possible in the calculation due to precision errors) and loaded as an `*.int` file for the refinement. After activating the *on-the-fly absorption correction* check box, the nuclear structure refinement can be done as usual.

In a second step, the refined nuclear structure from the first step should be used to apply the absorption correction on the raw data which are then eventually merged and exported (as explained in Sec. 4.2.2). The last step consists in refining the nuclear structure to the corrected and merged data set of step 2 (without the *on-the-fly* option), which should give similar results as in the first step, but with better agreement factors due to a reduced number of observations (due to the merging of equivalent reflections).

4.3 Correction for the spin-filter efficiency

Usually the efficiency of the ^{3}He spin-filter cell is monitored by measuring e.g. the polarization P_{zz} on a purely nuclear Bragg peak - which is known to be 1 - several times a day during the experiment. The reduction from the expected value is due to the initial polarization of the neutron beam (which can be set in the *Settings* menu) and the spin-filter efficiency. In the case of a loaded `*.fli` file the program analyzes the lines which signal a cell change and the time of the respective observations to show the decrease of efficiency as a function of hours. On D3 depending on the used cell the decay is usually between 10 and 20% per day. The reflection on which the calibration has been performed throughout the experiment and the polarization canal has to be selected followed by clicking *Apply*. The polarization data will now be corrected with respect to the decaying spin-filter efficiency according to

$$P_{corr} = P_{mes} \cdot \frac{P_0}{P_{cell}} \tag{4.5}$$

and repeated reflections will be merged (P_0 is the polarization of the incident neutron beam, note that setting this value to 1 in the settings of the program will correct the data also for the initial polarization). A more precise merging is possible, if the respective raw data Numors are put in the same folder as the `*.fli` file. Like this the individual counts (background - peak - background) can be summed up and weighted by the respective counting times. Otherwise, a weighted average will be calculated from the standard deviations given in the `*.fli` file. In order to interpolate the spin-filter efficiency for any

given time an exponential decay function of the form

$$P(t) = \tanh[O \cdot P_{0,He} \cdot \exp(-t/T_{1/2})] \tag{4.6}$$

is used, where $O = \lambda \cdot l \cdot p \cdot 7.282 \cdot 10^{-2}$ is the cell opacity at room temperature. The wavelength and the cell pressure p are fixed, while the halflife $T_{1/2}$ and the initial polarization of the cell $P_{0,He}$ are refined. The results can be seen by clicking on *View cell efficiency*, which opens a window similar to the one shown in Fig. 4.5. The different cells recognized
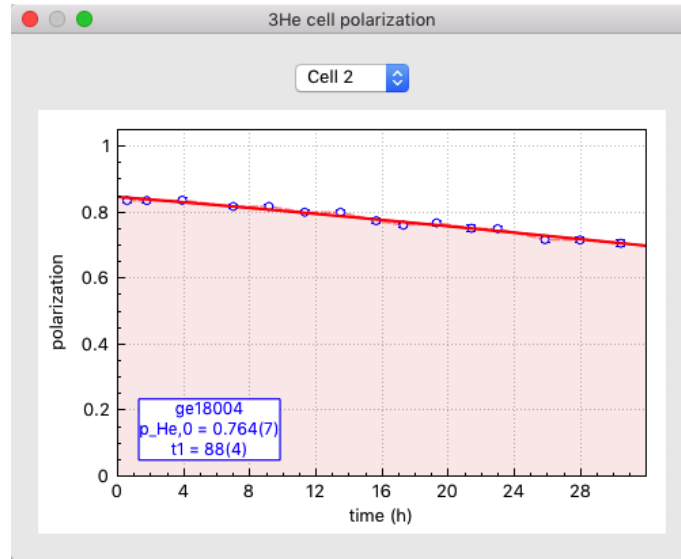
Figure 4.5: Visualization of the spin-filter efficiency decay as a function of time.

from the entries in the `*.fli` file can be chosen from the combo box. The legend shows the name of the cell as well as the refined values including standard deviations for the initial cell polarization and the halflife.

The corrected data can be saved from the fit window in order not to repeat this procedure.

Note that when chiral or nuclear-magnetic interference scattering is present, the polarization data should only be corrected to the spin-filter efficiency and not to the initial polarization (i.e. the P_0 value of the incident beam needs to be entered in the Mag2Pol settings) as the respective entries contain terms which are dependent on the initial neutron polarization and terms which are not. In order to analyze the raw data the checkbox *Refine on uncorrected data using cell efficiency* should be activated before you hit the button *Apply*. The program will still take into account the cell efficiency at a given time of an observation, but it will be used in combination with the initial neutron polarization to calculate the respective entry of the polarization matrix. In this case no merging of reflections is possible.

Loading Numors directly is intended for a special type of measurement, where the initial neutron spin is rotated within the local y-z plane. The positions and amplitudes of the minima and maxima allow important conclusions concerning the magnetic structure. In this case the polarization value (including the time of the observation) as well as the directions of the initial neutron polarization and analysis vector are extracted from the Numor files. As no information is present concerning any potential spin-filter cell changes only those data should be loaded which have been measured with the same cell. The correction with respect to the cell efficiency is done as described above (note that for a final polarization vector within the y-z plane no chiral scattering is present).

4.4 Refinement flags and constraints

All the magnetic ions defined within the magnetic structure will be listed in the same order under the *Magnetic moments* tab as M1, M2, ... The magnetic domains are shown under the *Domains* tab together with their corresponding symmetry, an eventual keyword signalling an inversion or chiral domain and their population. In the case of a multipole refinement on flipping ratio data, the coefficients C_l^m and the Slater coefficient Z are refinable parameters as well. By activating the checkbox next to a respective value, this parameter will be considered as a refined variable. Nuclear structure parameters can be refined, when the checkbox *Refine nuclear structure* is activated in the *Data* tab, which will insert a new tab called *Atoms* including the positions, thermal and occupational parameters, scale factor and extinction coefficients. Anisotropic displacement parameters can be flagged by chosing the *set betas* context menu entry after right-clicking an isotropic temperature factor. Constrained B_{ij} values and fit flags are disabled if they are constrained by symmetry.

Linear constraints can be set under the *Constraints* tab by chosing the variables and relations from the combo boxes and entering the proportionality factors and summands by hand. M1 refers to the whole vector of magnetic moment 1, |M1| refers to the modulus of the moment, whereas Mr1 and Mi1 would denote the real and imaginary part, respectively (note that vector quantities can only be constrained to other vector quantities and that a moment modulus can only be constrained to another moment modulus). In the case of non-zero real and imaginary components, MAG2POL will constrain Mr and Mi to be perpendicular, if they are not defined as parallel. If the real components are refined, the imaginary vector will be adjusted and vice versa. If both real and imaginary components are refined, the imaginary vector will be adjusted after each iteration.
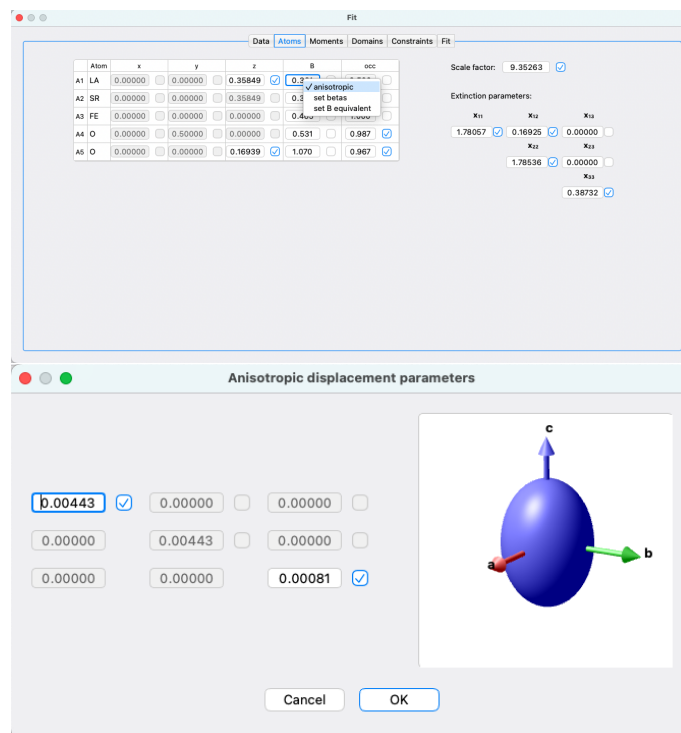
Figure 4.6: Anisotropic displacement parameters and the visualization of thermal ellipsoids.

The constraints take the form of

$$p_1 = a \cdot p_2 + b \tag{4.7}$$

where p_1 depends on p_2. If you choose the equal sign, the parameter p_1 is regarded as a constant (in relation to parameter p_2) and should therefore not be refined. For relations 'greater than' or 'smaller than' the constrained parameter p_1 should be marked as a refined parameter. If the multiplication factor a is 0, then p_2 is a dummy parameter which is not necessarily refined and p_1 is directly related to the scalar b. If $|a| > 0$, then p_2 needs to be set as a refined parameter as well (note that errors will be shown as pop-up warnings). The keyword *various* for parameter p_1 can be used to define multiple constraints. By choosing *various* a button will appear to the right which permits to select various parameters from a list which will be constrained to p_2 (see Fig. 4.7).

In the present version of MAG2POL up to 20 constraints can be set. In case of multiple magnetic domains or structural twins, the population of the first domain/twin is automically set to 1 minus the rest in each iteration. Constraints can be deleted by right-clicking the parameter to be constrained and then clicking *Delete*.
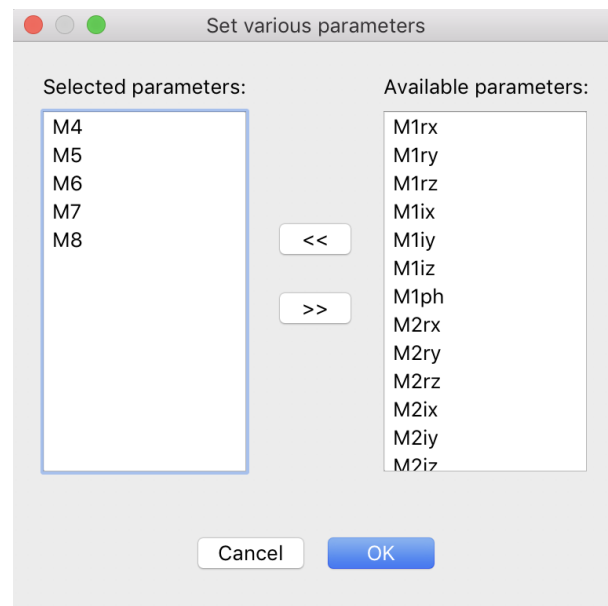
Figure 4.7: Multiple parameters can be selected after choosing *various*.

Note that constraints on atomic positions due to special Wyckoff sites, e.g. $(x \ x + \frac{1}{2} \ z)$ or $(x \ 2x \ \frac{1}{2})$, do not need to be set by the user, because MAG2POL will consider them automatically. The same applies to anisotropic temperature factors of atoms on special sites.

Simple constraints, i.e. of the form $p_1 = p_2$, can directly be set in the *Atoms*, *Moments* and *Domains* tabs by right-clicking the respective label and evoking context menus as shown in Fig. 4.8. Note that the parameter to which one wishes to constrain needs to be placed higher in the atom/moment/domain/twin list or it needs to be in a phase with lower index. E.g. the position of atom 3 in phase 2 can be constrained to atom 2 of the same phase or to atom 4 of phase 1. Parameters being lower in the list are automatically grayed out in the context menu.

In the case of atoms the parameters which can be constrained are

- position: x, y and z fractional coordinates

- B: isotropic temperature factor

- anisotropic B: all anisotropic displacement parameters

- occupation: the occupation factor

- all atomic parameters: all of the above

If the parameter in questions is a magnetic atom, the options are

- moment: all real and imaginary components

- moment modulus: the modulus of the moment

- real part: the parameters belonging to the real part of the complex magnetic moment

- real part modulus: the modulus of the real part of the complex magnetic moment

- imaginary part: the parameters belonging to the imaginary part of the complex magnetic moment

- imaginary part modulus: the modulus of the imaginary part of the complex magnetic moment

- phase: the magnetic phase

- all magnetic parameters: all real and imaginary components as well as the magnetic phase

In the case of domains and twins the population can be constrained to any other domain/twin population with a lower index similarly to what was explained above concerning atomic sites. Note that constraining a domain (twin) population to the first domain (twin) population equally distributes the remainder of the other domain (twin) populations to 1 (i.e. 1 minus the rest) on the constrained domains (twins), which is not supported when

using constraints under the *Constraints* tab. Setting a constraint in this way will disable the manual editing of the corresponding parameters and fit flags. In order to quickly find to which parameter a constraint is set, the corresponding menu fonts are set in italic. A constraint can be removed by unchecking it. Some constraint combinations will be automatically summarized as a different one, e.g. if the imaginary part of a magnetic moment is constrained after the real part was already constrained, then the constraint will be found under *Constrain moment*.

Changing a parameter will automatically update the parameter(s) which is/are constrained to it (both for constraints under the corresponding tab as well as for simple constrained which are set via context menues).
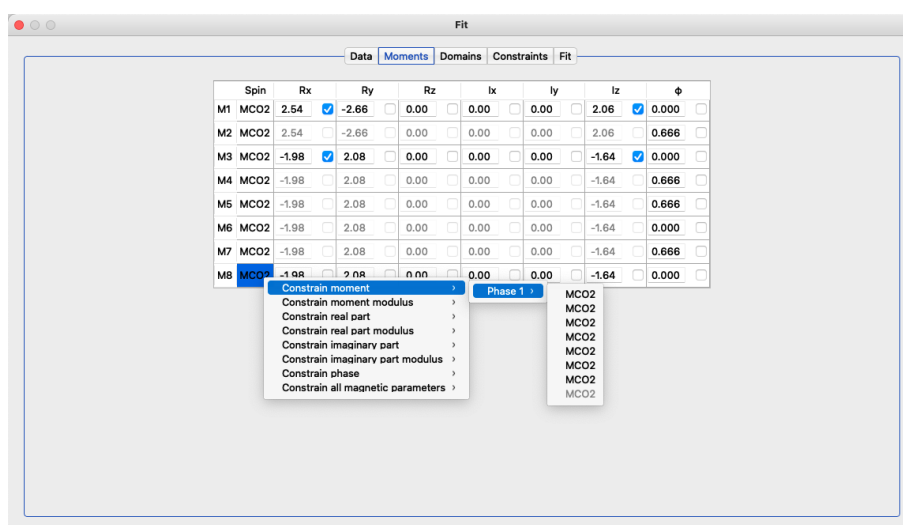
Figure 4.8: Simple constraints can conveniently be set using context menues.

4.5 Powder patterns

When at least one powder pattern has been loaded, the *Patterns* tab appears which is shown in Fig. 4.9. The left part of the tab features the pattern plot with the corresponding plot controls above it, while the scroll area on the right side contains all necessary parameters and fit flags separated into different categories. The category labels, e.g. *Geometry*, *Background*, etc., contain further options which can be evoked by right-clicking the label which opens a context menu. The context menu generally contains a list of loaded patterns and contributing phases in order to set constraints between them (see Sec. 4.5.6). Further options of certain categories are explained below. Note that the parameters depend on the type of data loaded, i.e. if it was taken on a constant-wavelength or a time-of-flight diffractometer.
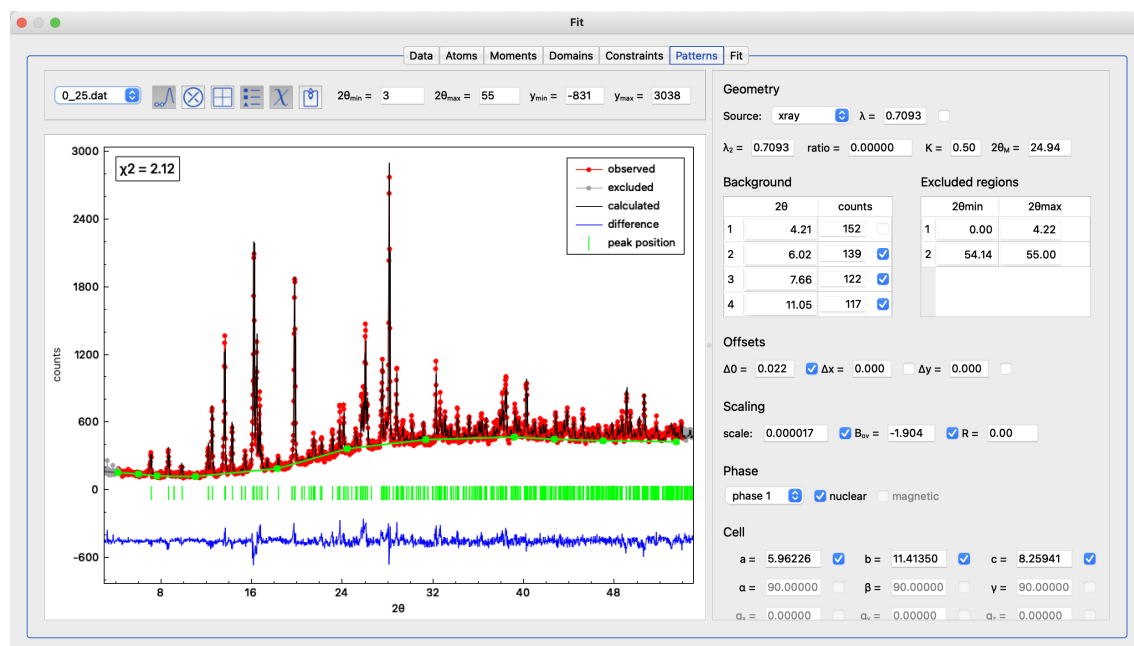
Figure 4.9: Pattern tab within the Fit window in which all parameters can be set which are necessary for the Rietveld refinement.

4.5.1 Plot controls

The plot always shows the observed data points in red, the calculated pattern in black and the difference between the two in blue. Furthermore, the positions of nuclear and magnetic Bragg reflections calculated from the underlying model(s) are shown as green markers between the data and the difference curve. Like in other 2D plots hovering the mouse over data points shows the respective coordinates, while hovering over the peak markers reveals the scattering angle (or time of flight), the Miller indices and the multiplicity of the Bragg reflection. When more than one pattern file was loaded, one can switch between them by choosing from the combo box in the upper-left corner. The two buttons to the right of the combo box toggle the background and excluded regions mode which will be explained in Secs. 4.5.3 and 4.5.4. The next 3 buttons toggle the plot grid, the legend and the χ^2 value on the plot, whereas the last button exports the plot into either a `pdf` or an `ASCII` file taking into account the actual zoom (note that for the `ASCII` output the excluded angles and peak markers are labelled with an asterisk). The plot boundaries for the 2θ and counts axes can be set further to the right. Those boundaries will also be used for the plot in the *Fit* tab. They can be reset to the optimal values by right-clicking on any of the 4 values and then clicking *reset boundaries.*

4.5.2 Geometry

The *Geometry* section concerns the basic information of the used instrument like the source (neutron or x-ray) and the wavelength. Note that constant-wavelength (CW) and time-of-flight (TOF) instruments in Debye-Scherrer geometry are currently supported in MAG2POL. For CW patterns the $\lambda/2$ contamination or the $K\alpha_2$ line can be entered in the λ_2 field with the corresponding intensity ratio between λ_1 and λ_2. When *x-ray* is selected, a right-click on the λ_1 value allows the selection between different frequently used x-ray $K\alpha_{1,2}$ lines. The values K and $2\theta_M$ are only needed in the x-ray case in order to calculate the monochromator polarisation within the Lorentz factor (see Sec. 7.7.1). For TOF patterns the detector bank angle $2\theta_B$ has to be given. From the *Geometry* context menu the instrument configuration of different ILL and ISIS instruments can be loaded, which include the wavelength, the resolution, the peak shape and asymmetry parameters for constant-wavelength diffractometers as well as time-of-flight, detetor bank, rise and decay and peak shape parameters for TOF. This is a convenient way of setting up a starting point of the refinement, see Fig. 4.10.
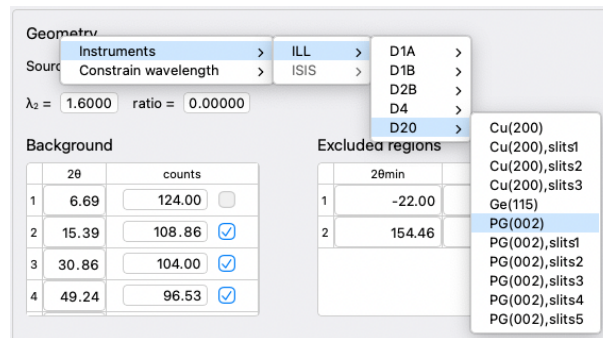
Figure 4.10: Selection of predefined instrument configurations.

4.5.3 Background

There are different ways to introduce the background of a powder pattern. The first is to give a list of points between which a linear interpolation is calculated. In order to do so the background mode needs to be activated by clicking on the first button next to the pattern file name. If a background is already defined it will be shown as green squares connected by green lines (see e.g. Fig. 4.9). A background point is simply added by left-clicking on the pattern. A green square will be added to the plot and the corresponding 2θ value and counts will be added to the table on the right. An already drawn point can be moved by placing the mouse over it which will turn the mouse cursor into an open hand symbol. Now simply click and drag the background point to the desired position. The coordinates

of each point can also be modified by directly editing them in the table. A background point can be deleted by right-clicking it. The pattern will be calculated using the newly defined background after leaving the background mode, i.e. by clicking the corresponding button.

The background can also be modeled with a polynomial function of different degrees or with a Debye-like model (see Sec. 7.7.1.7 for more information). In order to change the background type, simply right-click the *Background* label in the scroll area and select one of the diffent models, see Fig. 4.11. Note that when you select *polynomial (6 coeffs)* and you have manually introduced points before, the program will fit the coefficients (if they are all equal to 0) to the linear interpolation as a convenient starting point. From there you can eventually choose one of the two more complex models.
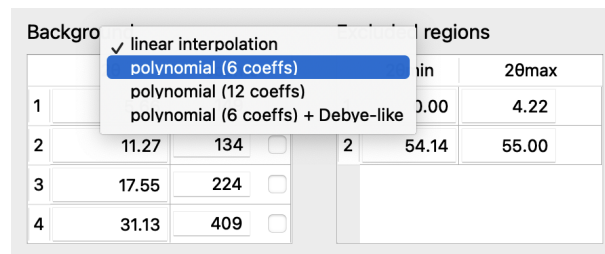
Figure 4.11: Selection of different background models.

4.5.4 Excluded regions

All regions of the powder pattern which cannot be explained by the underlying model(s), e.g. direct beam, negative intensities, zero sigmas, parasitic peaks etc., should be excluded from the refinement and from the calculation of agreement factors. In order to do so one has to activate the excluded region mode by clicking the second icon next to the pattern file name. Now, exluded regions can be drawn by left-clicking and draggin which will create a gray box (note that zooming is disabled when excluded region mode is activated). Already drawn excluded regions can be modified by placing the moue over one of the limits which will change the mouse cursor into horizontal arrows. The lower/upper limit can now be dragged. The excluded regions can also be modified in the table on the right. An excluded region can be deleted by right-clicking it in the pattern plot. Note that depending on the chosen option in the settings menu the pattern is nevertheless calculated in these regions, but not included in the calculation of χ^2.

4.5.5 Pattern and phase parameters

In order to allow the correlated refinement of powder patterns and single-crystal data at different temperatures, the overall temperature factor B_{ov} has a special function. If it is set to 0 and is not refined, then the temperature factors listed in the *Atoms* tab will also be used for this particular powder pattern. If a non-zero value is entered for B_{ov} or if it is flagged as a refined parameter, only the B_{ov} value will be used in the powder pattern, while the B values in the *Atoms* tab are applied to the single-crystal data. Like this it is also possible to use anisotropic temperature displacement factors for single-crystal data sets, while using an overall isotropic temperature factor for the powder data at the same time.

The remaining parameters grouped in the *Offsets/Time of flight* and *Scaling* categories are explained in Secs. 7.7.1 and 7.7.1.6.

More than one phase can contribute to a single pattern and in that case multiple phases have to be set up in the main window (see Sec. 2.2). The parameters which are grouped in *Cell*, *Profile*, *Asymmetry/Rise and decay*, *Preferred orientation* and *Absorption and extinction* (only for TOF) concern a specific phase in a specific pattern. The pattern can be specified - as explained above - by choosing from the combo box in the upper-left part of the tab. The phase can be chosen in the *Phase* category. Furthermore, it can be defined if the phase has a nuclear contribution, a magnetic contribution or both. Having different sets of parameters for the same phase, which contributes to different patterns, allows for example the co-refinement of two patterns at two very different temperatures resulting in different lattice constants. The only part which is common to all patterns (and other types of data of the same phase) are the parameters listed under the *Atoms* and *Moments* tabs (except for the temperature factors if $B_{ov} > 0$ in the powder pattern). Therefore, one has to keep in mind that co-refining different data sets is only meaningful if one can assume that the fractional atomic parameters do not change too much. Note that the information given in the *Domains* tab is ignored for the calculation of powder patterns, i.e. only a single twin with a single magnetic domain is considered. If different phases with different cell metrics contribute to the powder pattern, the option *Ignore secondary phases for single crystal* needs to be checked in the settings menu, if a co-refinement with single-crystal data is intended. Otherwise, the contribution of secondary phases will be considered to the (hkl) reflections of the main phase, which is not correct.

Note that after accepting a fit result (click on the *Accept* button) the lattice constants and the propagation vector(s) are not automatically transferred to the model(s) in the main window as those values are in principle used in the reduction and refinement of single-crystal data (the cell and **q** are of course saved in the powder model). One can however transfer these parameters between the main window and the models for powder patterns

by right-clicking the label *Cell* or *Propagation vector q* (in the *Symmetry* and *Spins* tab of the main window) and choosing the corresponding option and pattern number.

4.5.6 Constraints

If one can safely assume that the same structural model contributes to different patterns, e.g. a neutron and an x-ray pattern taken at the same temperature or two neutron patterns taken with different wavelengths, then constraints should be set. In such a case it would be a good idea to constrain the cell parameters. Or if two phases contribute to the same pattern and one can exclude peak broadening due to strain, then the profile parameters could be constrained. Constraints can conveniently be set by right-clicking the respective category label and then choosing the pattern and phase to which the parameters should be constrained (in analogy to simple constraints described in Sec. 4.4). The example in Fig. 4.12 shows how the cell parameters of phase 1 in pattern 2 are constrained to the cell parameters of phase 1 (i.e. the same phase) in pattern 1. After setting a constraint the corresponding values are directly synchronized and the fit flags (in this case of phase 1 in pattern 2) are disabled. It is not necessary to constrain the profile and asymmetry parameters of the magnetic contribution to the nuclear contribution, since all magnetic parameters are Δ values, i.e. they are added to their nuclear counterparts. In other words, if a magnetic Δ parameter is 0, it is automatically constrained to the nuclear parameter.
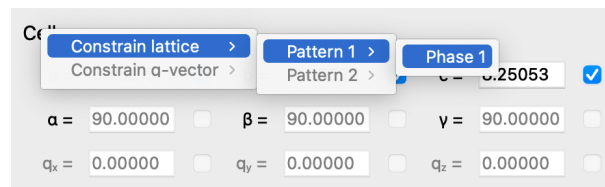
Figure 4.12: Example of how the cell parameters of one phase can be constrained to be the same in two different patterns.

4.6 Refinement and results

Once the data are loaded and the refinement flags and constraints are set, one can proceed to the *Fit* tab. Here one can control how the eventual co-refinement should be weighted. This is visualized by a weight triangle in which a draggable dot marks the different weights in trilinear coordinates (see Fig. 4.13). The weights of the respective data sets sum to 1 and are shown on the left of the triangle where they can also be set manually. If only one type of data was loaded, then the dot is fixed in one of the three corners. If two types are loaded, the user can drag the dot on one of the three lines of the triangle. And when all

three data types were loaded, the dot can be dragged everywhere within the triangle. For convieniency the dot snaps to the center of the triangle and to the bisections.
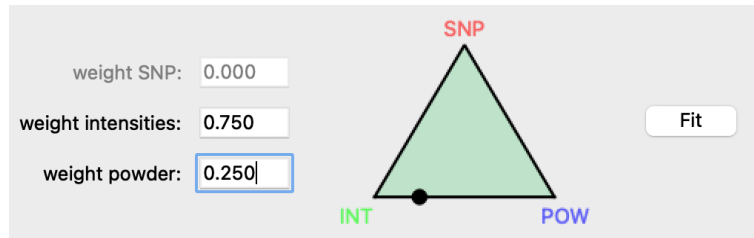
Figure 4.13: The weight triangle is a graphical way to set the respective weights of the data sets. When 2 (3) different types of data were loaded the dot can be dragged within a line (within the whole triangle). When only a single data type is present, the dot stays in the respective corner. The weights can also be set in the respective boxes, which are synchronized with the triangle.

The least-squares refinement will therefore minimize

$$\chi^2 = w_{SNP} \cdot \chi^2_{SNP} + w_{INT} \cdot \chi^2_{INT} + w_{POW} \cdot \chi^2_{POW} \tag{4.8}$$

where χ^2_{SNP}, χ^2_{INT} and χ^2_{POW} are the respective χ^2 values of the polarimetry, integrated intensities and powder data, respectively. Note that the weight given for intensity and powder data is further split if multiple data sets exist for which the individual weights can be set in the *Data* tab. The convergence criterium ϵ can be set in the *Settings* of the program and it refers to the maximum relative shift of a parameter in an iteration divided by its standard deviation. The refinement stops when

$$\Delta(p)/\sigma(p) < \epsilon \tag{4.9}$$

where $\Delta(p)/\sigma(p)$ represents the maximum value in an iteration for parameter p. Also the maximum number of iterations can be set.

The refinement can be started by clicking the *Fit* button and the progress as well as the results are shown in the text field to the left. For every iteration the χ^2 value will be printed together with the maximum relative parameter shift. Either when the maximum number of iterations has been reached, the convergence criterium is fullfilled or the *Stop* button is clicked (the *Fit* button changes label automatically), the refinement will stop and list the χ^2, reduced χ^2 and R_F value (the last only applies for the integrated intensities and powder patterns). The refined parameters with their respective standard deviation are shown below.

The refinement is visualized on the right-hand side of the window (see Fig. 4.14), where

the integrated intensites are shown in an I_{obs}-vs-I_{cal} plot (flipping ratios are shown in an R_{obs}-vs-R_{cal} plot), powder patterns are represented as usual with the observed, calculated and difference lines and the polarization matrices are shown for each magnetic Bragg reflection. The latter is achieved by showing the observed polarization matrix entries as circles and the calculated ones as squares. The color code is red for x, green for y and blue for z, while those colors refer to initial polarization P_i for the marker face color and to the final polarization P_f for the marker edge color. E.g. a red square with a blue edge refers to an initial neutron polarization along the local x axis and a analysis direction along the local z axis, i.e. to the term P_{xz} of the polarization matrix. In case of multiple data sets of a single type (intensities or powder patterns) the one to plot can be selected from the combo box in the upper-right corner of the window (appears only when multiple data sets are loaded). If you have loaded Numors corresponding to a rotation of the incident
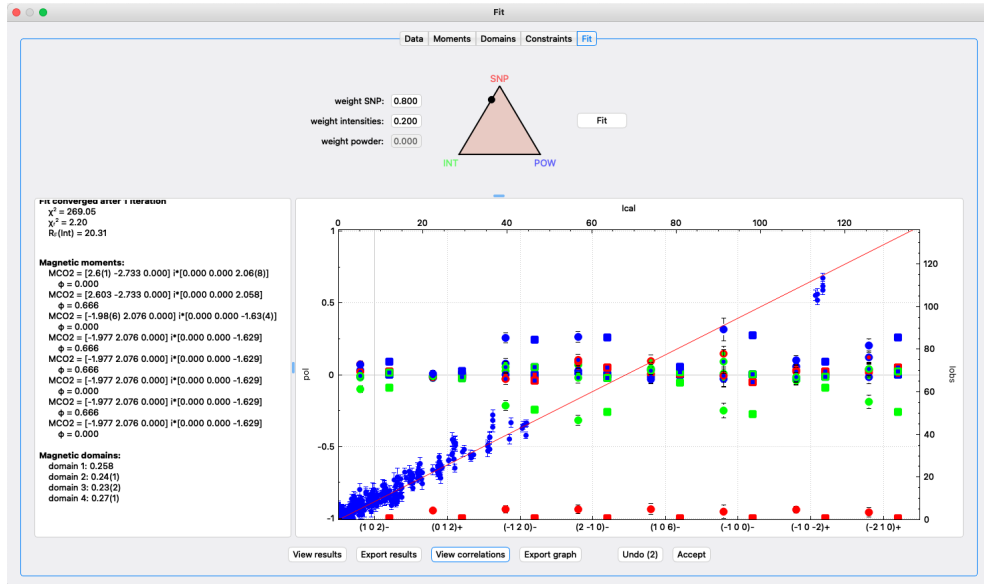
Figure 4.14: Output and visualization of the fit results.

neutron polarization within the y-z plane, the resulting plot contains the curves for each magnetic Bragg reflection on which this measurement was done (Fig. 4.15). The usual zoom controls work on this plot and the mouse can be hovered over a data point to obtain the exact values. A table of the observed and calculated intensities (also derived from powder patterns) as well as polarization matrices can be seen by clicking on *View results*, the same table can also be exported into an ASCII file by clicking on *Export results*. For powder patterns, more information is displayed, e.g. the scattering angle, d value, FWHM, line shift and F^2 values.
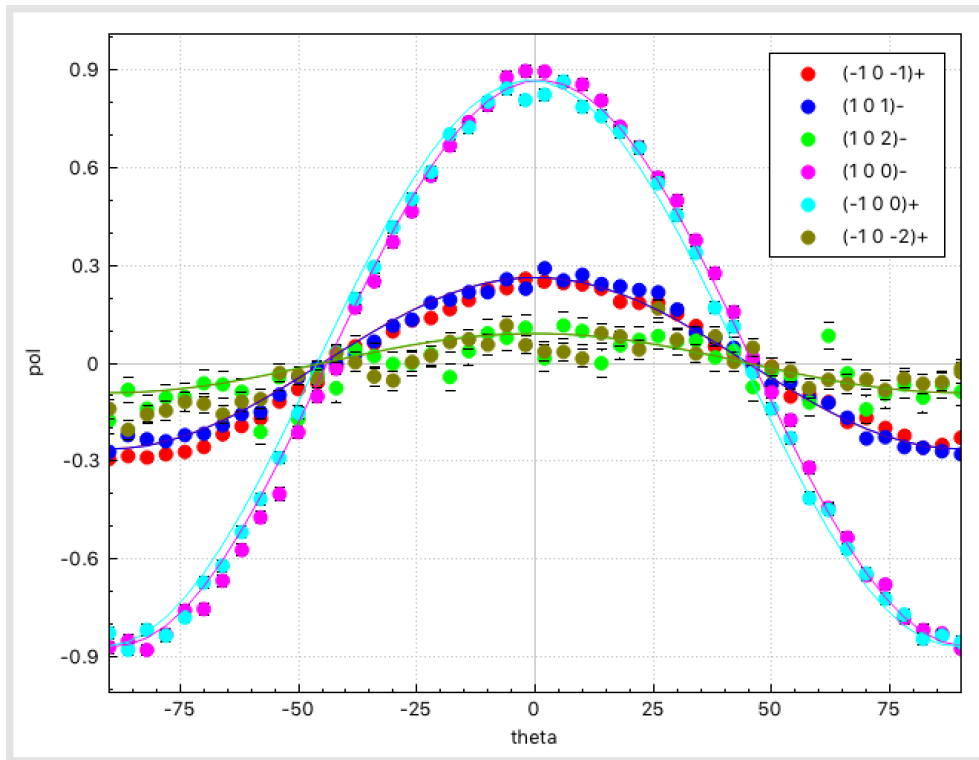
Figure 4.15: Visualization of the fit results when the data correspond to a rotation of the initial neutron polarization within the *y-z* plane.

When more than one parameter is refined, the *View correlations* button is enabled which, when pressed, opens a window in which the correlation and the covariance matrix is shown. Note that if correlations exceeding 70% are present the *View correlations* button will be given the focus in order to notify the user. Within the correlations window, the (anti)correlations with more than 70% will be marked. This threshold value can be modified in order to focus on weaker or stronger correlations. Note that this window can be kept open for subsequent refinement steps, which will automatically update the values of the correlation matrix. The button focus will be set according to the actual threshold value in the correlation matrix window.

If you are satisfied with the refinement (step) you can click the button *Accept*. This will pass on the refined parameters to the main window, replot the magnetic structure and you can afterwards save it to your input file. If the fit diverged or did not improve you can close the window without clicking *Accept*, like this the initial parameters before the respective refinement step are kept in the main window. It is also possible to (repeatedly) click the *Undo* button (or CTRL/CMD + Z) which reloads the parameters and flags which were present before clicking the *Fit* button.

4.7 Batch fitting

Batch fitting is presently only possible for powder patterns. It first requires to refine a single powder pattern as described in Sec. 4.5 and accept the fit in order to transfer the refined parameters to the main window. Note that the fit flags and eventual constraints need to be set in this single refinement and will be used in the batch fit afterwards. It is also possible to open an `xml` file to which fit results have been saved previously. If an initial model is present the action *Batch fit* will be enabled in the *Fit* menu of the main window. When entering the *Batch fit* window the initial model and its corresponding pattern will be shown in the upper-right part of the window. The same functionalities are enabled as for the pattern plot in the *Fit* window.

A sequence of powder patterns can be loaded in the upper-left part of the window by clicking on the *Load* button. The sequence can consist e.g. of powder patterns of a sample recorded at different temperatures or of different samples with varying composition. For a meaningful use of the batch fit option the powder patterns should not vary too much from step to step. The loaded samples will be shown in the item list below the *Load* button and clicking the different items will show the different patterns in the pattern plot together with the initial model. If the loaded patterns contain metadata like temperatures (set point, regulation, sample) or composition it can be sorted according to that parameter by clicking on the *Sort* button. A dialog box will open which contains the possible variables,

note that sorting according to the file name is always possible. The loaded patterns can be cleared by clicking on the *Clear* button.

When a sequence of powder patterns is loaded the refinement can be started by clicking on *Fit batch*. By using the option *refined values = next start values* it is more probable to have a converging fit from pattern to pattern. Otherwise, the same start parameters of the initial model will be used for every single pattern in the list. The fit progress is shown for every pattern by outputting the iterations and χ^2 values like for standard refinements. After each fit the corresponding pattern is shown in the pattern plot. When the last pattern has been processed the refined parameters are shown in the parameter table in the center of the window. The current pattern or all patterns at one time (the pattern number will be added as an extension to the chosen file name) can be exported into `pdf` format.

Variables can easily be plotted by ticking either the check box *Plot 1* or *Plot 2* which refer to the left or right y-axis of the parameter plot on the lower-right part of the window. The plot style can be customized by chaning the color, the line style and width as well as marker type and size. Legend entries and axes labels can be entered in the corresponding text fields which are synchronized with the parameter plot. The plot can be exported either as `pdf` or `ASCII`.
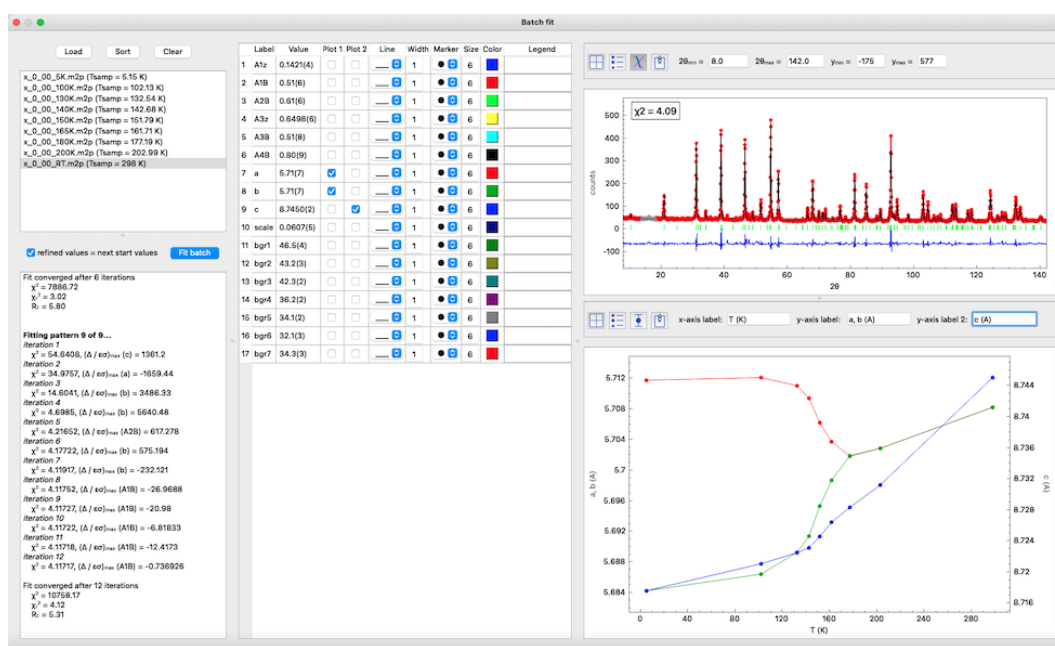

Figure 4.16: Batch fit window allowing to sequentially refine powder patterns. The refined parameters can easily be plotted against temperature, composition or pattern number.

5 Reflection lists, powder patterns and maps

5.1 Reflection lists and intensity maps

Once a crystal and magnetic structure has been set up reflection lists can be generated via the menu entry *Generate→Reflection list* or using its toolbar icon or shortcut (CTRL/CMD + L). A window will pop up in which the criteria like the (hkl) range, nuclear and magnetic structure factors, polarization values can be set. If an orientation matrix has been entered, then the diffractometer angles (calculated according to the instrument definition, see Sec. 3.9) can be used as a criterium as well. In that case it can be chosen, if only accessible reflections should be listed. By clicking *Create list* a table will be created which can be ordered according to a specific value by right-clicking on the horizontal header entry and choosing ascending or descending. The table can be exported in a format directly readable by MAD or NOMAD (running on ILL diffractometers) by clicking *Save*. A demo video can be seen here.

Intensity maps can be generated by triggering *Generate→Intensity map*, using its toolbar icon or shortcut (CTRL/CMD+ M). All nuclear and magnetic structure factors for integer and satellite reflections will be calculated (for the current phase in the main window) in the range from -10 to 10 for h, k and l. The initial view is the ($hk0$) plane, which can be altered by choosing the plane from the combo box or the layer in the spin box (see Fig. 5.1). The boundaries can be set for the horizontal and vertical axes in the second line. The resolution corresponding to the full width at half maximum of a 2D Gaussian function can be set individually for the h, k and l directions. The intensity maps' intensity color scale will automatically be rescaled to the minimum and maximum intensity of the actual map. In order to compare intensities between different maps or layers, the check box *Rescale* can be unchecked, which will therefore conserve the scale. Furthermore, a logarithmic scale can be chosen or nuclear scattering can be hidden. The maximum and minimum values of the intensity scale can be modified by the vertical sliders to the right of the map. This can be useful to emphasize weak reflections.
In case of multi-q magnetic structures scattering from differently modulated components

of the magnetic structures can be added. For that the magnetic structure in the main window should be modified (especially the propagation vector) and regenerated. Alternatively, a second phase can be added in the main window and set as the current one. Afterwards, the scattering from that new magnetic structure can be added to the intensity map by clicking *Add*. The x, y and intensity values are visualized by hovering the mouse over the map. Zooming in and out are achieved with the usual mouse controls. Intensity maps can be saved as pdf or ASCII files by clicking the corresponding button at the bottom. By holding down the CTRL/CMD key while drawing a rectangle a projection will automatically be calculated and plotted in a new window (see Fig. 5.2). The projection is always along the shorter side of the rectangle. Zooming and point labels are enabled and the projection can be saved as pdf and ASCII as well.

It is also possible to view maps in 3D (see lower panel of Fig. 5.1). This feature is particularly interesting for non-orthogonal systems in order to appreciate the real crystal symmetry. By clicking on the buttong VIEW 3D a new window will open, showing the map with the same boundaries and color code in three dimensions. The intensity scale (peak amplitude) and appearance of axis and labels can be adjusted before creating a high-quality picture.

5.2 Powder pattern

MAG2POL features the quick simulation of powder patterns which can be done via the menu entry *Generate→Powder pattern* or the toolbar icon (see also this demo video). A new window will open showing the global pattern, i.e. the sum of all phases (see Fig. 5.3). In the lower left corner of the window the geometry of the instrument can be changed, i.e. the source (neutron or X-ray), the wavelength and the resolution function via the *uvw* parameters of the Caglioti formula:

$$FWHM^2 = u \tan^2 \theta + v \tan \theta + w$$

The powder diffractometers of the ILL (D1B, D2B, D20) can be chosen with different configurations from the combo boxes which will set the respective parameters automatically. When *xray* is chosen as source, then a right-click context menu is enabled for the wavelength value from which different standard x-ray wavelengths can be chosen, which will automatically use the α_1 and the α_2 line.

The plot of the powder pattern can be zoomed in with the usual rectangle zoom and zoomed out with a right click. Hovering over the peak markers below the pattern will show a tool tip containing the scattering angle and the corresponding (hkl) reflections.

In the lower right corner the user can change the appearance of the powder pattern (colours
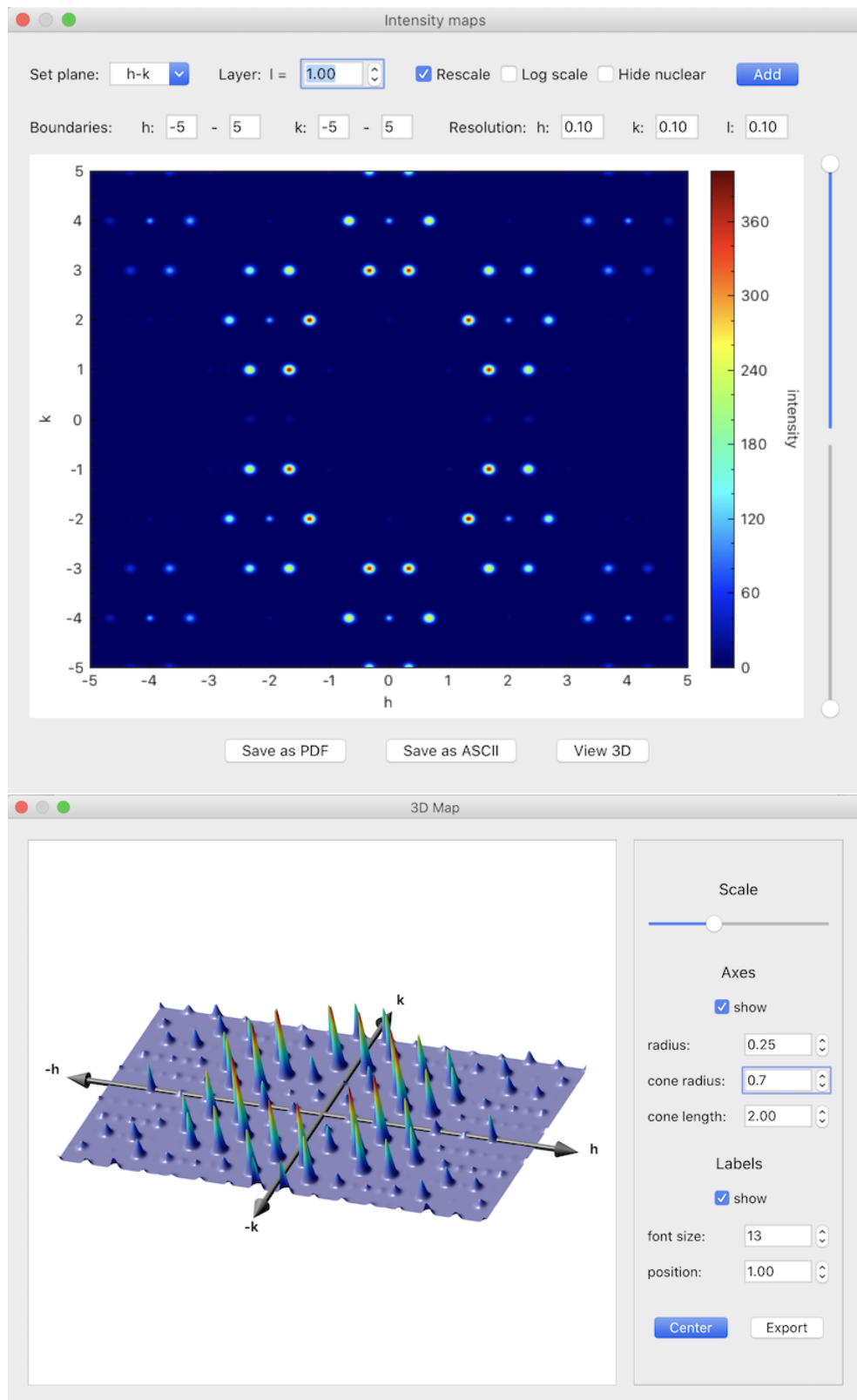
Figure 5.1: Intensity map in the $(hk1)$ plane.
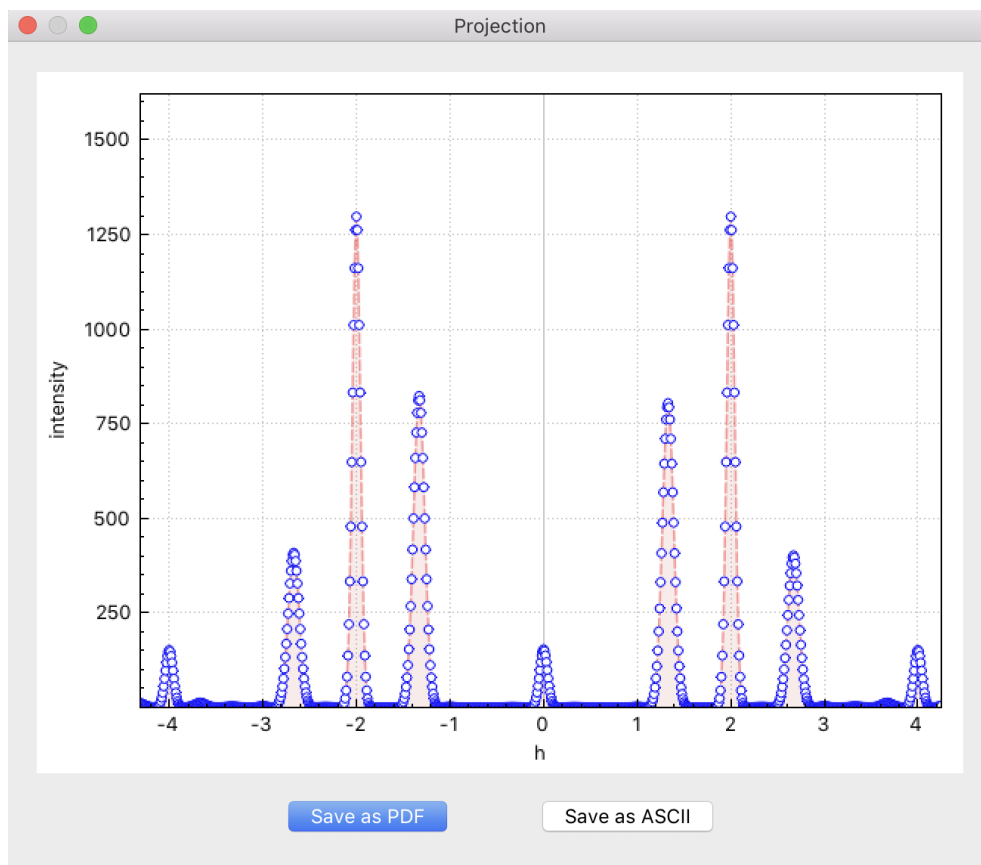
Figure 5.2: Projection along k of the scattered intensity along the $(h20)$ line of the map shown in Fig. 5.1.
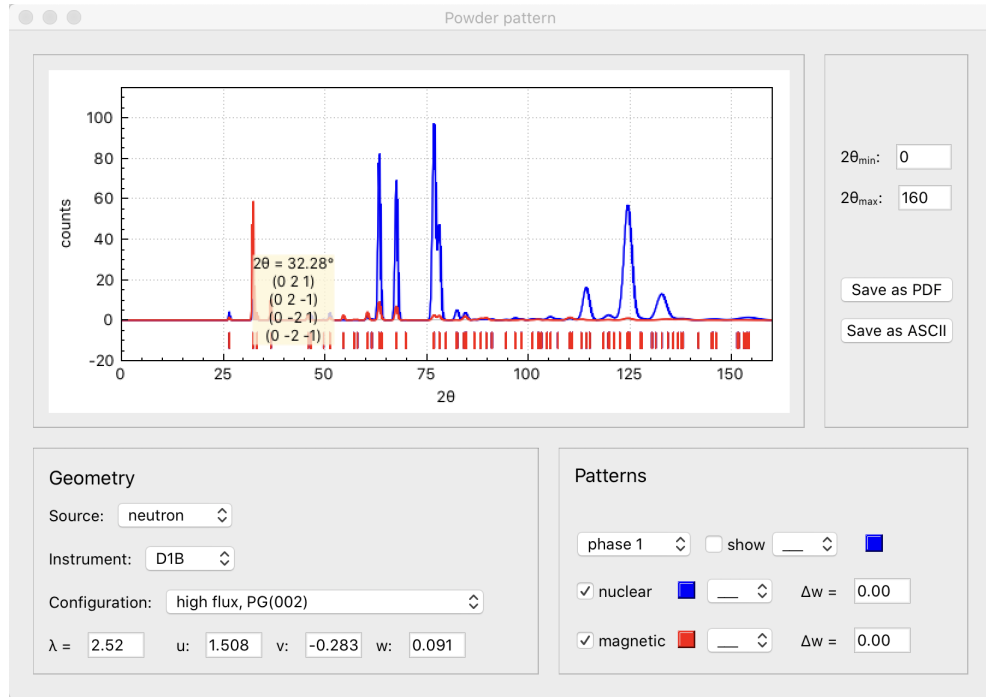
Figure 5.3: Powder pattern showing the nuclear and magnetic contribution separately.

and line styles) and choose whether nuclear and/or magnetic patterns should be shown individually. An additional broadening of the peaks can be introduced through the Δw value for the nuclear and magnetic patterns separately. The individual patterns can be exported into a text file or the visualized pattern(s) can be exported as a PDF file.

5.3 Magnetization density maps

Magnetization density maps (see an example in Fig. 5.4) can be created by calculating a Fourier inversion according to:

$$\rho(\mathbf{r}) = \frac{1}{V} \sum_{hkl} M \exp[2\pi i(hx + ky + lz)]$$

where the Fourier coefficients are the magnetic structure factors M. Projections, like e.g. onto the x-y plane are obtained by

$$\rho(\mathbf{r}) = \frac{1}{bc} \sum_{hkl} M \exp[2\pi i(hx + ky)]$$

Note that the theoretical magnetic structure factor of the experimentally inaccessible (000) reflection is added for scaling purposes in both calculated and observed maps. Different
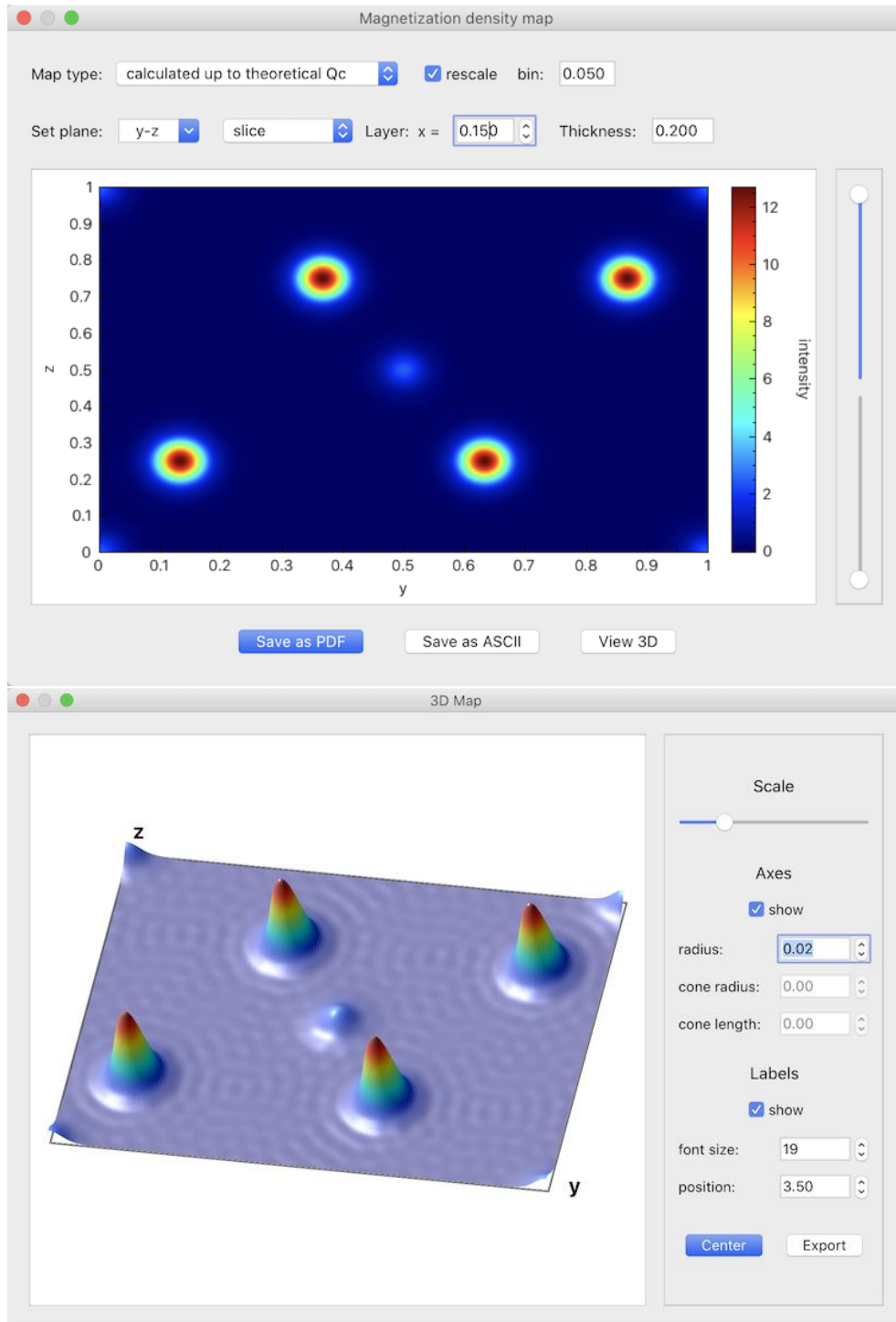
Figure 5.4: Slice of 0.2 Å thickness around $x = 0.15$ in the y-z plane in 2D (upper panel) and 3D (lower panel). The Fourier inversion is taken up to the highest measurable Q_c with the given wavelength.

Fourier maps can be chosen from the combo box, e.g. calculated maps with different cut-off angles corresponding to a critical Q_c, observed maps from `*.int` or `*.fli` flipping ratio input files or difference maps. Furthermore, the user can choose from projections, cuts or slices within the $x - y$, $x - z$ or $y - z$ plane. The different layers, or the vertical parameter, can be changed using the arrow buttons. A right-click on the layer value will pop up a context menu from which either the single step value can be set to the actual shown value or the whole range of layers from 0 to 1 can be calculated at once. For all calculations the program will make use of the nuclear symmetry in order to speed up the process. Note that each map is only calculated once, i.e. repeated scrolling through already calculated maps will not cost calculation time. However, when the bin value is changed, all previously calculated maps will be deleted. It has to be noted that the maps will sometimes show unusual details coming from binning artefacts. Therefore, the default bin has been set to 0.1 Å and the lattice constants are rounded, which usually gives good results for the Fourier maps.

The magnetization density maps can also be viewed in 3D (see Fig. 5.4). This feature is particularly interesting for non-orthogonal systems in order to visualize the correct symmetry (see also this demo video).

6 Tools

6.1 Sample information

Once a nuclear and/or magnetic structure model has been entered it is possible to see a summary of the main parameters via the menu entry *Tools→Sample info* or the toolbar icon. Under the *Crystal structure* tab (see Fig. 6.1) the real and reciprocal lattice paramters and volumes are shown together with a list of all the atoms in the unit cell. A list with magnetic moments and Fourier coefficients can be found under the *Magnetic structure* tab. All information related to the absorption correction are shown under *Absorption*. Note that the interactive tool to create the sample model (Sec. 4.2.2) can directly be accessed from here. The last refinement results can be viewed unter the *Fit* tab.
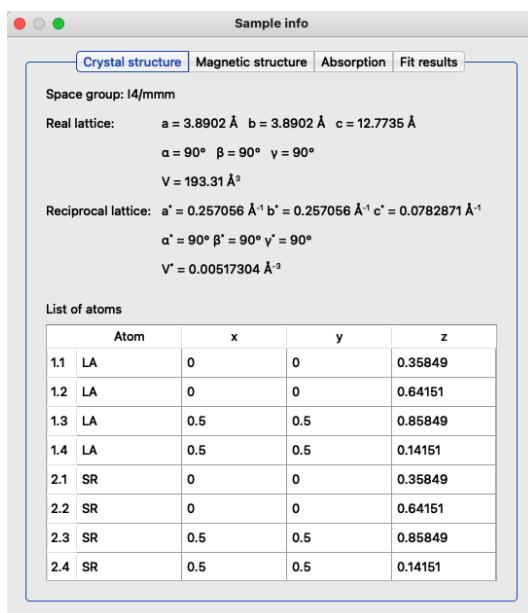

Figure 6.1: Summary of basic parameters entered by the user.

6.2 Space group tables

The space group tables and conversion tools for crystallographic (CSG), magnetic (MSG) and magnetic superspace groups (MSSG) can be consulted under *Tools→Space group tables* or via its corresponding toolbar icon. When entering the window without a previously defined structure model, the symmetry operators and Wyckoff positions as well as basis vectors for MSGs can be viewed for any space group with or without basis transformation. Selecting a space group to set up a structure model including the transformation of the unit cell and atomic positions is only possible with a previously defined structure model.

The *Space group tables* window is organized in four tabs, from which the first three are: CSGs, MSGs and MSSGs (see Fig. 6.2). Space groups can be entered via their (numerical) labels, e.g. $I4/mmm$ or 139, $Pm'n'a$ or 53.326, $P2.1'(0,0,g)0s$ or 3.1.5.3.m2.2, or they can be chosen from the combo boxes where they can also be sorted by system for easier navigation. As stated in Sec. 2.2, all information concerning MSGs and MSSGs is based on the computer-readable tables available on the ISOTROPY SOFTWARE SUITE website [1–3] and the work published in [4–6]. For further information, the reader may refer to the excellent reviews [24, 25]. If a space group has been correctly entered its label will be shown in green (red if not) and the crystallographic information will be shown in the text window below. This information consists of the operators of the space group (including time inversion operator for MSGs and the internal variable for MSSGs) followed by the Wyckoff positions in case the space group has been entered in its standard setting (a few non-standard CSGs are implemented in MAG2POL). The basis of any space group can be transformed to another setting which can be useful to compare a structure with another one published in a different setting, and is necessary for a reasonable use of MSGs and MSSGs. The transformation operator can be entered either by writing a string in standard notation which will display the rotational part R and translational part t of the operator, or vice versa, by entering R and t which will display the transformation string. The correct syntax will be shown in green and requires the transformation string to be enclosed in parantheses, the rotational and translational part to be separated by a semicolon and the individual axes to be separated by a comma. The identity would be expressed as (`a, b, c; 0, 0, 0`), where the spaces are optional. A swapping of the a and b axes with an origin shift along c would correspond to (`b, -a, c; 0, 0, 1/2`). Note the minus sign to conserve a right-handed set of axes and the possibility of entering fractions. The correct application of basis transformations, especially when entering information obtained from other tools (e.g. BILBAO CRYSTALLOGRAPHIC SERVER or ISOTROPY), will be shown in the next sections.

The fourth tab *Preview* serves to visualize the crystal and magnetic structure in the main window and allows to modify the degrees of freedom, i.e. atomic positions and basis vectors of magnetic moments respecting the underlying symmetry. If bonds and polyhedra were drawn beforehand, the program will show their deformation in real time.
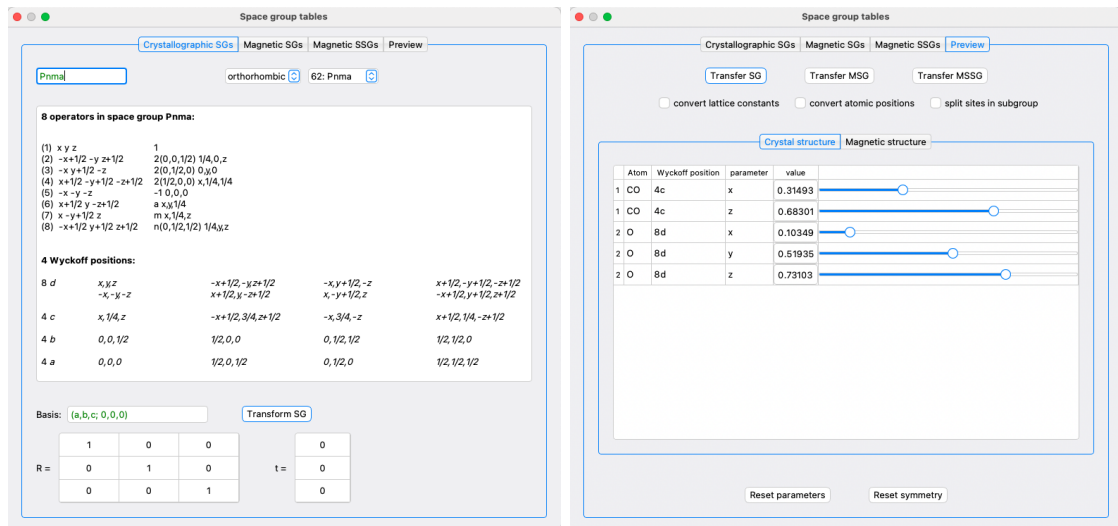
Figure 6.2: Left: Space group tables for crystallographic, magnetic and magnetic super-space groups containing information about symmetry operators, Wyckoff positions and basis vectors. Furthermore, any transformation can be applied to any of the space groups. Right: Preview window allowing to transfer a space group to the main window, to modify the degrees of freedom and to visualize the crystal and magnetic structure.

6.2.1 Space group transformations

After choosing a space group from the combo boxes or by entering its (numerical) label, MAG2POL will always load the untransformed operators and Wyckoff sites regardless of the given transformation operator. The basis transformation is only applied when clicking on *Transform SG*, which will update the crystallographic information in the text box above, which is also shown by the basis transformation string next to the space group label.

If the user wishes to transfer the space group to the structure model initiated in the main window, this can be achieved by clicking *Transfer SG* in the *Preview* tab. Several options exist which depend on what the user wishes to achieve. If the checkbox *convert lattice constants* is activated, the rotational part of the transformation operator is applied to the lattice which will be updated in the main window. The same applies to *convert atomic positions* which - if activated - will convert the position vectors by taking into account

the rotational and translational part. The last checkbox *split sites in subgroup* should be activated, when a group was chosen in the *Space group tables* which is a subgroup of that in the main window. In this case, the program will identify the symmetry operators missing in the subgroup and create new atoms in the structure model, if sites split into different orbits. Two examples will clarify the use of these checkboxes:

- Convert a structure expressed in *Pnma* to *Pnam*

  Enter the *Space group tables* with a *Pnma* structure model in the main window. The transformation to *Pnam* is expressed by (`a, c, -b; 0, 0, 0`) or equivalently by (`a, -c, b; 0, 0, 0`) which should be entered in the corresponding field under the *Crystallographic SGs* tab. Alternatively, the rotation matrix can be entered, which will create the transformation string as a confirmation. Click *Transform SG* to apply the transformation and check the results in the text box above.

  Now switch to the *Preview* tab. Due to the swap of b and c axes the lattice parameters and the atomic positions previously defined in the main window should be updated in order to conserve the structure. Therefore, *convert lattice parameters* and *convert atomic positions* should be activated. On the other hand, all symmetry operators of *Pnam* will be different from the ones in *Pnam*, but the site multiplicity remains unchanged. Therefore, the *split sites in subgroup* checkbox should not be activated. Now click *Transfer SG* and inspect the structure in the main window. You can move the sliders or enter values for free positional parameters to verify the structural degrees of freedom and you can go back to the initial values by clicking *Reset parameters*. If the transformation does not show the expected results, it can be reverted by clicking *Reset symmetry* which will take the structure back to its state before entering the *Space group tables* window. If the *Space group tables* window was closed after transferring the space group and converting the structural data, it is still possible to recover the original structure by right-clicking the *Space group* label in the main window and choosing the appropriate action from the *reset transformation* menu. Any of the options will set the transformation operator to identity, i.e. the symmetry operators of the original space group will be used to generate the cell. The optional conversion of the lattice parameters and the atomic positions will be done with the inverse of the former transformation operator. In this example, the correct option would therefore be *convert both*.

- Convert a structure expressed in *Pnma* to its non-isomorphic subgroup $P2_1ma$

  From the International Tables Vol. A [8] one can obtain the following information concerning the non-isomorphic subgroup: $P2_1ma$ ($Pmc2_1$, 26) 1; 4; 6 ;7. The subgroup $P2_1ma$ is a non-standard setting of space group 26, $Pmc2_1$, and the symmetry operators 1, 4, 6 and 7 of *Pnma* are conserved. Since MAG2POL lists the opera-

tors in the exact same order, it is straightforward to compare the respective space groups. First, set up the structure in *Pnma* symmetry in the main window and then enter the *Space group tables* window (copy the symmetry operators for a more comfortable comparison afterwards). Choose space group *Pmc*2$_1$ under the *Crystallographic SGs* tab, which now has to be converted to *P*2$_1$*ma*. The rotational part of the transformation is easy to extract by comparing the two space group labels. Therefore, in a first step the transformation (`c, a, b; 0, 0, 0`) can be entered followed by a click on *Transform SG*. Now, paste the *Pnma* symmetry operators below the converted ones and compare operators 1, 4, 6 and 7. It is apparent that a rotation of the basis is not sufficient and that a shift of origin is necessary. It can be verified that the correct transformation is (`c, a, b; 1/4, 1/4, 0`). Enter the string and click *Transform SG* (note that for each transformation the original space group is reloaded before applying the transformation, i.e. one cannot do a chain of transformations), which should produce the four symmetry operators of *Pnma* numbered 1, 4, 6 and 7. The transfer of the new symmetry to the main window is effectuated in the *Preview* tab. In this case, the axes and atomic positions have been transformed to match those of the original structure in *Pnma*, so the first two checkboxes should not be activated. On the other hand, since the general multiplicity of *P*2$_1$*ma* is 4, while it is 8 in *Pnma* not all atomic positions will be generated in the subgroup, for which the *split sites in subgroup* option needs to be activated. Finally, click on *Transfer SG* and verify the result.

The conversion from the non-standard setting *P*2$_1$*ma* to *Pmc*2$_1$, if intended, can be done by closing the *Space group tables* window and by resetting the transformation via the *Space group* label context menu as explained in the previous point.

6.2.2 Magnetic space group transformations

The basic use of magnetic space groups and their transformations is very similar to the explanations in the previous section with a few exceptions. The first is related to the fact that the transformation operators are always applied to the parent space group which is the definition used by the programs of the BILBAO CRYSTALLOGRAPHIC SERVER for example. Therefore, the chosen magnetic space group is transformed with the inverse of the shown transformation, since the direct transformation is applied to the parent space group which is (related to) the paramagnetic space group. The second difference concerns the transformation of lattice constants and atomic positions which are always calculated according to the transformation operator under the *Crystallgraphic SGs* tab. This makes it possible to effectuate complex transformations of both the CSG and the MSG to obtain the desired result. A good starting point for finding appropriate MSGs is the use of the

MAXMAGN program [25] on the BILBAO CRYSTALLOGRAPHIC SERVER. After entering the crystallographic space group and the commensurate propagation vector one obtains a list of maximal magnetic space groups. By clicking the *Show* button in the *General positions* column one can obtain both the augmented transformation matrix for the CSG and for the MSG. How to correctly enter this information will be shown in the following example from [25].

- Magnetic space group P_aca2_1 as a child of the parent space group *Pbam*
  The use of MAXMAGN with space group *Pbam* and propagation vector $\mathbf{q} = (^1\!/_2\ 0\ 0)$ reveals four maximal magnetic space groups, one of them being P_aca2_1 (#29.104), but in a special setting. First of all, set up the paramagnetic *Pbam* structure in the main window and enter the *Space group tables* window. Here, enter the basis transformation of the parent space group which is given as (`2a, b, c; 0, 0, 0`) on the *General positions* page of the MAXMAGN output. Click *Transform SG* which will result in doubling the symmetry operators of space group *Pbam* due to the additional translation $t(^1\!/_2\ 0\ 0)$. Now switch to the *Magnetic SGs* tab and enter either `P_aca2_1` or `29.104` which will show the symmetry operators, Wyckoff positions and basis vectors for that magnetic space group. Enter the transformation of the MSG, this time given in matrix form in the MAXMAGN output, which becomes (`a, -c, b; 1/8, 0, 0`), and click *Transform MSG*. At this point it is important to compare the symmetry operators in both tabs. If the transformations were applied correctly, the MSG should be a subgroup of the SG and reveal a subset of the symmetry operations (primed or unprimed) of the latter. In this example the 8 MSG operators can be found in the CSG (operators 1, 3, 6, 8, 9, 11, 14 and 16). Now the MSG can be transferred from within the *Preview* tab. Since the CSG was adapted to the doubling along the *a* axis, the lattice parameters and the atomic positions need to be changed accordingly, i.e. the *convert lattice constants* and *convert atomic positions* checkboxes need to be activated. Furthermore, since the MSG only reveals a subset of the symmetry operators in the CSG, not all the atomic positions can be generated, for which the *split sites in subgroup* checkbox needs to be activated as well. Now, click *Transfer MSG*, inspect the resulting structure in the main window by adjusting the degrees of freedom under the *Crystal structure* and *Magnetic structure* tabs and accept the result by closing the *Space group tables* window. As described above, the transformation of the MSG can be converted back to the original P_aca2_1 setting by evoking the context menu on the *Space group* label in the main window.

6.2.3 Magnetic superspace group transformations

The use of MSSGs is almost the same as for MSGs with the exception that no transformation of the parent paramagnetic space group is necessary. When selecting a MSSG symmetry (either by typing its label or by choosing it from the list) and transferring it to the main window in the same way as described for MSGs, MAG2POL automatically calculates the basis vectors for all the magnetic ions in the structure model. Depending on their point symmetry certain components may be extinct or relations between real and imaginary components might exist. Note that the order of basis vectors is not necessarily the same as shown in the ISOVIZ plotting tool and that split sites are treated as independent sites in MAG2POL. The interested reader may consult [24] for a complete overview on MSSGs.

A good starting point to identify possible MSSGs for the underlying crystal structure and incommensurate propagation vector is the use of the ISOTROPY SOFTWARE SUITE website [1–3]. A `*.cif` file can be exported from MAG2POL and loaded on the website to start a new distortion (choose only magnetic). Enter the propagation vector using *Method 2: General method - search over specific k points*, enter the necessary propagation vector coefficients, set the number of incommensurate modulations to 1 [note that only (3+1)d modulations can be treated with the present version of MAG2POL] and click *OK*. On the next page all necessary input parameters can be found for the different possible modes. Either extract the information from this page or select a mode and click *OK*. On the next page it is possible to download an `*.isoviz` or `*.cif` file, from which the latter can be directly loaded in MAG2POL after changing its extension to `*.mcif`. The `*.mcif` files downloaded from the ISOTROPY SOFTWARE SUITE contain the original setting and the one adapted to a standard paramagnetic space group. On loading the file, it can be chosen which setting to employ. Note that for MSSGs with origin translations **t** such that the dot product with the propagation vector **q** is non-zero, the visualization in the conventional cell might look different than that of the untransformed MSSG. The correct use of the MSSG transformation is shown in the following example.

- Magnetic superspace group $P2_1/b.1'(0,0,g)00s$ as a child of the parent space group $P2_1/c$ with propagation vector $\mathbf{q} = (0\ 0.32\ 0)$
  First, set up a structure in $P2_1/c$ symmetry and export is to a `*.cif` file which can be uploaded on the ISOTROPY SOFTWARE SUITE website. Enter the propagation vector under *Method 2* by choosing *LD, k3 (0, b, 0)* and enter $b = 0.32$, set the number of incommensurate modulations to 1 and click *OK*. On the next page, select the first mode corresponding to the MSSG $P2_1/b.1'(0,0,g)00s$. From here the necessary input can already be transferred to MAG2POL by entering the given basis transformation. In this example the output `basis={(1,0,0,0),(0,0,1,0),(0,-1,0,0),(0,0,0,1)}`,

`origin=(0,0,0,0)` needs to be entered as

$$R = \begin{pmatrix} 1 & 0 & 0 & 0 \\ 0 & 0 & -1 & 0 \\ 0 & 1 & 0 & 0 \\ 0 & 0 & 0 & 1 \end{pmatrix} \qquad t = \begin{pmatrix} 0 \\ 0 \\ 0 \\ 0 \end{pmatrix} \tag{6.1}$$

followed by a click on *Transform MSSG*. At this point, it should be verified that the transformed operators constitute a subset of the ones in the parent space group $P2_1/c$. As this is the case one can transfer the MSSG from the *Preview* tab. The parent space group is left unchanged for which no conversion of lattice constants and atomic positions is necessary. Furthermore, the general site multiplicity is the same in both MSSG and CSG. Therefore, all the options should be unchecked before clicking *Transfer MSSG*.

6.3 Data converter
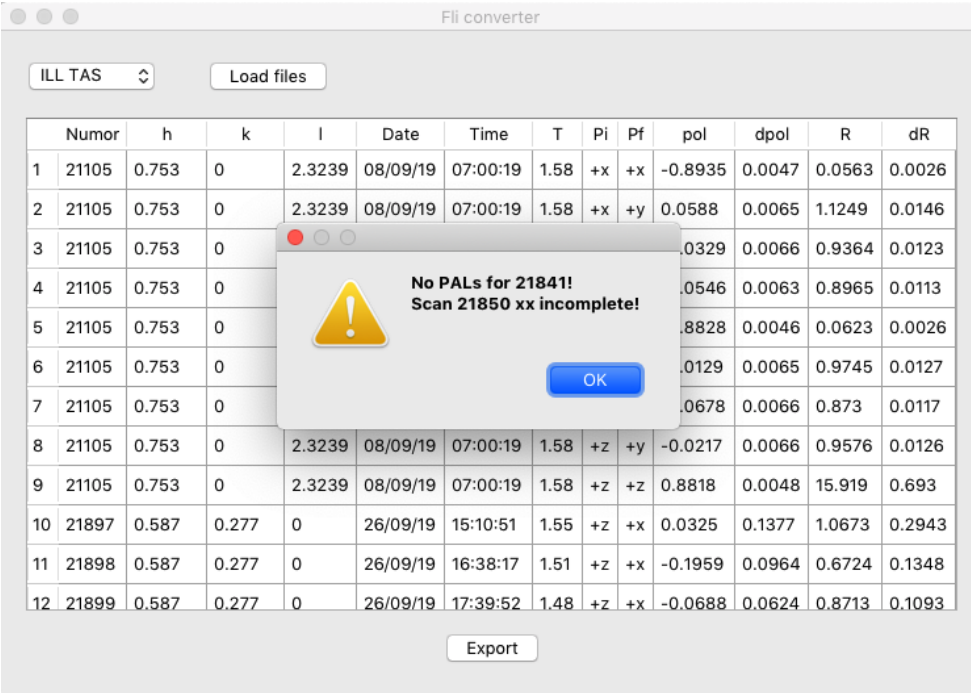
Data from ILL Triple Axes Spectrometers (TAS) can be opened with MAG2POL and converted to a `*.fli` file under certain conditions:

- each Numor contains a 1-point (peak) or 3-point scan (left background - peak - right background)

- the scan was done using a PAL file which defines the polarization channels to measure

- the information concerning $\mathbf{P}_i$ and $\mathbf{P}_f$ are listed as output parameters for each point of the scan

If these criteria are not met, the program will show an error message for each corresponding Numor which could not be (fully) loaded (see Fig. 6.3).

6.4 Irreducible representations

MAG2POL offers the possibility to calculate the irreducible representations (irreps) which yield magnetic structure models with different symmetries that are allowed by the underlying crystal structure and the propagation vector (see this demo video). The method of obtaining the irreps is based on the induction method which is very well explained in [26]. In fact, in order to obtain the irreps of space group $G(\mathbf{k})$ one has to find the irreps of its invariant subgroup $G'(\mathbf{k})$ of index 2 or 3. This co-set decomposition is done iteratively until the translation group or a cyclic group is reached, whose irreducible representations can readily be written down. The case of cubic space groups is dealt with separately in

Figure 6.3: List of loaded polarization data. Incomplete information will be output with a warning message.

the original paper and has been adopted as well in Mag2Pol.

The menu item *Generate→Irreducible representations* and the toolbar icon will be enabled after generating a structure with at least one magnetic site. Note that depending on the remaining magnetic symmetry operators certain magnetic sites split into several orbits. This will automatically be updated by the program in the main window (note that split sites should be grouped together in the atom list, when a structure model is entered manually, i.e. without using the irrep tool). Similarly, if the given structure already contains split sites (either because the user entered them or because the irreps calculation has already been run at least once), they will not be split again. I.e. the irreps calculation can be performed several times without the need of modifying the sites in the main window. Triggering *Generate→Irreducible representations* will open a new window in which a summary of the symmetry information will be shown in the *Symmetry* tab (see Fig. 6.4).

The symmetry operators are shown exactly as in the International Tables for Crystallography Vol.A including the same order. Further below, the symmetry operators of the little group are shown, i.e. those symmetry operators which are compatible with the magnetic translation symmetry. Then a list containing the magnetic atom positions is shown including the information if a split orbit is present and which symmetry operator (lost in
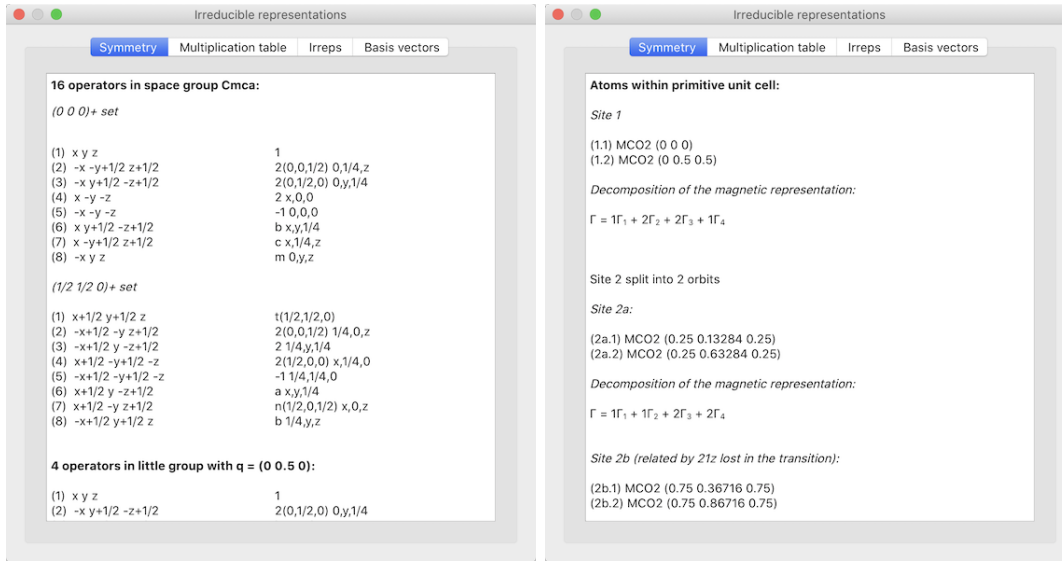
Figure 6.4: Irreducible representations window showing the symmetry operators, the atomic positions and a summary of the calculation.

the transition) relates the orbits. Under the tab *Multiplication table* (see the left panel of Fig. 6.5) one can see how the symmetry operators act under the group multiplication. The note below the table changes depending on the active cell and adds the information if a phase shift needs to be applied, when a non-zero propagation vector is present.

The tab *Irreps* contains the table of the irreducible representations (see central panel of Fig. 6.5). Eventual exponential factors are abbreviated and explained in the legend below the table. A right-click on the vertical header item, e.g. Γ_1, pops up a menu in which this particular irrep can be transferred to the current phase in the main window. By highlighting two irreps and right-clicking either one a mixed irrep can be set. If no particular basis vectors are selected in the tab *Basis vectors* all basis vectors are transferred to the current magnetic structure in the main window. Note that a maximum of 6 basis vectors can be used per site, for which an error message will pop up, if this number is exceeded. In that case, or also if certain basis vectors can be excluded, the basis vectors to export can be highlighted in the *Basis vectors* tab (see right panel of Fig. 6.5) for the corresponding irrep(s). The basis vectors can be visualized in different ways: basis vector of the first atom of each site normalized to 1, normalized with abbreviated exponential factors or with the smallest component normalized to 1. Note that the basis vector will always be exported with the basis vector of the first atom normalized to 1 so that the multiplying coefficients can be interpreted as Bohr magnetons. Each basis vector can (repeatedly) be multiplied by i, e.g. to combine two irreps in phase quadrature.

By setting the coefficients, which are multiplied to the basis vector, in the main window
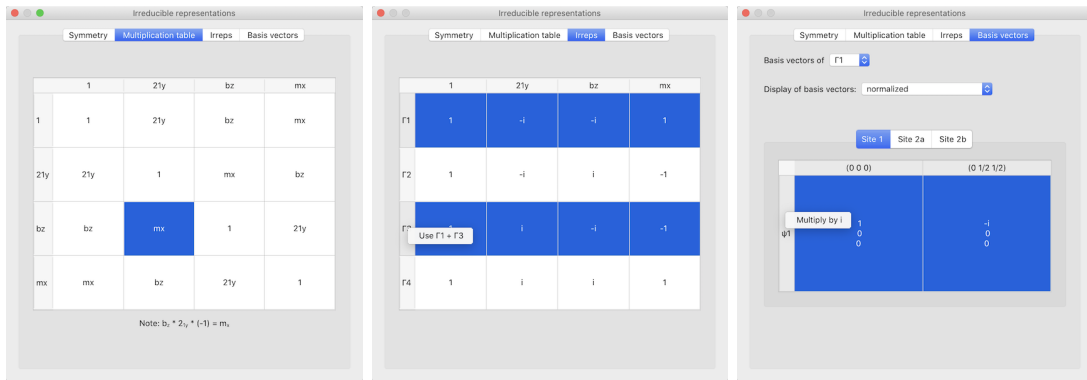
Figure 6.5: Irreducible representations window showing the multiplication table, the irreducible representations and the basis vectors.

(under the *Magnetic structure* tab) to a non-zero value, the magnetic structures can be visualized instantly and compared to each other. The irreps information will be saved in the input file, so that the calculation does not need to be repeated. Hovering over the coefficients in the main window will show tool tips explaining to which irrep and basis vector the coefficients belong. Note that when the magnetic structure results from an irrep calculation it is not necessary to explicitly enter the magnetic symmetry operators by hand. They are internally stored together with the corresponding magnetic phases. One can also look up the basis vectors in *Structure→Basis vectors* and change the way of setting up the magnetic strucure, i.e. use symmetry-adapted basis vectors from the irreps calculation, use user-defined basis vectors or use no basis vectors at all (i.e. use *uvw* coefficients).

6.5 Spin correlations

MAG2POL offers a spin-correlation tool which calculates the spin-correlation function $\langle S(\mathbf{R}) \rangle$, the intensity as a function of Q and the magnetic pair distribution function (mPDF). To calculate those distributions it is only necessary to enter a magnetic structure in the main window and click on *Tools→Spin correlations* or the corresponding toolbar icon. A new window will open and the 3 distribution functions will be calculated based on the R_{min} and R_{max} values which can be set to the right of the $\langle S(\mathbf{R}) \rangle$ plot. For the $I(Q)$ and mPDF plots start and end values as well as a step width can be chosen. For the latter the resolution can be taken into account via a $FWHM$ value. The underlying formalism is explained in Sec. 7.6.

The structure plot offers the same functionalities as the main window, i.e. one can click on the atoms and spins to retrieve information concerning the position, spin components,

distances and angles. In the spin-correlations window the 3D plot is interactively linked with the 2D plots of the respective distribution functions. Shift-clicking two atoms to evoke their distance will automatically show the corresponding distance in the $\langle S(\mathbf{R}) \rangle$ and mPDF plots. It also works the other way round: clicking on a bar in the $\langle S(\mathbf{R}) \rangle$ bar plot will draw the bond between all spins separated by this particular distance. This offers an intuitive way to understand the correlation functions. All distribution functions can be exported either as PDF or ASCII via the *File→Export* menu.

The spin-correlation tool furthermore offers the possibility to visualize the results of reverse Monte-Carlo simulations performed with the SPINVERT program [27]. This can be done by opening a *_spins_xx.txt file containing the spin configuration within the supercell. Note that the atomic positions in SPINVERT and MAG2POL should roughly agree (precision of 0.01) in order to identify the correct positions for plotting the structure. The R_{max} value will be set automatically depending on the used supercell. Eventually there is a huge number of spins in the supercell, therefore, in order to increase rendering speed and fluidity the object resolution can be reduced. The visualized supercell can also be adapted using the box boundary values.
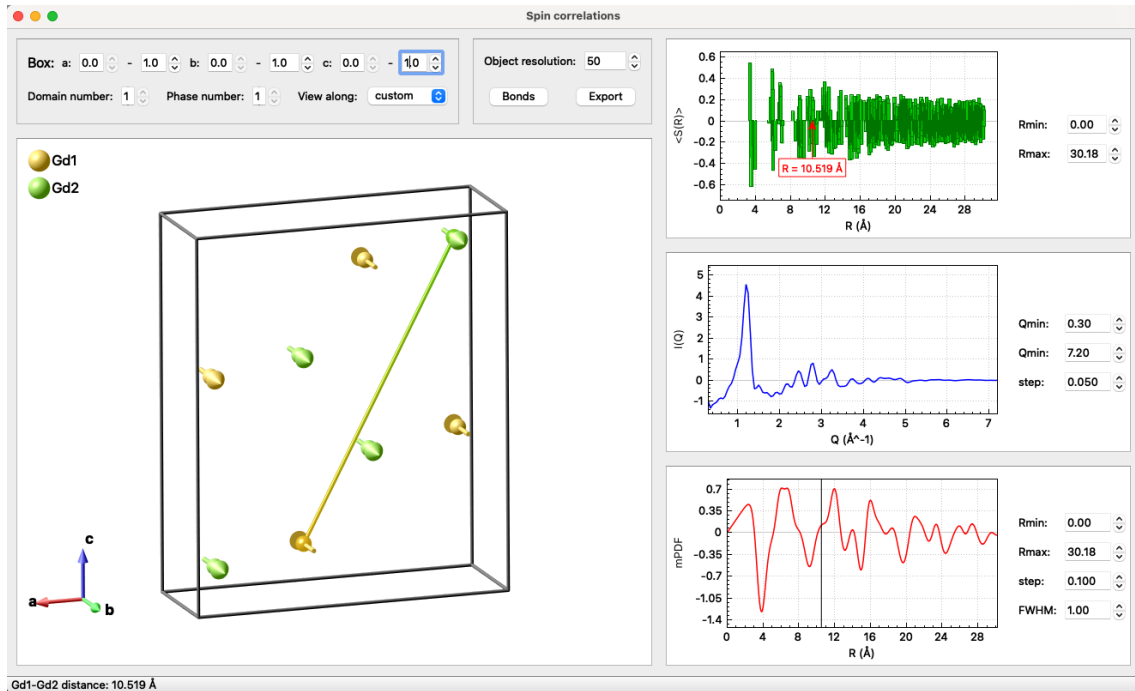
Figure 6.6: Spin-correlation window showing the magnetic structure and the different distribution functions. The 2D and 3D plots are interactively linked to each other so as to identify correlations at a particular distance.

6.6 Multi-q magnetic structures

Multi-**q** magnetic structures, e.g. conical or fan-like structures, are not only beautiful but also tricky to visualize. With MAG2POL this is very easy to do. One only needs to set up two phases in the main window (see Sec. 2.2) which have exactly the same crystal structure (note that different space groups may be used as long as the atomic positions coincide), but different magnetic parameters. In the example shown in Fig. 6.7 a ferromagnetic (**q**=0) component along the c axis has been used together with a helical component in the a-b plane modulated by the propagation vector **q**=(0 0 ¹/7). In order to visualize the resulting multi-**q** structure one has to click on *Tools→Multi-q structure* or the corresponding toolbar icon, which will open a new window. Note that for the moment only two different **q** vectors can be combined. Furthermore, the case might occur where the different components have been set up with a different number of magnetic domains. If the domain number to plot is superior than the number of domains in that phase, then the first domain is chosen by default.
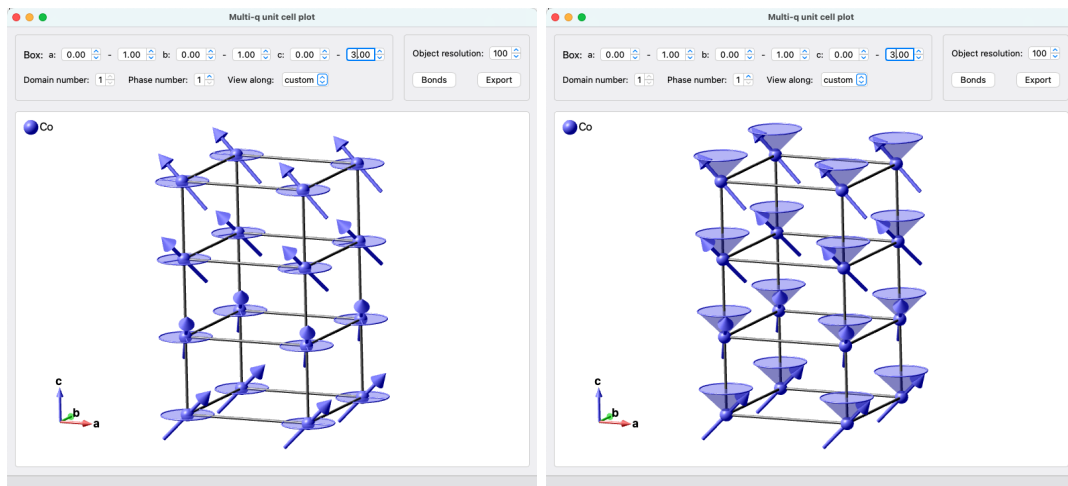
Figure 6.7: Multi-**q** window showing the superposition of two magnetic structure components, one being ferromagnetic along the c axis and the other one being a helically modulated component in the a-b plane. The resulting superposition is a conical magnetic structure. The modulated in-plane component can be emphasized by an ellipse, where the spin direction is marked by a thin cylinder (left panel) or by a cone tracing the spin rotation (right panel).

6.7 LaTeX export

The presentation of nuclear and magnetic structure parameters as well as information about the magnetic symmetry are the central part of a scientific report or publication. With MAG2POL it is possible to create tables in LaTeX format containing

- nuclear structure parameters (including standard deviations from the last accepted and saved refinement)

- magnetic structure parameters (including standard deviations from the last accepted and saved refinement)

- the multiplication table of the given space group or little group

- the table of irreducible representations

- the table of basis vectors for a given irreducible representation and atomic site

These tables can be copied to the clipboard by clicking on *Tools→LaTeX export* and pasted into an open `*.tex` document.

6.8 Pattern editor

The pattern editor is a tool which offers the following features

- plot patterns in 1D, 2D and 3D and export as `*.pdf`

- add offsets on the 2θ and counts axes of loaded patterns

- create new patterns by building sums and differences

- export patterns in the MAG2POL format

Patterns can be loaded by clicking the *Load* button and then selecting the corresponding format from the input dialog window. If the wrong format was chosen, an error message will be shown, otherwise the patterns will be shown as a 1D-plot in the panel on the left part of the window. The patterns and the corresponding properties are shown in the table on the right. It contains the file name, wavelength, temperature, offsets and plot styles. The table can be sorted according to file name, wavelength or temperature by right-clicking the respective column header and choosing either ascending or descending from the *Sort* menu. The listed temperature can be switched between sample, regulation and setpoint by right-clicking the temperature header and selecting from the list within the *Temperature* menu.

As in all other plots zooming is done by clicking and dragging, while a right-click re-establishes the boundaries which are specified above the plot. If these are changed by the user they can be reset to the optimal values by right-clicking any of these values and then clicking *reset boundaries*. The 3 symbols to the right of the plot boundaries toggle the legend, error bars and plot grid, respectively. Hovering the mouse over the data points shows the 2θ values and counts when no more than 5 patterns are plotted.

The appearance of each data set can be modified with the respective line and marker options and the checkbox *Show* allows to show or hide a particular pattern. A right-click on the *Show* header allows to select between *Show all*, *Show every nth* and *Hide all*. Choosing the second option will open an input dialog in which the value n can be entered. In 1D-plotting mode or in order to manipulate and export patterns, offset values can be added to the 2θ or counts axes. There is a convenient way to apply a gradual offset and even a gradual color change to all visible patterns: Select the offset/color of the first and last visible pattern in the table and then right-click on the respective column header and select *Set gradient*. Choosing *Set as first* obviously sets the respective property to the one for the first pattern in the list. The legend entries can be either typed in manually or set to the temperature (the one selected in the table) or to the file name by right-clicking the *Legend* header and selecting the corresponding option.

When at least 2 patterns are visible the *View 2D* button is enabled which - after activating it - shows all visible 1D patterns in a 2D plot where the vertical axes corresponds to the temperature and the intensity is represented in a color code. Zoom and plot boundaries work as in 1D mode, additionally, the minimum and maximum values of the color bar can adjusted by the vertical sliders on the right side of the plot. Note that any offset values in 2θ and counts are only considered in 1D plots. Clicking the button *Export plot* will save the shown plot (1D or 2D) in `*.pdf` format. As for other 2D maps holding down the CTRL/CMD button and zooming will calculate the projection of the data along the shorter side of the rectangle and the result will be shown in a new window. After a 2D map has been plotted it can also be shown in 3D by clicking on the enabled button *View 3D* which opens a OPENGL plot. Like for intensity and magnetization density maps the plot appearance can be adjusted and the plot can be exported in high resolution.

The loaded list can be cleared or exported in MAG2POL format with `*.m2p` extension by clicking on the *Clear* or *Save all* button, respectively. Individual patterns can be exported or removed by right-clicking the vertical header number. The file name shown in the table will be used to save the file, however, the program will remove any other extension and replace it with `*.m2p`, therefore, no original data can be overwritten. New patterns can

be created from the loaded ones, e.g. sums or differences, by typing an equation in the field below the table. Each pattern is represented by the letter `p` and by its corresponding number in the table. Each pattern, e.g. `p3`, needs to be preceded by a multiplying factor, e.g. `2*p3` and the different patterns are combined by either the $+$ or $-$ sign, e.g. `2*p3-1*p4`. The correct syntax is visualized by a green font, while a red font means that there is an error in the equation. When the font is green, the *Create* button becomes active and clicking it creates a new pattern which is added to the table and plotted. At the same time the standard deviations are calculated according to the error propagation rule.

6.9 Guides to the eye

Certain nuclear and magnetic structures benefit from guides to the eye which highlight their peculiarities. With Mag2Pol such hints can be added to the OpenGL unit cell plot in 3D through the following objects (with their corresponding customizable properties):

- Arrow (position, direction, shaft radius, cone radius, cone length, color)

- Cylinder (start position, end position, radius, start color, end color, transparency, gradient)

- Sphere (position, radius, color)

- Ellipse (position, first axis, second axis, color, transparency)

- Torus (position, first axis, second axis, radius, color)

- Spiral (position, first axis, second axis, radius, height, windings, phase, start color, end color)

- Sine (position, propagation direction, amplitude, radius, cycles, phase, start color, end color)

- Plane (at least 3 points, color, transparency)

- *hkl* plane (*hkl* indices, color, transparency, family)

- Box (position, length, width, height, color, transparency)

- Text (position, text, font size, color)

All positions are given in fractional coordinates with respect to the unit cell (just like atomic positions), while all vector quantities are defined in units along the crystallographic
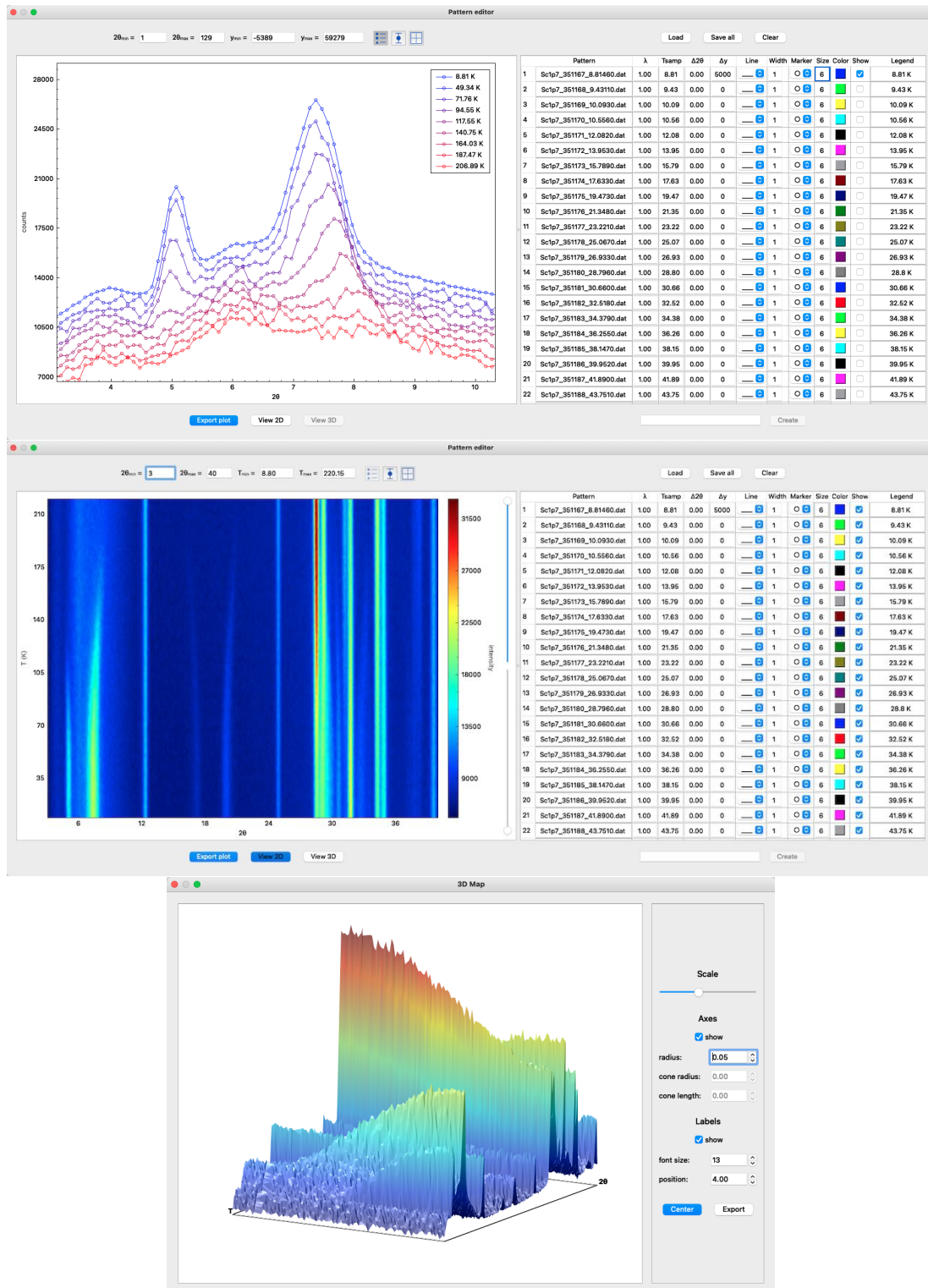
Figure 6.8: Upper panel: Pattern editor showing diffraction patterns in 1D mode. Center panel: When at least 2 diffraction patterns are set to be shown, a 2D thermodiffractogram can be shown by clicking on the *View 2D* button. Bottom panel: After viewing the plot in 2D the *View 3D* button can be clicked which opens a 3-dimensional OPENGL plot of the thermodiffractogram.

axes, i.e. in the same way as magnetic moments (the length corresponds to the that of magnetic moments with a plot scale of 1.0). Note that the vectors are not normalized, i.e. the size of an ellipse or the wavelength of a sine (through the propagation direction) depend on the length of the vectors. The best way to invert the handedness of a spiral is to define negative number of windings (it is also possible to define a negative height, but the spiral will propagate in the opposite direction). Depending on the object it is possible to define the transparency or a color gradient.

The *Guides to the eye* window can be accessed via the *Tools* menu or directly via its toolbar icon. It shows a list of all guides to the eye presently defined in the unit cell plot. From here it is possible to create a new guide to the eye (*New* button), modify a present one (*Edit* button), duplicate (*Duplicate* button) or delete it (*Delete* button). A click on the *New* button opens a dialog from which one of the listed objects can be chosen. This opens another window in which the respective properties can be entered (see Fig. 6.9). The visibility of guides to the eye can be triggered in the settings window under the *Plot*
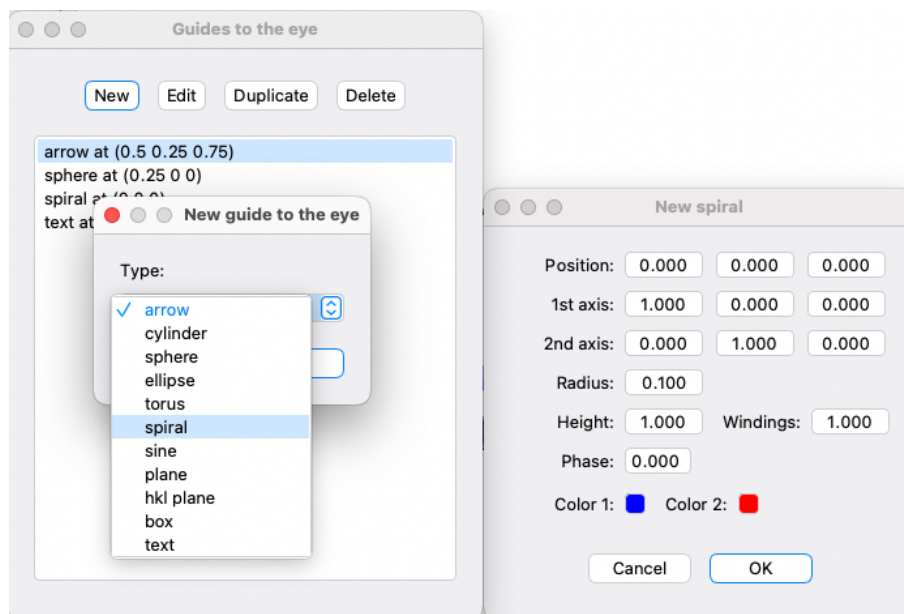
Figure 6.9: *Guides to the eye* window (left) showing a list of objects which are depicted in the unit cell plot. New guides to the eye can be created, edited or deleted. A click on the *New* button opens a dialog from which one of the implemented objects can be chosen. Afterwards, the object can be customized in the object property window (right).

tab. The figures below show some examples in which 3-dimensional guides to the eyes may be useful (and one example where they are absolutely useless).
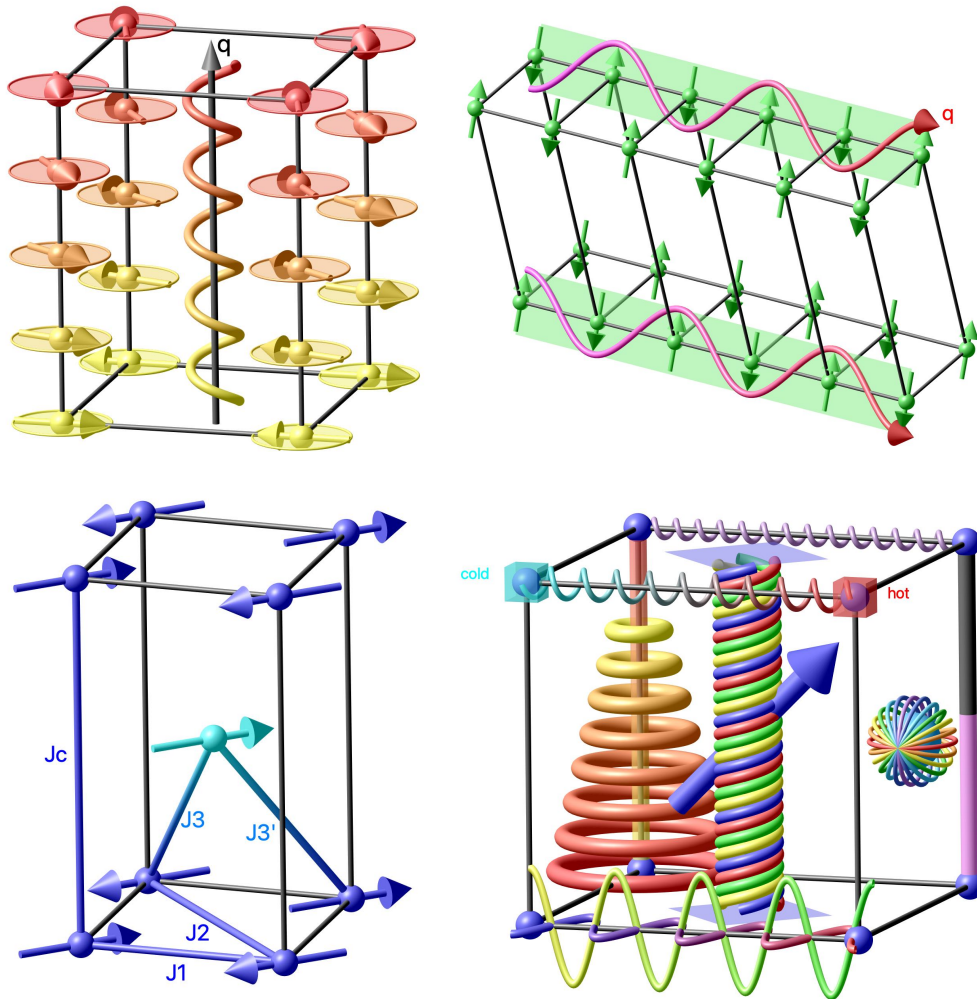
Figure 6.10: Examples of 3-dimensional guide-to-the-eye objects.

6.10 Phase transitions

In single-crystal diffraction experiments, nuclear and/or magnetic phase transitions are best identified and illustrated by following e.g. the integrated intensity of selected Bragg reflections as a function of temperature, magnetic field or pressure. MAG2POL offers a *Phase transition* tool which helps to find appropriate (hkl) reflections showing a significant difference between the involved structures, or - the other way round - to check if certain structures explain an observed transition. In order to use this tool it is necessary to define at least 2 phases in the main window, which are listed in the upper left part of the *Phase transitions* window. Each phase is given an x value according to its number, which can be changed in order to be taken into account in the plot on the right part of the window. In the lower left part, a list of Bragg reflections reflections can be created by entering the h, k, l and $\pm\mathbf{q}$ values and clicking the *Add* button. The quantities according to the combo boxes *y axis1* and *y axis 2* will be calculated and plotted against the different phases. The plot can be modified with respect to the marker and line styles (note that a different style is automatically applied for the right y axis, if enabled). User-defined axes, tick and legend labels can be entered to customize the plot, which can be exported as a `pdf` or `ASCII` file. Reflections can be removed by right-clicking the vertical header labels and then clicking *Remove reflection*.
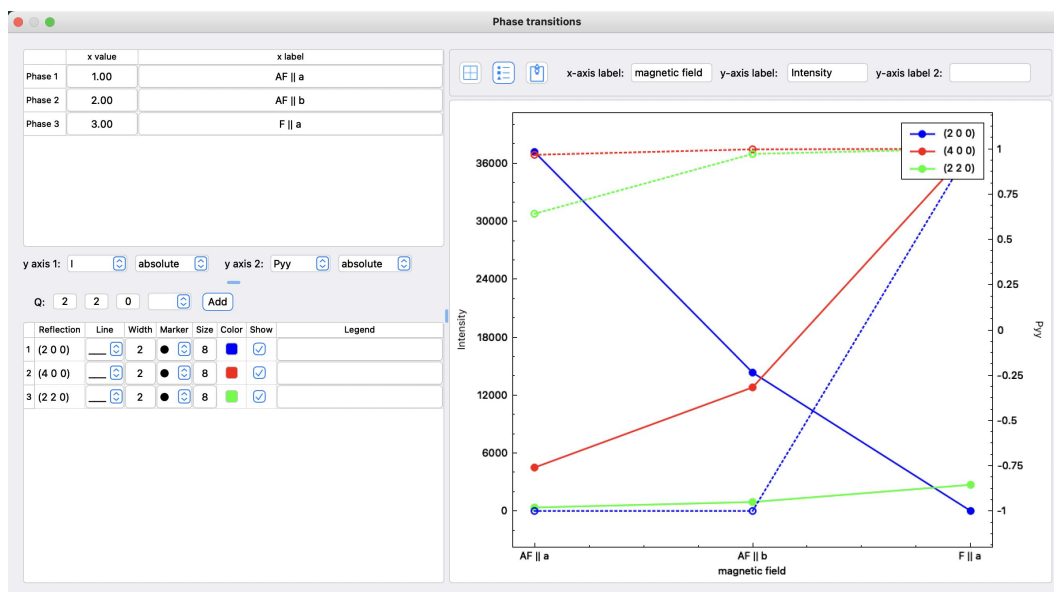
Figure 6.11: Phase transitions window.

7 Mathematical information

7.1 Basic equations

MAG2POL uses the plane wave function following conventions of quantum mechanics, which is generally used for neutron scattering and which is the complex conjugate of that used in x-ray scattering:

$$\psi_{QM} = \psi_{XR}^* = e^{i(\mathbf{kr} - \omega t)}$$

which requires

$$b = b' - ib'' \quad with \quad b'' > 0$$

for the scattering length and yields the scattered wave as a superposition of the plane wave and the spherical wave in the form of

$$\psi(\mathbf{r}) = e^{i\mathbf{kr}} + f(\theta, \phi)\frac{e^{ikr}}{r}.$$

The scattering amplitude is the Fourier transform of the scattering potential and is given by

$$f(\theta, \phi) \propto - \int V(\mathbf{r})e^{-i\mathbf{Qr}}d\mathbf{r}$$

with the scattering vector $\mathbf{Q} = \mathbf{k}_f - \mathbf{k}_i$. Note that using the conventions for X-ray scattering or $\mathbf{Q} = \mathbf{k}_i - \mathbf{k}_f$ leads to the complex conugate of the scattering amplitude. The nuclear structure factor can therefore be written as

$$N(\mathbf{Q}) = \sum_j o_j b_j e^{-2\pi i(hx_j + ky_j + lz_j)} e^{-B_j \sin^2\theta/\lambda^2}$$

with the second exponential term being the Debye Waller factor. The sum is done over all the atoms in the unit cell and o_j denotes the multiplicity and occupation of atom j. Note that the leading minus sign has been dropped as the square of the structure factor is used in all calculations.

The magnetic structure factor writes as

$$\mathbf{M}(\mathbf{Q}) = \sum_j p_n o_j \mathbf{S}_j f_j(\mathbf{Q}) e^{-2\pi i(hx_j + ky_j + lz_j)} e^{-B_j \sin^2\theta/\lambda^2}$$

where $p_n = 0.2695420113693928312$ is the conversion factor between Bohr magnetons and scattering lengths. A factor 0.5 is applied, when the non-zero propagation vector $+\mathbf{q}$ is

inequivalent to $-\mathbf{q}$. $\mathbf{S}_j$ are the Fourier coefficients of the magnetic moment expansion according to

$$\boldsymbol{\mu} = \frac{1}{2} \sum_{\mathbf{q}} S_{\mathbf{q}} e^{i\mathbf{q}\mathbf{R}} + S_{\mathbf{q}}^* e^{-i\mathbf{q}\mathbf{R}}$$

The Fourier coefficients of a given magnetic moment contain a phase factor determined by symmetry and a refinable one. For the calculation of $(hkl) - \mathbf{q}$ satellites the complex conjugate of $\mathbf{S}_j$.

The calculated intensities, which are to be compared to the observed ones, are given by

$$I_N(\mathbf{Q}) = scale \cdot y \cdot NN^*$$

and

$$I_M(\mathbf{Q}) = scale \cdot y \cdot \mathbf{M}_\perp(\mathbf{Q})\mathbf{M}_\perp{}^*(\mathbf{Q})$$

with the magnetic interaction vector

$$\mathbf{M}_\perp = \hat{\mathbf{Q}} \times (\mathbf{M}(\mathbf{Q}) \times \hat{\mathbf{Q}})$$

scale is a simple scaling factor and y is the extinction correction mentioned in Sec. 3.2.

7.2 Polarization matrices

The polarization values are calculated using the density matrix formalism [28] according to

$$P_f = \frac{\mathrm{Tr}(\boldsymbol{\sigma} \cdot \mathcal{M} \cdot \boldsymbol{\rho} \cdot \mathcal{M}^\dagger)}{\mathrm{Tr}(\mathcal{M} \cdot \boldsymbol{\rho} \cdot \mathcal{M}^\dagger)}$$

with

$$\boldsymbol{\sigma} = \begin{pmatrix} P_{f,z} & P_{f,x} - iP_{f,y} \\ P_{f,x} + iP_{f,y} & -P_{f,z} \end{pmatrix},$$

$$\boldsymbol{\rho} = \frac{1}{2} \begin{pmatrix} 1 + P_{i,z} & P_{i,x} - iP_{i,y} \\ P_{i,x} + iP_{i,y} & 1 - P_{i,z} \end{pmatrix},$$

and

$$\mathcal{M} = \begin{pmatrix} N + M_{\perp,z} & -iM_{\perp,y} \\ iM_{\perp,y} & N - M_{\perp,z} \end{pmatrix}.$$

$\mathcal{M}^\dagger$ denotes the conjugate transpose of $\mathcal{M}$. The coordinates x, y and z refer to the local coordination system, where x is always parallel to the scattering vector $\mathbf{Q}$, z is vertical and y completes the right-handed coordination system. The initial neutron polarization is considered by multiplying it to the matrix of the incident beam $\boldsymbol{\rho}$. The finite ^{3}He cell

efficiency is considered in the same way in the matrix of the analyzed beam $\boldsymbol{\sigma}$.

The final neutron spin $\mathbf{P}_f$ is related to the initial one by

$$\mathbf{P}_{i,f} = \mathcal{P}\mathbf{P}_i + \mathbf{P}'$$

where $\mathcal{P}$ is a rotation matrix acting on the initial neutron spin $\mathbf{P}_i$ and $\mathbf{P}'$ is the created/annihilated polarization. By aligning the initial neutron polarization along the directions x, y or z and by analyzing the component of the final neutron spin along these directions, one can summarize nine measurements in the so-called polarization matrix, which is better defined as a pseudomatrix, since it combines the rotation and the created/annihilated polarization. For the general case, i.e. including nuclear, magnetic and interference terms as well as different degrees of polarization and analyzer efficiency for the different directions, the polarization matrix is

$$\mathbf{P}_{f,i} = \begin{pmatrix} p_{fx}\frac{p_{ix}(N^2-M^2)-J_{yz}}{I_x} & p_{fx}\frac{-p_{iy}J_{nz}-J_{yz}}{I_y} & p_{fx}\frac{p_{iz}J_{ny}-J_{yz}}{I_z} \\[2mm] p_{fy}\frac{p_{ix}J_{nz}+R_{ny}}{I_x} & p_{fy}\frac{p_{iy}(N^2+M_{\perp y}^2-M_{\perp z}^2)+R_{ny}}{I_y} & p_{fy}\frac{p_{iz}R_{yz}+R_{ny}}{I_z} \\[2mm] p_{fz}\frac{-p_{ix}J_{ny}+R_{nz}}{I_x} & p_{fz}\frac{p_{iy}R_{yz}+R_{nz}}{I_y} & p_{fz}\frac{p_{iz}(N^2-M_{\perp y}^2+M_{\perp z}^2)+R_{nz}}{I_z} \end{pmatrix}$$

with $N^2 = NN^*$, $M^2 = \mathbf{M}_\perp \mathbf{M}_\perp^*$, $M_{\perp,y}^2 = M_{\perp y}M_{\perp y}^*$ and $M_{\perp z}^2 = M_{\perp z}M_{\perp z}^*$. The mixed magnetic terms are $R_{yz} = 2\Re(M_{\perp y}M_{\perp z}^*)$ and $J_{yz} = 2\Im(M_{\perp y}M_{\perp z}^*)$, while the nuclear-magnetic interference terms are $R_{ny} = 2\Re(NM_{\perp y}^*)$, $R_{nz} = 2\Re(NM_{\perp z}^*)$, $J_{ny} = 2\Im(NM_{\perp y}^*)$ and $J_{nz} = 2\Im(NM_{\perp z}^*)$. The respective matrix elements are normalized to the scattered intensity depending on the initial neutron polarization:

$$I_x = N^2 + M_{\perp y}^2 + M_{\perp z}^2 + p_{ix}J_{yz}$$
$$I_y = N^2 + M_{\perp y}^2 + M_{\perp z}^2 + p_{iy}R_{ny}$$
$$I_z = N^2 + M_{\perp y}^2 M_{\perp z}^2 + p_{iz}R_{nz}$$

In the absence of nuclear scattering, i.e. for a purely magnetic peak, $N = R_{ny} = R_{nz} = J_{ny} = J_{nz} = 0$. One can in general assume the same degree of incident neutron polarization as well as analyzer efficiency for the different directions: $p_{ix} = p_{iy} = p_{iz} = p_0$ and $p_{fx} = p_{fy} = p_{fz} = p_f$. The latter is equal to 1 for data which have been already corrected for the analyzer efficiency. The above polarization matrix is obtained by applying the density matrix formalism for each individual element.

7.3 **Flipping ratios**

The flipping ratio R of a Bragg reflection is defined as the intensity ratio between spin-up and spin-down neutrons and is given by

$$R = \frac{I^+}{I^-} = \frac{NN^* + (N\mathbf{P}_0\mathbf{M}_\perp^* + N^*\mathbf{P}_0\mathbf{M}_\perp) + M_\perp M_\perp^*}{NN^* - (N\mathbf{P}_0\mathbf{M}_\perp^* + N^*\mathbf{P}_0\mathbf{M}_\perp) + M_\perp M_\perp^*}$$

where $\mathbf{P}_0$ is the vector of the initial neutron polarization to be taken along the vertical axis of the diffractometer and the dot product $\mathbf{P}_0\mathbf{M}_\perp$ gives the projection of the magnetic interaction vector onto the vertical polarization axis.

The extinction correction for flipping ratios corresponds to the one which is applied in FullProf [14], see the *Flipping Ratios in FullProf* manual. The flipping ratio is then written as

$$R = \frac{(NN^* + M_{\perp,z}M_{\perp,z}^*)p_p^+ + (N^*\mathbf{p}_m^+\mathbf{M}_\perp + N\mathbf{p}_m^+\mathbf{M}_\perp^*) + (1-q^2)M_\perp M_\perp^* y_{pm}}{(NN^* + M_{\perp,z}M_{\perp,z}^*)p_p^- + (N^*\mathbf{p}_m^-\mathbf{M}_\perp + N\mathbf{p}_m^-\mathbf{M}_\perp^*) + (1-q^2)M_\perp M_\perp^* y_{pm}}$$

with the correction factors

$$p_p^\pm = \frac{1}{2}\left[(1 \pm P_0)(1 + \frac{0.001 I^+ \lambda^3 x_{aniso}}{4\sin^2(\theta/\lambda)\sin(2\theta)})^{-1/2} + (1 \mp P_0)(1 + \frac{0.001 I^- \lambda^3 x_{aniso}}{4\sin^2(\theta/\lambda)\sin(2\theta)})^{-1/2}\right]$$

$$\mathbf{p}_m^\pm = \frac{1}{2}\left[(1 \pm P_0)(1 + \frac{0.001 I^+ \lambda^3 x_{aniso}}{4\sin^2(\theta/\lambda)\sin(2\theta)})^{-1/2} - (1 \mp P_0)(1 + \frac{0.001 I^- \lambda^3 x_{aniso}}{4\sin^2(\theta/\lambda)\sin(2\theta)})^{-1/2}\right]\hat{\mathbf{P}}_0$$

$$y_{pm} = (1 + \frac{0.001 x_{aniso}(1-q^2)M_\perp M_\perp^* \lambda^3 r}{4\sin^2(\theta/\lambda)\sin(2\theta)})^{-1/2},$$

where P_0 is the beam polarization and $I^\pm$ are the uncorrected intensities for a spin-up and spin-down beam, respectively. $q = \sin\alpha$ with α being the angle between the scattering vector and the vertical axis.

Mag2Pol version 3.0 introduced the feature of calculating magnetization density maps. For the observed maps and difference maps, the magnetic structure factors (the coefficients of the Fourier inversion) are obtained by isolating M from the flipping ratio expression:

$$M^2 + aM + b = 0$$

with

$$a = \frac{2Nq^2(Rp_m^- - p_m^+)}{q^4(Rp_p^- - p_p^+) + (1-q^2)q^2 y_{pm}(R-1)}$$

and

$$b = \frac{N^2(Rp_p^- - p_p^+)}{q^4(Rp_p^- - p_p^+) + (1 - q^2)q^2 y_{pm}(R - 1)}$$

Note that the present version of MAG2POL uses the calculated M to derive the extinction correction factors analytically although this is an approximation. A numeric method will be implemented in a future release.

7.4 Multipoles

The magnetization density $m(\mathbf{r})$ is described by

$$m(\mathbf{r}) = R_0' C_0'^0 d_0'^0(\hat{\mathbf{r}}) + \sum_{l=0}^{4} R_l(r) \sum_{m=-l}^{l} C_l^m d_l^m(\hat{\mathbf{r}})$$

where the d_l^m are the density-normalized real spherical harmonics y_l^m whose normalization constants can be found in [29]. The primed quantities denote the first monopole besides the one specified by R_0, C_0^0 and d_0^0. R_l is the radial dependence of a Slater-type orbital:

$$R_l(r) = \frac{Z^{n_l+3}}{(n_l + 2)!} r^{n_l} \exp(-Z_l r)$$

where n and Z can be chosen to be different for each l value. Z and the coefficients C_l^m are refinable parameters. The normalization is such that:

$$\int_{r=0}^{\infty} R_l r^2 dr = 1.$$

The real spherical harmonics y_l^m are obtained from the spherical harmonics Y_l^m according to

$$y_l^m = \begin{cases} \sqrt{2}\,\mathrm{Im}(Y_l^{|m|}), & \text{if } m < 0 \\ Y_l^0, & \text{if } m = 0 \\ \sqrt{2}\,\mathrm{Re}(Y_l^{|m|}), & \text{if } m > 0 \end{cases}$$

The spherical harmonics parametrized in the angles θ and φ are given by

$$Y_l^m(\theta, \varphi) = \sqrt{\frac{2l + 1}{4\pi} \cdot \frac{(l - m)!}{(l + m)!}} P_l^m(\cos \theta) e^{im\varphi}$$

As indicated e.g. in [30] the Condon-Shortley phase $(-1)^m$ which can be seen in some textbooks is included in the associated Legendre polynomials P_l^m so that, e.g. $P_1^1(x) =$

$-(1-x^2)^{\frac{1}{2}}$ and $P_1^{-1}(x) = -\frac{1}{2}P_1^1(x)$. Therefore, the density-normalized real spherical harmonics are normalized so that:

$$\int\limits_{\theta=0}^{\pi}\int\limits_{\varphi=0}^{2\pi} |d_l^m(\theta,\varphi)|\sin(\theta)d\varphi d\theta = \begin{cases} 1, & \text{for } l=0 \\ 2, & \text{for } l>0 \end{cases}$$

The magnetic form factor is given by the Fourier transform of the magnetization density and results in

$$f(\mathbf{Q}) = \langle j_l'(Q)\rangle C_0'^0 d_0'^0(\hat{\mathbf{Q}}) + \sum_{l=0}^{4} i^l \langle j_l(Q)\rangle \sum_{m=-l}^{l} C_l^m d_l^m(\hat{\mathbf{Q}})$$

where $\hat{\mathbf{Q}}$ is parametrized in terms of θ and φ and $\langle j_l(Q)\rangle$ being the Fourier-Bessel transform of the radial density:

$$\langle j_l(Q)\rangle = \int\limits_{r=0}^{\infty} R_l(r) j_l(Qr) 4\pi r^2 dr$$

$j_l(x)$ are the spherical Bessel functions:

$$j_0(x) = \frac{\sin x}{x}$$

$$j_1(x) = \frac{\sin x}{x^2} - \frac{\cos x}{x}$$

$$j_2(x) = \frac{3}{x^2-1}\frac{\sin x}{x} - \frac{3\cos x}{x^2}$$

etc. Note that in the spherical Bessel functions Q is expressed in atomic units by multiplying the Bohr atomic radius a_0 in Å and that $f(\mathbf{Q}{=}0){=}1$ for $C_0^0 = 1$, since $\langle j_0(0)\rangle = 4\pi$ and $d_0^0(\hat{\mathbf{Q}}) = \frac{1}{4\pi}$.

7.5 Orbitals

Here, the magnetization density $m(\mathbf{r})$ is given by

$$m(\mathbf{r}) = |\phi_l(\mathbf{r})|^2 = \left| R_l(r) \sum_{m=-l}^{l} C_l^m d_l^m(\hat{\mathbf{r}}) \right|^2 = R_l^2(r) \sum_{l'=0,2\ldots}^{2l} \sum_{m=-l'}^{l'} \beta_{l'}^m d_{l'}^m(\hat{\mathbf{r}})$$

The product of two spherical harmonics is expressed as a sum over spherical harmonics according to the contraction rule and the relation between the coefficients C_l^m and β_l^m are obtained by equating the orbital expansion with the multipole expansion which results in the so called **M** matrix (see [17]). Therefore, the magnetic form factor becomes

$$f(\mathbf{Q}) = \sum_{l'=0,2\ldots}^{2l} i^{l'} \langle j_{l'}(Q)\rangle \sum_{m=-l'}^{l'} \beta_{l'}^m d_{l'}^m(\hat{\mathbf{Q}})$$

with $\langle j_{l'}(Q) \rangle$ expressed like in the previous section

$$\langle j_{l'}(Q) \rangle = \int\limits_{r=0}^{\infty} R_{l'}^2(r) j_{l'}(Qr) 4\pi r^2 dr$$

The radial part can be expressed by using the tabulated $\langle j_{l'}(Q) \rangle$ as for the sum of radial integrals or by using Slater-like orbitals like in the multipole approach. A third option is the hydrogen-like radial function which writes as

$$R_{n,l} = \left[\frac{\xi}{2n}(n-l-1)!(n+l)! \right]^{\frac{1}{2}} \exp\left(-\frac{\xi r}{2} \right) (\xi r)^{l+1} \sum_{\nu=0}^{n-l-1} \frac{(-\xi r)^\nu}{\nu!(\nu+2l+1)!(n-l-1-\nu)!}$$

with $\xi = \frac{2Z}{na_0}$.

7.6 Spin correlations

Given a periodic magnetic structure or the result of a reverse Monte-Carlo simulation in a large supercell the intensities $I(Q)$ can be calculated according to

$$I(Q) = C[\mu f(Q)]^2 \cdot \frac{1}{N} \sum_{i,j} \left[A_{ij} \frac{\sin Qr_{ij}}{Qr_{ij}} + B_{ij} \left(\frac{\sin Qr_{ij}}{(Qr_{ij})^2} - \frac{\cos Qr_{ij}}{(Qr_{ij})^2} \right) \right], \qquad (7.1)$$

where $C = \left(\frac{\gamma_n r_e}{2} \right)^2 = 0.07265$ barn, μ is the effective magnetic moment, $f(Q)$ is the magnetic form factor, N is the number of atoms in the super cell, Q is the scattering vector and the sum runs over the pairs of spins i and j separated by the distance r_{ij}. In order to calculate the powder-averaged magnetic neutron scattering intensity for each spin pair in the sum a local coordination system is defined where z is along the vector r_{ij}, y is parallel to $\mathbf{S}_i \times \mathbf{z}$ and x completes the right-handed system. With this definition $A_{ij} = S_i^x S_j^x$ and $B_{ij} = 2S_i^z S_j^z - S_i^x S_j^x$ as implemented in SPINVERT [27].

The analytical form of the mPDF was derived for the first time in [31] by calculating the Fourier transform of the neutron scattering cross section from a collection of magnetic moments. We have adapted the original formula by adjusting the prefactors in order to be consistent with Eq. 7.1:

$$I(r) = \frac{C[\mu f(Q)]^2}{b_M^2} \cdot \frac{1}{N} \sum_{i,j} \left[\frac{A_{ij}}{r} \delta(r - r_{ij}) + B_{ij} \frac{r}{r_{ij}^3} [1 - \Theta(r - r_{ij})] \right]. \qquad (7.2)$$

b_M^2 is the square of the magnetic scattering length 3.055 barn/str/Gd and 0.635 barn/str/Nd, respectively. Furthermore, in order to allow the comparison with the Fourier transform of the corrected raw data (without dividing by the magnetic form factor) we have replaced

the delta function $\delta(r)$ and the step function $\Theta(r)$ by Gaussian and Error functions, respectively, with a full width at half maximum (FWHM) in real space corresponding to a Gaussian fit to the squared magnetic form factor in reciprocal space $[FWHM_R \approx 4 \cdot \ln(4)/(4\pi FWHM_{f^2(Q)})]$ (note that the factor 4π is due to the crystallographers' definition of Q widely used in particular for the analytical approximation of magnetic form factors, which is also adapted in MAG2POL).

7.7 Powder patterns

Rietveld refinement is a method which compares an experimentally observed powder (x-ray or neutron) diffraction pattern with a calculated line profile in a least-squares algorithm until the best possible agreement is found. MAG2POL supports diffraction patterns recorded on constant-wavelength and time-of-flight instruments and the data should contain the scattering variable 2θ or TOF, the intensity and eventually the standard deviation of the intensity. If the latter is not given (depending on the input file format), the program takes the square root of the intensity.

The following features and equations are based on the FULLPROF manual. For the sake of completeness of this manual, the implemented equations are listed here as well.

7.7.1 Calculated profile

The theoretical profile is calculated from the given structure model with nuclear and/or magnetic contribution. A single point in this profile is calculated according to

$$y_{cal,i} = \sum_P S_P \sum_Q I_{P,Q} \cdot \Lambda(2\theta_i - 2\theta_{P,Q} - \Delta 2\theta) + b_i$$

where the sum runs over the number of phases P and all Bragg reflections Q which contribute to the point $y_{cal,i}$. S_P is the scale factor of phase P, Λ is the profile function with its peak at $2\theta_{P,Q}$ ($\Delta 2\theta$ contains all systematic offsets, see Secs. 7.7.1.5 and 7.7.1.6) and b_i is the background which is calculated according to the model used (see Sec. 7.7.1.7). The intensity of the Bragg reflection Q of phase P writes as

$$I_{P,Q} = (m \cdot L \cdot A \cdot P \cdot T \cdot F^2)_{P,Q}$$

F^2 is the square of the nuclear/magnetic structure factor corresponding to NN^* or $\mathbf{M}_\perp \mathbf{M}_\perp^*$ as shown in Sec. 7.1 and m is the multiplicity of the peak [e.g. $m = 4$ for a (200) reflection in tetragonal symmetry]. The remaining quantities are described in the following sections.

7.7.1.1 Lorentz and polarisation factor

The Lorentz and polarisation factor L (in Debye-Scherrer geometry) is given by

$$L = \frac{1 - K + K\cos^2(2\theta_M)\cos^2(2\theta)}{2\sin^2(\theta)\cos(\theta)}$$

with θ_M being the monochromator take-off angle and K the polarization factor, which is 0 for neutrons, 0.5 for characteristic non-polarised x-ray radiation and around 0.1 for synchrotron radiation. Therefore, the take-off angle does not need to be given in the neutron case.

7.7.1.2 Asymmetry

A is the peak asymmetry, a function which is multiplied to the profile function

$$A(x) = 1 - \frac{A_1 F_a(x) - A_2 F_b(x)}{\tanh(\theta)} - \frac{A_3 F_a(x) + A_4 F_b(x)}{\tanh(2\theta)}$$

with

$$x = \frac{2\theta_i - 2\theta_Q - \Delta 2\theta}{FWHM}$$

$\Delta 2\theta$ combines all systematic line-shifts which are explained in more detail in Sec. 7.7.1.6. The functions $F_{a,b}(x)$ are given by

$$F_a(x) = 2z\exp(-z^2)$$

$$F_b(x) = (2z^2 - 3)F_a(x)$$

The parameters A_1 to A_4 can be refined. Note that the subtle differences in the equations in comparison to the FULLPROF manual are on purpose, they have been adapted to obtain the same asymmetries.

7.7.1.3 Preferred orientation

The two following preferred orientation functions are implemented in MAG2POL:

- Exponential function
  The correction factor for the calculated intensities is given by

$$P_Q = P_2 + (1 - P_2)\exp(-P_1\alpha_Q^2)$$

  α_Q is the acute angle between the scattering vector Q and the normal of the preferred orientation (hkl) vector which has to be defined by the user. P_1 and P_2 are refinable parameters.

- Modified March's function

  Here the correction is calculated by

$$P_Q = P_2 + (1 - P_2) \left\{ [P_1 \cos(\alpha_Q)]^2 + \frac{\sin^2(\alpha_Q)}{P_1} \right\}^{-\frac{3}{2}}$$

and P_1 and P_2 are again refinable parameters. $P_1 = 1$ means no preferred orientation, $P_1 < 1$ refers to a platy habit (α_Q is the acute angle between the scattering vector and the normal of the crystallites) and $P_1 > 1$ to a needle-like habit (α_Q is the acute angle bewteen the scattering vector and the axis of the needle).

7.7.1.4 Absorption and extinction

The effects of sample absorption depend on the scattering angle and can be corrected by the following transmission factor for constant wavelength and Debye-Scherrer geometry:

$$T_Q = \exp \left\{ - \left[1.7133 - 0.0368 \sin^2(\theta_Q) \right] \mu_\lambda R + \left[0.0927 + 0.375 \sin^2(\theta_Q) \right] [\mu_\lambda R]^2 \right\}$$

The linear absorption coefficient is automatically calculated based on the given structure model (averaged over the volumes of the contributing phases) and the corresponding wavelength (λ_1 or λ_2), but the radius R of the cylindrical sample has to be given by the user.

For time-of-flight data different refinable absorption models are implemented:

- Model 1

  Here the parameters μ_1 and μ_2 can be refined to mimic an effective $\mu_\lambda R$ according to

$$\mu_\lambda R = \mu_1 \cdot \lambda_Q + \mu_2$$

with λ_Q being the wavelength associated with the particular reflection Q and the transmission factor is given by

$$T_Q = \begin{cases} 1 - \mu_\lambda R(1 - \frac{2}{3}\mu_\lambda R), & \text{if } \mu_\lambda R \leq 0.001 \\ \frac{1 - \exp(-2\mu_\lambda R)}{2\mu_\lambda R}, & \text{if } \mu_\lambda R > 0.001 \end{cases}$$

- Model 2

  This model corresponds to the one for the constant-wavelength case, but with a refinable parameter μ_1 which is multiplied with λ_Q representing $\mu_\lambda R$:

$$T_Q = \exp \left\{ - \left[1.7133 - 0.0368 \sin^2(\theta_B) \right] \mu_1 \lambda_Q + \left[0.0927 + 0.375 \sin^2(\theta_B) \right] [\mu_1 \lambda_Q]^2 \right\}$$

Hereby, θ_B is half the scattering angle of the corresponding detector bank.

- Model 3

  Again, the parameter μ_1 is multiplied with λ_Q associated to the reflection Q, therefore describing an effective μR, and the transmission factor is

  $$T_Q = \exp(-\mu_1 \lambda_Q)$$

- Model 4

  This is the Loganov & alte da Veiga model [32]. For $\mu_1 \lambda_Q = \mu R < 3$ cm^{-1}

  $$T = \exp\left[-k_0 \mu_1 \lambda_Q - k_1 (\mu_1 \lambda_Q)^2 - k_2 (\mu_1 \lambda_Q)^3 - k_3 (\mu_1 \lambda_Q)^4\right]$$

  with

  $$
  \begin{aligned}
  k_0 =& 1.697653 \\
  k_1 =& \left[25.99978 - 0.01911\sqrt{\sin(\theta_B)}\right] \exp(-0.024514 \sin^2(\theta_B)) \\
  & + 0.109561 \sin(\theta_B) - 26.0456 \\
  k_2 =& -0.02489 - 0.39499 \sin^2(\theta_B) + 1.219077 \sin^3(\theta_B) - 1.31268 \sin^4 \theta_B \\
  & + 0.871081 \sin^5(\theta_B) - 0.2327 \sin^6(\theta_B) \\
  k_3 =& 0.003045 + 0.018167 \sin^2(\theta_B) - 0.03305 \sin^4(\theta_B)
  \end{aligned}
  $$

  For $\mu_1 \lambda_Q = \mu R > 3$ cm^{-1} the transmission factor is given by

  $$T = \frac{k_4 - k_7}{\left[1 + k_5(\mu_1 \lambda_Q - 3)\right]^{k_6}} + k_7$$

  with

  $$
  \begin{aligned}
  k_4 =& 1.433902 + 11.07504 \sin^2(\theta_B) - 8.77629 \sin^4(\theta_B) \\
  & + 10.02088 \sin^6(\theta_B) - 3.36778 \sin^8(\theta_B) \\
  k_5 =& \left[0.013869 - 0.01249 \sin^2(\theta_B)\right] \exp\left[3.27094 \sin^2(\theta_B)\right] \\
  & + \frac{0.337894 + 13.77317 \sin^2(\theta_B)}{\left[1 + 11.53544 \sin^2(\theta_B)\right]^{1.555039}} \\
  k_6 =& \frac{1.933433}{\left[1 + 23.12967 \sin^2(\theta_B)\right]^{1.686715}} - 0.13576 \sin(\theta_B) + 1.163198 \\
  k_7 =& 0.044365 - \frac{0.04259}{\left[1 + 0.41051 \sin^2(\theta_B)\right]^{148.4202}}
  \end{aligned}
  $$

For time-of-flight data a primary extinction correction is implemented which is calculated according to [33]. The extinction correction E is a combination of Bragg and Laue components

$$E = E_B \sin^2(\theta_B) + E_L \cos^2(\theta_B),$$

where

$$E_B = \frac{1}{\sqrt{1+x}}$$

and

$$E_L = 1 - \frac{x}{2} + \frac{x^2}{4} - \frac{5x^3}{48} + ... \text{ for } x < 1$$

or

$$E_L = \sqrt{\frac{2}{\pi x}} \left(1 - \frac{1}{8x} - \frac{3}{128x^2} - \frac{15}{1024x^3} - ... \right) \text{ for } x > 1$$

where

$$x = r_{bl} \left(\frac{\lambda_Q F}{V} \right)^2$$

where F is the calculated structure factor and V is the unit cell volume. r_{bl} is a refinable parameter and is a measure of the mosaic block size in μm^2. Note that a direct comparison of this value with FULLPROF is only possible, if the `*.pcr` file contains the occupation factor as the ratio between special site and general site multiplicity.

7.7.1.5 Profile functions

Except for the numerical and the split Pseudo-Voigt profile all constant-wavelength profile functions available in FULLPROF are implemented in MAG2POL, in the current version two time-of-flight peak profiles are implemented. If not otherwise specified, for all constant-wavelength profiles the full width at half maximum Γ is composed of the Cagliotti formula (u, v, w refinable parameters) and isotropic Gaussian broadening (I_G refinable parameter):

$$\Gamma^2 = u \cdot \tan^2(\theta) + v \cdot \tan(\theta) + w + \frac{I_G}{\cos^2(\theta)}$$

- Gaussian

$$\Lambda(x) = G(x) = \frac{2}{\Gamma} \sqrt{\frac{\ln 2}{\pi}} \exp\left(-\frac{4 \ln 2}{\Gamma^2} x^2 \right)$$

- Lorentzian

$$\Lambda(x) = L(x) = \frac{a_L}{1 + b_L x^2}$$

$$a_L = \frac{2}{\pi \Gamma} \qquad b_L = \frac{4}{\Gamma^2}$$

- Modified Lorentzian

$$\Lambda(x) = \frac{a_{ML}}{\left(1 + b_{ML} x^2 \right)^2}$$

$$a_{ML} = \frac{4\sqrt{\sqrt{2}-1}}{\pi\Gamma} \qquad b_{ML} = \frac{4(\sqrt{2}-1)}{\Gamma^2}$$

- Intermediate Lorentzian

$$\Lambda(x) = \frac{a_{IL}}{(1+b_{IL}x^2)^{3/2}}$$

$$a_{IL} = \frac{\sqrt{2^{2/3}-1}}{\Gamma} \qquad b_{IL} = \frac{4(2^{2/3}-1)}{\Gamma^2}$$

- Pearson VII

$$\Lambda(x) = \frac{a_{VII}}{(1+b_{VII}x^2)^m}$$

$$a_{VII} = \frac{\Gamma(m)}{\Gamma(m) - 1/2} \frac{2\sqrt{2^{1/m}-1}}{\sqrt{\pi}\Gamma} \qquad b_{VII} = \frac{4(2^{1/m}-1)}{\Gamma^2}$$

The refinable parameter m can optionally be set to be a function of the scattering angle (in degrees):

$$m = m_0 + \frac{100 \cdot X}{2\theta} + \frac{1000 \cdot Y}{(2\theta)^2}$$

where X and Y are further refinable parameters.

- Pseudo-Voigt

$$\Lambda(x) = pV(x) = \eta \cdot L(x) + (1-\eta) \cdot G(x) \qquad 0 \le \eta \le 1$$

where $L(x)$ and $G(x)$ have the same full width at half maximum Γ. The mixing parameter η can optionally be set to be a function of the scattering angle (in degrees):

$$\eta = \eta_0 + X \cdot 2\theta$$

- Tripled Pseudo-Voigt

$$\Lambda(x) = X \cdot pV(x-D) + (1-X-Y) \cdot pV(x) + Y \cdot pV(x+D)$$

$$D = \frac{S}{d\cos(\theta)}$$

where d is the d-spacing of the (hkl) reflection for which the profile is calculated and S is a refinable parameter. The three Pseudo-Voigt profiles have the same η_0 and Γ and are mixed according to the refinable parameters X and Y.

- Pseudo-Voigt with Finger-Cox-Jephcoat asymmetry [34]

$$\Lambda(x) = \frac{\sum\limits_{n=1}^{N_{max}} \frac{w_n W(\delta_n, 2\theta) pV(x+2\theta-\delta_n)}{h(\delta_n)\cos(\delta_n)}}{\sum\limits_{n=1}^{N_{max}} \frac{w_n W(\delta_n, 2\theta)}{h(\delta_n)\cos(\delta_n)}}$$

The sum is a numerical integration corresponding to a Gauss-Legendre quadrature procedure with w_n and x_n being the Gauss-Legendre weights and abscissae associated with the nth point and N_{max} is the number of points chosen. In the original paper it is recommended that $N_{max} \geq 30$ for values within six half-widths of the profile peak and $N_{max} = 10$ outside this region. Mag2Pol uses $N_{max} = 30$ for every point which yields smooth peak profiles with sufficiently fast calculation times.

$$h(\delta) = \sqrt{\frac{\cos^2(\delta)}{\cos^2(\theta)} - 1} \qquad \delta_n = \frac{1}{2}(2\theta + 2\varphi_{min}) + \frac{x_n}{2}(2\theta - 2\varphi_{min})$$

$$W(2\varphi, 2\theta) = \begin{cases} S_L + D_L - h(\delta_n), & \text{for } 2\varphi_{min} \leq 2\varphi < 2\varphi_{infl} \\ 2\min(S_L, D_L), & \text{for } 2\varphi_{infl} \leq 2\varphi \leq 2\theta \\ 0, & \text{else} \end{cases}$$

The inequalities above apply to $2\theta < 90°$ and have to be inverted for $2\theta > 90°$. Bragg peaks with a scattering angle closer than $0.1°$ to $90°$ are not corrected in Mag2Pol. The respective limiting 2φ angles are given by

$$2\varphi_{min} = \cos^{-1}\left[\cos(2\theta)\sqrt{(S_L + D_L)^2 + 1}\right]$$

$$2\varphi_{infl} = \cos^{-1}\left[\cos(2\theta)\sqrt{(D_L - S_L)^2 + 1}\right]$$

The parameters S_L and D_L are refinable. The first refers to half the sample height divided by the sample-to-detector distance and the second is half the detector height divided by the sample-to-detector distance. The implemented code was successfully compared to the example given in the original paper as well as with FullProf examples. The recast of variables for special values of S_L and D_L in the refinement procedure as proposed in [35] is implemented but needs to be tested more throroughly as the resulting standard deviation proved to be a bit high for some examples.

- Thompson-Cox-Hastings Pseudo-Voigt with Finger-Cox-Jephcoat asymmetry
  In comparison to the Pseudo-Voigt profile above the parameter η is not refinable but calculated from the Lorentzian and Gaussian linewidths:

$$\Gamma_G = \sqrt{u \cdot \tan^2(\theta) + v \cdot \tan(\theta) + w + \frac{I_G}{\cos^2(\theta)}}$$

$$\Gamma_L = X \cdot \tan(\theta) + \frac{Y}{\cos(\theta)}$$

with X and Y being refinable parameters The numerical Pseudo-Voigt approximation of the convolution between the Lorentzian and a Gaussian function yields

$$\Gamma = \left(\Gamma_G^5 + 2.69269 \cdot \Gamma_G^4 \Gamma_L + 2.42843 \cdot \Gamma_G^3 \Gamma_L^2 + 4.47163 \cdot \Gamma_G^2 \Gamma_L^3 + 0.07842 \cdot \Gamma_G \Gamma_L^4 + \Gamma_L^5\right)^{1/5}$$

$$\eta = 1.36603 \cdot \frac{\Gamma_L}{\Gamma} - 0.47719 \cdot \left(\frac{\Gamma_L}{\Gamma}\right)^2 + 0.11116 \cdot \left(\frac{\Gamma_L}{\Gamma}\right)^3$$

These values Γ and η are then used in the Pseudo-Voigt function $pV(x)$ and the optional Finger-Cox-Jephcoat asymmetry is calculated as described in the previous point.

- Convolution of Pseudo-Voigt with a pair of back-to-back exponentials

$$\Lambda(x) = pV(x) \circledast E(x) = \int\limits_{-\infty}^{\infty} pV(x-t)E(t)dt$$

$$= (1-\eta)N\left[e^u \operatorname{erfc}(y) e^v \operatorname{erfc}(z)\right] - \frac{2N\eta}{\pi}\left\{\Im[e^p E_1(p)] + \Im[e^q E_1(q)]\right\}$$

with erfc being the complementary error function, E_1 the exponential integral and

$$N = \frac{\alpha\beta}{2(\alpha+\beta)}.$$

The exponents u and v are given by

$$u = \frac{1}{2}\alpha(\alpha\sigma_G^2 + 2x) \quad u = \frac{1}{2}\beta(\beta\sigma_G^2 - 2x),$$

the arguments y, z by

$$y = \frac{\alpha\sigma_G^2 + x}{\sqrt{2\sigma_G^2}} \quad z = \frac{\beta\sigma_G^2 - x}{\sqrt{2\sigma_G^2}}$$

and the arguments p and q by

$$p = \alpha x + \frac{i\alpha\Gamma}{2} \quad p = -\beta x + \frac{i\beta\Gamma}{2}.$$

The Gaussian component of the Pseudo-Voigt function is expressed by

$$\sigma_G^2 = \sigma_0 + \sigma_1 \cdot d^2 + (\sigma_2 + I_G) \cdot d^4 = \frac{\Gamma_G^2}{8\ln 2}$$

and the Lorentzian component writes as

$$\gamma_L = \gamma_0 + \gamma_1 \cdot d + \gamma_2 \cdot d^2 = \Gamma_L.$$

Note that the Lorentzian size broadening is not yet implemented in MAG2POL. The relations between Γ_G, Γ_L and Γ as well as η are the same as for the Thompson-Cox-Hastings Pseudo-Voigt function. The rise and decay constants α and β are given by

$$\alpha = \alpha_0 + \frac{\alpha_1}{d_Q} \quad \beta = \beta_0 + \frac{\beta_1}{d_Q^4}$$

- Convolution of Pseudo-Voigt with the Ikeda-Carpenter function

  The Ikeda-Carpenter function is the result of the convolution of two functions

$$S_k(t) = \frac{\alpha^3}{2}t^2 e^{-\alpha t} \quad R_k(t) = (1-R)\delta(t) + R\beta e^{-\beta t},$$

which describe leakage of fast and slow neutrons from the moderator with the fast and slow decay constants α and β:

$$I_k(t) = S_k(t) \circledast R_k(t) = (1-R)S_k(t) \circledast \delta(t) + R\beta S_k(t) \circledast e^{-\beta t}$$

$$= (1-R)S_k(t) + R\beta \int_{-\infty}^{\infty} S_k(\tau) \left[e^{-\beta(t-\tau)} \right] d\tau$$

$$= (1-R)S_k(t) + R\beta e^{-\beta t} \int_{0}^{t} S_k(\tau) e^{\beta t} d\tau$$

$$= \frac{\alpha^3}{2} \left\{ (1-R)t^2 e^{-\alpha t} + \frac{2R\beta}{(\alpha-\beta)^3} \left[e^{-\beta t} - e^{-\alpha t} \left((\alpha-\beta)^2 \frac{t^2}{2} + (\alpha-\beta)t + 1 \right) \right] \right\}$$

The implemented peak profile is obtained by the convolution of a Pseudo-Voigt function with the Ikeda-Carpenter function:

$$\Lambda(x) = pV(x) \circledast I_k(x) = \int_{-\infty}^{\infty} pV(x-t)I_k(t)dt = N\left[(1-\eta)\Lambda_G(x) + \eta\Lambda_L(x)\right]$$

with

$$N = \frac{\alpha(1-k^2)}{4k^2}$$

The Gaussian part Λ_G is given by

$$\Lambda_G(x) = N_u e^u \operatorname{erfc}(y_u) + N_v e^v \operatorname{erfc}(y_v) + N_s e^s \operatorname{erfc}(y_s) + N_r e^r \operatorname{erfc}(y_r)$$

with

$$N_u = (1 - R\frac{\alpha^-}{w}) \quad N_v = (1 - R\frac{\alpha^+}{z}) \quad N_s = -2(1 - R\frac{\alpha}{y}) \quad N_r = 2R\alpha^2\beta\frac{k^2}{wyz}$$

and

$$y_u = \frac{\alpha^-\sigma_G^2 - x}{\sqrt{2\sigma_G^2}} \quad y_v = \frac{\alpha^+\sigma_G^2 - x}{\sqrt{2\sigma_G^2}} \quad y_s = \frac{\alpha\sigma_G^2 - x}{\sqrt{2\sigma_G^2}} \quad y_r = \frac{\beta\sigma_G^2 - x}{\sqrt{2\sigma_G^2}}$$

where $k = 0.05$, $R = \exp\left(-\frac{81.799}{\kappa \lambda^2}\right)$, $\alpha^- = \alpha(1-k)$, $\alpha^+ = \alpha(1+k)$, $w = \alpha^- - \beta$, $y = \alpha - \beta$ and $z = \alpha^+ - \beta$. The parameters α and β are

$$\alpha = \frac{1}{\alpha_0 + \lambda \alpha_1} \quad \beta = \frac{1}{\beta_0}$$

The u, v, s and r arguments of the exponential functions are

$$u = \frac{1}{2}\alpha^-(\alpha^- \sigma_G^2 - 2x) \quad v = \frac{1}{2}\alpha^+(\alpha^+ \sigma_G^2 - 2x) \quad s = \frac{1}{2}\alpha(\alpha \sigma_G^2 - 2x) \quad r = \frac{1}{2}\beta(\beta \sigma_G^2 - 2x)$$

The Lorentzian part is described by

$$\Lambda_L(x) = -\frac{2}{\pi}\left\{N_u \Im\left[e^{z_u} E_1(z_u)\right] + N_v \Im\left[e^{z_v} E_1(z_v)\right] + N_s \Im\left[e^{z_s} E_1(z_s)\right] + N_r \Im\left[e^{z_r} E_1(z_r)\right]\right\}$$

with the z_n being

$$z_s = -\alpha x + \frac{1}{2}i\alpha \gamma_L \quad z_u = -\alpha^- x + \frac{1}{2}i\alpha^- \gamma_L \quad z_v = -\alpha^+ x + \frac{1}{2}i\alpha^+ \gamma_L \quad z_r = -\beta x + \frac{1}{2}i\beta \gamma_L$$

Note that σ_G and γ_L have the same definition as for the previous peak profile (convolution of Pseudo-Voigt and back-to-back exponentials).

7.7.1.6 Offsets / Time of flight

Systematic line-shifts in a powder pattern can occur due to an improper alignment of the sample and/or the detector. The first offset parameter, $\Delta 0$ simply adds to the calculated 2θ value of a Bragg reflection and corresponds to the zero-shift of the detector. The sample-dependent line-shifts result from the eccentricity e of a sample with radius R from the central position

- perpendicular to the incident beam direction

$$\Delta 2\theta = \frac{e}{R}\cos(2\theta) = \Delta x \cos(2\theta)$$

- parallel to the incident beam direction

$$\Delta 2\theta = \frac{e}{R}\sin(2\theta) = \Delta y \sin(2\theta)$$

The above equations apply to the Debye-Scherrer geometry and the parameters Δx and Δy are refinable. Note that the correction perpendicular to the incident beam direction is different from the $\cos(\theta)$ term in the FULLPROF manual, but both programs yield no shift for $2\theta = 90°$.

For TOF data the instrumental offsets in the peak positions are given by the 3 parameters Z_0, D_1 and D_2 which yield the time of flight T_Q for a reflection Q with d-spacing d_Q:

$$T_Q = Z_0 + D_1 \cdot d_Q + D_2 \cdot d_Q^2$$

7.7.1.7 Background

The different possibilities to describe the background of a powder diffraction pattern in MAG2POL are explained below

- linear interpolation
  The user defines a number of discrete background points as explained in Sec. 4.5.3 and the program calculates a linear interpolation. The slope beyond the first and last point is simply continued. When 0 points are defined, the background is 0 everywhere; when 1 point is defined, the background is flat and goes through that point.

- polynomial (6 coefficients)

$$b_i = \sum_{m=0}^{5} C_m \left(\frac{2\theta_i}{B_0} - 1 \right)^m$$

  where the coefficients C_0 to C_5 are refinable parameters and B_0 is the adaptable origin of the polynomial.

- polynomial (12 coefficients)

$$b_i = \sum_{m=-3}^{-1} C_m \left(2\theta_i \right)^m + \sum_{m=0}^{8} C_m \left(\frac{2\theta_i}{B_0} - 1 \right)^m$$

  where the coefficients C_{-3} to C_8 are refinable parameters and B_0 is the adaptable origin of the polynomial.

- polynomial (6 coefficients) + Debye-like

$$b_i = \sum_{m=0}^{5} C_m \left(\frac{2\theta_i}{B_0} - 1 \right)^m + \sum_{n=1}^{6} C'_n \frac{\sin(Q_i r_n)}{Q_i r_n}$$

  with $Q_i = 4\pi \frac{\sin(\theta_i)}{\lambda}$. The coefficients C_0 to C_5 as well as C'_1 to C'_6 and r_1 to r_6 are refinable parameters and B_0 is the adaptable origin of the polynomial.

7.8 Standard deviations and agreement factors

The standard deviations σ are obtained by taking the square root of the diagonal of the covariance matrix $\mathbf{C}$:

$$\mathbf{C} = \boldsymbol{\alpha}^{-1} \cdot \chi_r^2$$

The correlation matrix is obtained by dividing the elements $C_{i,j}$ by the standard deviations $\sigma_i \cdot \sigma_j$. $\boldsymbol{\alpha}$ is a $n \times n$ square matrix with n the number of refined parameters x_j:

$$\boldsymbol{\alpha} = \mathbf{D}^T \cdot \mathbf{D}$$

with $\mathbf{D}$ being a $m \times n$ matrix (m is the number of observations $y_{obs,i}$ or calculated values $y_{cal,i}$) where the jth column is given by:

$$\mathbf{D}^{(j)} = \frac{y_{cal,i}(x_j + \Delta) - y_{cal,i}(x_j - \Delta)}{2\Delta\sigma_i}$$

The reduced χ_r^2 value is defined as

$$\chi_r^2 = \frac{\chi^2}{(m-n)}.$$

and χ^2 is expressed by

$$\chi^2 = \sum_i \left(\frac{y_{obs,i} - y_{cal,i}}{\sigma_i} \right)^2 .$$

The observed and calculated values, $y_{obs,i}$ and $y_{cal,i}$, can be integrated intensities, polarization matrix elements or a point in a diffraction pattern.

The crystallographic R_F factor is given by

$$R_\mathrm{F} = 100 \cdot \frac{\sum\limits_Q |F_{obs,Q} - F_{cal,Q}|}{\sum\limits_Q F_{obs,Q}}$$

and is calculated when integrated intensities or powder patterns are refined. In the case of powder data refinement the observed quantities $F_{obs,i}$ are calculated from the Rietveld formula:

$$I_{obs,Q} = I_{cal,Q} \cdot \frac{\sum\limits_i w_i \cdot \frac{y_{obs,i} - b_i}{y_{cal,i} - b_i}}{\sum\limits_i w_i}$$

with

$$w_i = \Lambda(2\theta_i - 2\theta_Q - \Delta 2\theta) \cdot A$$

i.e. the observed intensities are extracted based on the underlying structure model and peak clusters are proportionally decomposed depending on the calculated intensities which contribute. The weighting factors correspond to the amplitude within a specific profile function multiplied by the asymmetry function (note that the asymmetry is not included in FULLPROF, which, however does not make a difference).

For the determination of the standard deviations of the observed intensities the error propagation of the quantity $(y_{obs,i} - b_i)/(y_{cal,i} - b_i)$ is derived which results in

$$\sigma(I_{obs,Q}) = \frac{I_{cal,Q}}{\sqrt{\sum\limits_i w_i}}$$

with

$$1/w_i = \sigma^2(y_{obs,i}) \cdot \left\{ \frac{1}{(y_{cal,i} - b_i)^2} + \left[\frac{y_{obs,i} - b_i}{(y_{cal,i} - b_i)^2} \frac{y_{cal,i}}{y_{obs,i}} \right]^2 + \left[\frac{y_{obs,i} - y_{cal,i}}{(y_{cal,i} - b_i)^2} \frac{b_i}{y_{obs,i}} \right]^2 \right\}$$

The observed structure factor is then obtained from the observed intensity corrected for the peak multiplicity and the Lorentz factor:

$$F_{obs,Q} = \sqrt{\frac{I_{obs,Q}}{m \cdot L}}.$$

Bibliography

[1] H. T. STOKES, D. M. HATCH AND B. J. CAMPBELL. ISOTROPY.

[2] H. T. STOKES, D. M. HATCH AND B. J. CAMPBELL. ISO-MAG. doi:iso.byu.edu/iso/magneticspacegroups.php.

[3] H. T. STOKES, D. M. HATCH AND B. J. CAMPBELL. ISO(3+d)D. doi:iiso.byu.edu/iso/ssg.php.

[4] H. T. STOKES, B. J. CAMPBELL AND S. VAN SMAALEN. Generation of (3+d)-Dimensional Superspace Groups for Describing the Symmetry of Modulated Crystalline Structures. *Acta Crystallogr., Sect. A: Found. Crystallogr.* **67** 45 (2011).

[5] B. J. C. S. VAN SMAALEN AND H. T. STOKES. Equivalence of Superspace Groups. *Acta Crystallogr., Sect. A: Found. Crystallogr.* **69** 75 (2013).

[6] H. T. STOKES AND B. J. CAMPBELL. Enumeration and tabulation of magnetic (3+d)-dimensional superspace groups. *Acta Crystallogr., Sect. A: Found. Crystallogr.* **78** 364 (2022).

[7] W. J. A. M. PETERSE AND J. H. PALM. The anisotropic temperature factor of atoms in special positions. *Acta Crystallogr.* **20** 147 (1966).

[8] T. HAHN, ed. International Tables for Crystallography, Volume A: Space Group Symmetry (D. Reidel Publishing Company, 1983).

[9] W. C. HAMILTON. On the isotropic temperature factor equivalent to a given anisotropic temperature factor. *Acta Crystallogr.* **12** 609 (1959).

[10] J. SCHWINGER. On the Polarization of Fast Neutrons. *Phys. Rev.* **73** 407 (1948).

[11] C. G. SHULL. Neutron Spin-Neutron Orbit Interaction with Slow Neutrons. *Phys. Rev. Lett.* **10** 297 (1963).

[12] C. G. SHULL. *Trans. Amer. Cryst. Assoc.* **3** 1 (1967).

[13] G. P. FELCHER AND S. W. PETERSON. Schwinger and Anomalous Scattering of Neutrons from CdS. *Acta Crystallogr., Sect. A: Found. Crystallogr.* **31** 76 (1975).

[14] J. Rodríguez-Carvajal. Recent advances in magnetic structure determination by neutron powder diffraction. *Physica B* **192** 55 (1993). doi:10.1016/0921-4526(93)90108-I.

[15] G. M. Sheldrick. A short history of *SHELX*. *Acta Crystallogr., Sect. A: Found. Crystallogr.* **64** 112 (2008). doi:10.1107/S0108767307043930.

[16] P. J. Brown. Spherical Neutron Polarimetry. *In* Neutron Scattering from Magnetic Materials, edited by T. Chatterji, chap. 5, p. 215 (Elsevier, 2006).

[17] A. Holladay, P. Leung and P. Coppens. Generalized Relations Between d-Orbital Occupancies of Transition-Metal Atoms and Electron-Density Multipole Population Parameters from X-ray Diffraction Data. *Acta Crystallogr., Sect. A: Found. Crystallogr.* **39** 377 (1983).

[18] W. R. Busing and H. A. Levy. Angle Calculations for 3- and 4-Circle X-ray and Neutron Diffractometers. *Acta Crystallogr., Sect. A: Found. Crystallogr.* **22** 457 (1967).

[19] C. Wilkinson, H. W. Khamis, R. F. D. Stansfield and G. J. McIntyre. Integration of single-crystal reflections using area multidetectors. *J. Appl. Cryst.* **21** 471 (1988).

[20] H.-C. Hu, C. Yang and K. Zhao. Absorption correction A^* for cylindrical and spherical samples with extended range and high accuracy calculated by the Thorkildsen and Larsen analytical method. *Acta Crystallogr., Sect. A: Found. Crystallogr.* **68** 778 (2012).

[21] J. A. K. Howard, O. Johnson, A. J. Schultz and A. M. Stringer. Determination of the Neutron Absorption Cross Section for Hydrogen as a function of Wavelength with a Pulsed Neutron Source. *J. Appl. Cryst.* **20** 120 (1987).

[22] W. R. Busing and H. A. Levy. High-Speed Computation of the Absorption Correction for Single Crystal Diffraction Measurements. *Acta. Crystallogr.* **10** 180 (1957).

[23] A. N. Lowan, N. Davids and A. Levenson. Table of the zeros of the Legendre plynomials of order 1-16 and the weight coefficients for Gauss' mechanical quadrature formula. *Bull. Amer. Math. Soc.* **48** 739 (1942).

[24] J. M. Perez-Mato, J. L. Ribeiro, V. Petricek and M. I. Aroyo. Magnetic superspace groups and symmetry constraints in incommensurate magnetic phases. *J. Phys.: Condens. Matter* **24** 163 (2012). doi:10.1088/0953-8984/24/16/163201.

[25] J. M. Perez-Mato, S. V. Gallego, E. S. Tasci, L. Elcoro, G. de la Flor and M. I. Aroyo. Symmetry-Based Computational Tools for Magnetic Crystallography. *Annu. Rev. Mater. Res.* **45** 217 (2015). doi:10.1146/annurev-matsci-070214-021008.

[26] N. Neto. Irreducible Representations of Space Groups. *Acta Crystallogr., Sect. A: Found. Crystallogr.* **29** 464 (1973).

[27] J. A. M. Paddison, J. R. Stewart and A. L. Goodwin. Spinvert: A program for refinement of paramagnetic diffuse scattering data. *J. Phys.: Condens. Matter* **25** 454220 (2013).

[28] O. Schärpf. Polarization elements. *In* Lecture Notes on Polarized Neutron Scattering, edited by T. Brückel and W. Schweika, vol. 12 (Schriften des Forschungszentrum Jülich, Series Matter and Materials, 2002).

[29] N. K. Hansen and P. Coppens. Testing Aspherical Atom Refinements on Small-Molecule Data Sets. *Acta Crystallogr., Sect. A: Found. Crystallogr.* **34** 909 (1978).

[30] J. R. Michael and A. Volkov. Density- and wavefunction-normalized Cartesian spherical harmonics for $l \leq 20$. *Acta Crystallogr., Sect. A: Found. Crystallogr.* **71** 245 (2015).

[31] B. A. Frandsen, X. Yang and S. J. L. Billinge. Magnetic pair distribution function analysis of local magnetic correlations. *Acta Crystallogr., Sect. A: Found. Crystallogr.* **70** 3 (2013).

[32] N. N. Lobanov and L. alte da Veiga. Abstract P12-16. *In* 6th European Powder Diffraction Conference (1998).

[33] T. M. Sabine, R. B. von Dreele and J.-E. Jørgensen. Extinction in tim-of-flight neutron powder diffractometry. *Acta Crystallogr., Sect. A: Found. Crystallogr.* **44** 374 (1988).

[34] L. W. Finger, D. E. Cox and A. P. Jephcoat. A Correction for Powder Diffraction Peak Asymmetry due to Axial Divergence. *J. Appl. Cryst.* **27** 892 (1994).

[35] J. R. Hester. Improved asymmetric peak parameter refinement. *J. Appl. Cryst.* **46** 1219 (2013).